COMPARING EARLY SEEDLING TRAITS OF *PINUS ALBICAULIS* AND *PINUS FLEXILIS* ACROSS CLIMATES AND RUST RESISTANCE LEVELS

by

Jessica Ann Harris

A thesis submitted in partial fulfillment
of the requirements for the degree

of

Master of Science

in

Biological Sciences

MONTANA STATE UNIVERSITY
Bozeman, Montana

August 2025

DEDICATION

I want to dedicate this to my angels, Grandpa Al, Aunt Luanne, Grandma Helen, and my dad, Michael Harris, who passed away during my time here. Thank you, grandma, for loving me and for teaching me how to love. Thank you dad, for going for walks in the woods, taking me hunting, and for climbing trees with me. You gave me your adventurous and generous spirit, which I will be forever thankful for.

ACKNOWLEDGEMENTS

I want to thank Danielle Ulrich for giving me the opportunity to not only grow in my knowledge of science, but also for the hours of editing, long emails, and problem solving over the years. I also thank my committee members, Brian Smithers and Justin Runyon, for help with greenhouse processing methods and VOC/phloem analysis. I thank my fellow lab members, Teo Rautu, Katie Sparks, Lou Duloisy, Sean Hoy-Skubik, Steve Huysman, Chloe Wasteneys, Franklin Alongi, and Kelsey Flathers for all the help with greenhouse sowing, GIS, stats, and writing. I thank my undergraduate assistants, Sam Bowne, Jasmine Pflugmacher, Gabrielle Ostrowitz, and William Lutz, for all the help. We are also thankful for the seed that was donated from the Dorena Genetic Resource Center, the British Columbia Forest Service Provincial Tree Seed Centre, and the Alberta International Tree and Seed Centre. Thanks to MSU's Plant Growth Center for providing us with the greenhouse materials and space. Thanks to the Whitebark Pine Ecosystem Foundation and the Department of Ecology for funding support. Thanks to Teo Rautu, Elisabeth Krieger, Lauren Gedlinske, Kadie Heinle, Hannah Stapleton, Robert Eckelbecker, and Anna French for all the support throughout the years. Thank you to Caroline Muller for our weekly "podcast talks" and for our decade of friendship. Thank you to the Ortons for welcoming me into their family. Thank you to my brother, Jacob Harris, for our weekly phone calls, for daily walks in the woods growing up, and for encouraging my love of nature and trees. Thank you to my mom, Lisa Harris, who has made it possible for me to go to undergraduate and graduate school and for teaching me how to be kind, but tough. I love you both. Thank you to my partner, Luke Orton, who is my best friend. Thank you for your support during both challenging and beautiful times. I know it's only the beginning.

TABLE OF CONTENTS

TABLE OF CONTENTS CONTINUED

LIST OF TABLES

LIST OF TABLES CONTINUED

Table Page

LIST OF TABLES CONTINUED

LIST OF TABLES CONTINUED

LIST OF FIGURES

Figure Page

LIST OF FIGURES CONTINUED

LIST OF FIGURES CONTINUED

ABSTRACT

Whitebark pine (*Pinus albicaulis*; PIAL) and limber pine (*Pinus flexilis*; PIFL) are high-elevation five-needle (high-5) white pines (Pinaceae, *Pinus*, *Strobus*), keystone and foundational subalpine species in western North America. Both species are declining due to threats including climate change and white pine blister rust. The primary restoration strategy for PIAL is outplanting rust resistant seedlings. Seedling establishment is critical for successful restoration and shapes future forest composition. However, the mechanisms underlying first-year-germinant seedling establishment are poorly understood. We measured 10 phenological and survival, 56 growth, and 18 NSC traits in <1-year-old greenhouse-grown seedlings in a common garden setup. Seedlings originated from 51 PIAL families that spanned 32 to 54°N in latitude and –127 to –115°E in longitude across Washington and Oregon, U.S. (USFS Region 6) and British Columbia (B.C.), and 12 PIFL families from Alberta. For Question 1, we observed that U.S. and B.C. PIAL seedlings originating from higher latitudes exhibited adaptations to colder and shorter days and growing seasons, including higher survival to each phenological stage, reaching each stage earlier, shorter height, higher biomass allocation belowground to roots than aboveground, and lower leaf and root sucrose concentrations than those originating from lower latitudes. For Question 2, PIAL seed zones 3, 4, and 5 had the highest survival to each phenological stage, but survival appeared to be driven by contrasting resource use strategies: acquisitive in zones 3 and 5, and conservative in zone 4. For Question 3, more resistant PIAL seedlings had higher survival and reached each phenological stage earlier higher biomass allocation aboveground to tough, large leaves, lower biomass allocation belowground, lower leaf starch, and higher leaf sugars than less resistant seedlings. For Question 4, PIFL exhibited a mix of acquisitive and conservative resource use traits compared to PIAL including: lower survival to emergence and needle burst, later needle burst timing, higher aboveground and lower belowground biomass allocation, higher leaf sugars, and lower leaf starch. In contrast to PIAL, PIFL exhibited only one trait difference between resistant and susceptible groups. Our results may improve restoration efforts to conserve these iconic and beloved species in the North American West.

INTRODUCTION

Background

Whitebark pine (*Pinus albicaulis* Engelm.; PIAL) and limber pine (*Pinus flexilis* James.; PIFL) are two high-elevation, five-needle (High-5) white pine species (Family Pinaceae, Genus *Pinus*, subgenus *Strobus*) among six closely related High-5 species that serve as keystone and foundational species in subalpine ecosystems of western North America. High-5 species are often the only trees capable of establishing in these harsh environments, withstanding intense sun, extreme cold (−40 °C), high winds (up to 100 km/h), drought, a short growing season, and nutrient-poor, rocky soils (Tomback et al., 2022). They are slow-growing, stress-tolerant, and long-lived, at the cost of lower competitive capacity. PIAL and PIFL can live for ~1,300 and 1,500 years, respectively (Perkins & Swetnam, 1996; Smithers, 2017; Smithers et al., 2018). PIAL and PIFL have similar growth forms and are often indistinguishable without mature cones (Alongi et al., 2020).

PIAL has the broadest and most northern range of all High-5 species, reaching some of the highest elevations of any North American tree (Tomback et al., 2011). It spans 36˚–56˚N and 107˚–128˚W, occurring at ~1,370–3,660 m in the upper subalpine to treeline (Keane et al., 2017). PIFL occurs from 32˚–52˚N and 105˚-117˚W, occurring at ~870–3810 m in elevation (Ulrich et al., 2023) from lower treeline to upper treeline, including more eastern and southern U.S. regions and at lower elevations than PIAL (Letts et al., 2009; Hankin et al., 2023; Ulrich et al., 2023). As a result, PIAL has been viewed as a specialist and PIFL a generalist (Hankin & Bisbing, 2021; Tomback et al., 2011; Ulrich et al., 2023).

Keystone and foundational species both have a disproportionately large effect on their environment relative to their abundance and provide habitat and resources for other species. Moreover, a keystone species is critical for maintaining the structure, diversity, and functioning of an ecosystem while a foundational species physically defines an ecosystem by providing habitat and resources for other organisms. Both tree species rely on Clark's nutcracker (*Nucifraga columbiana*) for seed dispersal, grow on well-drained, nutrient-poor soils, and are quasi fire-dependent for regeneration (Ulrich et al., 2023; Tomback et al., 2022). Inhabiting high elevations, they help retain snowpack, regulate snowmelt for soil moisture and streamflow (Hankin & Bisbing, 2021), reduce soil erosion (Keane et al., 2022), and create microclimates that support shade-tolerant species by increasing soil moisture, providing shade and wind protection, and buffering temperature extremes (Brodersen et al., 2019; Hankin & Bisbing, 2021; Tomback et al., 2022). Their large, nutrient-rich seeds are key food sources for Clark's nutcracker, red squirrels (*Tamiasciurus hudsonicus*), and the threatened grizzly bear (*Ursus arctos horribilis*). PIAL and PIFL also served as an episodic food for western Native American tribes and remains an iconic species among outdoor enthusiasts (Tomback et al., 2011).

Despite their ecological importance, both species are declining at alarming rates due to climate change, white pine blister rust (WPBR; caused by the exotic fungal pathogen, *Cronartium ribicola* J. C. Fisch), mountain pine beetle (MPB; *Dendroctonus ponderosae* Hopkins), and habitat encroachment and competition with shade-tolerant conifers due to fire exclusion (Keane et al., 2022; Tomback et al., 2022). In the U.S., the percentage of dead PIAL trees increased from 12% to 54% between 1999 and 2020 (Goeking & Windmuller-Campione, 2021), with PIAL stands having more dead than live trees for all but the smallest diameter class (Goeking & Izlar, 2018). PIFL shows similar but lagging trends in mortality compared to PIAL, where mortality increased from 8% to 42% from 1999 to 2019 (Goeking & Windmuller-Campione, 2021; Borgman et al., 2015). As a result, PIAL and PIFL were listed as endangered in Canada under the Species at Risk Act (SARA) in 2012 and 2014, respectively (COSEWIC, 2014). In the U.S., PIAL was listed as threatened under the ESA in 2022,—and is the widest-ranging tree species included on the list (U.S. Fish and Wildlife Service, 2022). PIFL was designated as special status species in Wyoming by the U.S. BLM in 2010.

Climate Change

With increasing frequency and intensity of drought and heat stress worldwide, drought alone has doubled forest mortality rates across much of North and South America in the past 40 years (Allen et al., 2010; McDowell et al., 2020). These mortality trends are pronounced in high-elevation forests in western North America, where warming is occurring faster than the global average (Rangwala & Miller, 2012). Much of PIAL's U.S. range lies in the northwestern U.S. (WA, OR, ID, northern CA, western MT), where mean annual temperatures rose by 1.3°F from 1895–2011 and are projected to increase by 0.8–2.9°C by 2050 and 2–5°C by 2070 under moderate emissions scenarios (Mote & Salathé, 2010). In the western U.S., snowpack is projected to decline by 20–70% by 2100 with the largest percent decline predicted for Washington and Oregon's Cascade Mountains. In the Great Yellowstone Ecosystem (GYE), a greater fraction of total precipitation is expected to fall as rain instead of snow (though total precipitation is predicted to rise in the winter season) (Mahalovich, 2013). As a result of decreased moisture availability, drought is expected to become a key driver of mortality in subalpine systems (Allen et al., 2015). Warmer temperatures and reduced moisture availability have been prompting PIAL and PIFL migration northward or towards higher elevations (Hansen et al., 2021; Monahan et al., 2013). Species distribution models project PIAL will lose 73% of its current climatic niche in British Columbia by 2085 but may gain a similar-sized range farther northwest in British Columbia (McLane & Aitken, 2012). In the U.S., PIAL could lose over 97% of species' distribution area by 2090 (Warwell et al., 2006). For PIFL, the USDA Forest Service National Insect and Disease Risk Map predicts a 44% reduction in PIFL basal area by 2027 due to combined effects of WPBR, MPB, and dwarf mistletoe (*Arceuthobium cyanocarpum*) (Krist et al., 2014). PIAL and PIFL will need to rapidly adapt (~200 years (Hendry et al., 2011) to keep pace with drastic environmental change. However, natural gene flow and migration may be too limited to support timely adaptation when environmental changes are relatively acute for species with long generation times (~50-200 years for low cone crops (Keane et al., 2017, 2022), low rates of seedling establishment (Coop & Schoettle, 2009), and limited dispersal ranges via the Clark's nutcracker (~32 km radius (McKinney et al., 2009) and gene flow due to high-elevation trees being located in isolated areas separate from other high-elevation populations (Aitken et al., 2008; Bisbing et al., 2021).

High-5 pines are threatened not only by climate change-induced heat and drought stress alone, but also by exacerbating the severity and frequency of other threats. Drought and heat stress increase susceptibility of trees to biotic stressors. For example, tree defense against MPB, a prominent native agent of adult tree mortality, and WPBR is costly, exhausting tree C reserves and water through resin and terpene production to resist MPB and barrier tissue formation to resist WPBR (Bentz et al., 2022). Drought-stressed trees also have been observed to increase volatile emissions that attract MPB (Anderegg et al., 2015; Runyon et al., 2022). Additionally, climate change has shortened winters (Chmura et al., 2011), which has increased MPB winter survival and reproduction rates while also possibly increasing WPBR prevalence by inducing warmer and wetter conditions (Shanahan et al., 2016; Thoma et al., 2019). Fire exclusion, combined with climate-driven increases in fuel loads, wind, and lightning, intensifies wildfire frequency, duration, and upslope spread (McDowell et al., 2020; Stevens-Rumann et al., 2018). Fire exclusion also limits high-5 regeneration and promotes competition with Englemann spruce (*Picea engelmannii* Parry ex Engelm) and subalpine fir (*Abies lasiocarpa* var. *lasiocarpa*) in limited high-elevation habitats. Together, these interacting threats contribute significantly to PIAL and PIFL decline.

White Pine Blister Rust (WPBR)

While multiple threats have caused the decline of PIAL and PIFL (and all high-5 species), WPBR has been considered the primary agent of mortality (Shanahan et al., 2016; Thoma et al., 2019). *C. ribicola* is a non-native, heteroecious, fungal pathogen that causes the disease white pine blister rust (WPBR) on white (five-needle) pines (soft pines within the subgenus Strobus) in western North America (Jacobi et al., 2018). All white pines are susceptible to the pathogen and are *C. ribicola's* primary hosts (Schoettle et al., 2022). *C. ribicola* entered Western North America through Vancouver, B.C. in 1906 and was first reported on PIAL in 1926 and limber pine in 1945 (Hoff et al., 2001). Since then, it has spread southwards and eastwards through the Cascade Mountains in Washington and Oregon, U.S., the Sierra Nevada in California and Nevada, U.S., and the intermountain West and the Rocky Mountains of both U.S. and Canada, infecting High-5 pines including PIAL and PIFL (Burns et al., 2023; Cleaver et al., 2015; J. Dudney et al., 2021; J. C. Dudney et al., 2020; Shanahan et al., 2016; Shepherd, 2018, 2018; Thoma et al., 2019). In high-hazard areas such as the northern U.S. Rockies and adjacent parts of Canada, WPBR has caused mortality rates exceeding 90% (Burns et al., 2023; Shepherd, 2018). Infection rates are lower in the southern Sierra Nevada (0–2%), although they have risen compared to two decades ago (Dudney et al., 2020). In Canada, WPBR incidence in PIFL increased from 33% to 50% between 2004 and 2019 (Shepherd, 2018), while in southwestern Montana, Wyoming, and northern Colorado, 73% of stands averaged 26% infection, with a 6% increase over 8–9 years (Cleaver et al., 2015; Shepherd et al., 2025).

WPBR forms resinous cankers that interrupt the transport of nutrients and water within host stems and branches, girdling and killing the tree. WPBR affects all tree ages but has historically been known to be particularly lethal to smaller trees (≤20 cm) since 2000 because there is less distance to travel from needle to bole and MPB targets larger trees (Aubry et al., 2008; Geils et al., 2010). However, it has been found to infect larger trees more often in recent years because smaller size classes have already died from infection and bigger trees have a greater chance of intercepting basidiospores through larger crowns (Shepherd et al., 2025; Thoma et al., 2019). While larger trees may survive infection longer, WPBR cankers reduce forest regeneration through crown dieback, reducing seed and pollen cone production in the crowns of reproductive trees (Geils et al., 2010).

Each of the five sporulation stages of WPBR’s life cycle requires specific temperature, moisture, and timing thresholds. High humidity, free water (dew), and moderate temperatures during early spring and late summer promote spore production, infection, and germination (Jacobi et al., 2018; Shepherd, 2018; Thoma et al., 2019). Cool summer nights, high soil moisture, and downslope winds further enhance infection risk (Vogler et al., 2017), with infection requiring at least two consecutive favorable days (Jacobi et al., 2018). Some studies predict that WPBR infection may decline under warmer, drier conditions that are less favorable for spore survival and infection (Sturrock et al., 2011). Although climate change expanded WPBR's potential habitat by approximately 778 km² between 1996 and 2016 in the southern Sierra Nevada, where sugar pine (*Pinus lambertiana* Douglas) is the primary host, mean disease prevalence declined by about 33%, likely due to drought-pathogen interactions and reduced alternate host availability at higher elevations (Dudney et al., 2021). While hotter and drier conditions may inhibit the pathogen, climate change could still increase WPBR severity by predisposing heat- and drought-stressed trees to infection (Burns et al., 2023). Although North American white pines did not co-evolve with *C. ribicola*, all High-5 pines exhibit some degree of natural genetic resistance albeit at low population frequencies. PIFL primarily exhibits qualitative resistance (also called major gene or complete resistance) through the R gene *Cr4*, which prevents disease upon infection (Schoettle et al., 2014; Sniezko & Liu, 2022). Therefore, selection for resistance can quickly increase within a population if *C. ribicola* pressure is high. Fortunately for PIFL, the frequency of *Cr4* is relatively high compared to resistant genes found in other High-5 species (Schoettle et al., 2014). Population frequencies of *Cr4* range from 0% to 13.8% and average 5% with the highest concentrations found in southern Colorado and the lowest concentrations in Alberta (Schoettle et al., 2014; Sniezko & Liu, 2022). *Cr4* has yet to be found within other areas of PIFL's distribution (Schoettle et al., 2022). A limitation of qualitative resistance is that it consists of only one gene, meaning that a mutation in *C. ribicola* can overcome host resistance as previously seen in sugar pine and western white pine (*Pinus monticola* Douglas ex D. Don)(Schoettle et al., 2014).

In contrast to PIFL, PIAL exhibits quantitative resistance (also called partial or polygenic resistance) through multiple genes (polygenic) and physiological mechanisms, suppressing but generally not preventing disease. Because there are multiple genes involved, quantitative resistance is thought to be more durable to virulence than qualitative resistance (Sniezko et al., 2020). Symptoms depend on which and how many genes an individual has inherited that result in a resistant phenotype so that resistance exists on a spectrum from A-F, where resistance level A indicates ‘resistant’ (the progeny of that parent tree had the highest level of being symptom-free one year post inoculation) while resistance level F indicates ‘susceptible’ (95% of the progeny of that parent tree had stem symptoms one year post inoculation). Resistant PIAL seedlings have a reduced number of needle spots and early stem symptoms while having increased callus formation (callus is a mass of undifferentiated cells that attempt to compartmentalize or seal off the infection), walling-off cankers, survival with active cankers, shedding of infected spotted needles in the first fall following inoculation, and isolation of infected needle fascicles (Mahalovich et al., 2006). The no-spot and needle-shed resistance mechanisms are present in very low frequencies (<1%) while the short shoot resistance mechanism is present in a low frequency (5.2%) (Mahalovich et al., 2006). The most resistant PIAL seed sources (indicated by low early stem infection) have been found in the Cascade Mountains of Oregon and Washington, while the most susceptible seed sources have been found in eastern Oregon, the Interior West, California, and British Columbia (Sniezko et al., 2018). Like PIFL, historical estimates of PIAL resistance frequencies prior to WPBR introduction are around 1% (Hoff et al., 2001) and increase to 25-50% post-invasion, suggesting strong selective pressure has occurred in high mortality stands (Mahalovich et al., 2006; Schoettle & Sniezko, 2007).

Outplanting Rust Resistant Seedlings for Restoration

Though current restoration practices focus on conserving genetic diversity (greater genetic variation increases adaptive potential (Lind et al., 2017)), protecting seed sources, and deploying restoration treatments while mitigating climate change (Keane et al., 2022; Tomback et al., 2022), the primary restoration strategy for PIAL is outplanting rust-resistant seedlings to increase the frequency of genetic resistance and enhance population resilience (Schoettle et al., 2022; Schoettle & Sniezko, 2007). Several large-scale applied programs have been developed to identify rust resistant trees (known as 'plus' or 'elite' trees (Frankham et al., 2014) and to plant the progeny of these trees. Resistant seed is obtained from surviving trees located in severely infected areas (Tomback et al., 2022). Seeds are germinated into seedlings in a nursery and then are exposed to WPBR spores and monitored for infection symptoms (Sniezko et al., 2011). Resistant seedlings' parent tree seeds are used to grow 2-3-year-old seedlings for outplanting, develop seed orchards, and promote genetic conservation and clone bank contributions (Sniezko & Liu, 2022). While a worthwhile and research-backed endeavor, outplanting is time intensive and financially expensive. Time from seed collection to outplanting is at least 3 years and nursery processing and outplanting cost ~$1,980-$2,400 per ha (Pansing & Tomback, 2019). While PIFL mortality lags behind PIAL's and they are not being outplanted to the same degree as PIAL, the fact that WPBR is still spreading across forests indicates that PIFL may need outplanting efforts in the future.

Given the considerable time and financial investments of outplanting, ensuring that seedlings establish and survive into adulthood is critical for successful restoration and will shape future forest composition (Johnson et al., 2011; Markesteijn & Poorter, 2009). However, the seedling life stage (germinated-2 years old) is inherently vulnerable compared to adult trees.

Seedlings have a shallow, underdeveloped root system, immature and unhardened aboveground tissue with minimal photosynthetic capacity, and limited carbon reserves (Johnson et al., 2011). Given their small stature, seedlings are more susceptible and exposed to abiotic and biotic stressors than adults, including drought, frost heave, wind, pathogens, and animal disturbance—especially at elevational extremes (Kerr et al., 2015; Rank et al., 2022; Smithers et al., 2021). For instance, seedlings are found within the boundary layer of the soil surface, where air temperatures can exceed 60 ˚C and leaf temperatures can be 15 ˚C greater than ambient air temperatures (Johnson et al., 2011; Kolb & Robberecht, 1996). Therefore, summer soil surface temperatures can exceed adult canopy temperatures by up to 25 ℃ (Kueppers et al., 2017; Lazarus et al., 2018; Moyes et al., 2013).

As a result, seedlings are especially sensitive to climatic variation and disproportionately impacted by climate change (Brodersen et al., 2019). The establishment stage—marked by the development of primary leaves and cotyledon senescence—is an especially challenging bottleneck for tree populations (Brodersen et al., 2019) as long-term species persistence depends on surviving this vulnerable stage (Brodersen et al., 2019; Hankin et al., 2023; Johnson et al., 2011; McLane & Aitken, 2012). High-5 species have extremely high mortality rates prior to establishment (>90%) (Maher & and Germino, 2006), while survival rates improve significantly post-establishment (Leck et al., 2008). These vulnerabilities lead to seedling-specific responses compared to mature trees, even under the same environmental conditions (Smithers, 2017), especially in early successional pioneer species like PIAL and PIFL (Máliš et al., 2016).

Despite these differences between life stages, most research has focused on the physiology and survival of adult trees (Keane et al., 2017) with studies only recently examining early seedling function within the last decade and few studies examining seedling traits in the first 12 months of life. Currently, most species distribution models match adult presence with climate to predict future distributions (Smithers, 2017). However, given seedling-specific vulnerabilities, drivers of adult survival differ from those of seedling establishment and survival. Adult trees have broader climatic tolerances where their distributions reflect conditions suitable for reproduction (Dobrowski et al., 2015). Therefore, predictions based solely on adult distributions can be misleading. For example, smaller PIAL (<1 cm DBH) were located at lower elevations than expected by a GYE climate model that solely made predictions on reproductive-sized individuals, showing that without including juveniles, the effects of climate change were estimated to be more severe than in actuality (Hansen et al., 2021). Therefore, examining physiological mechanisms of seedling establishment will improve predictions of future forest composition and species distributions under climate change (Reinhardt et al., 2015).

Physiological mechanisms of seedling establishment include the ability of leaves to use CO_2, photosynthetically active radiation (PAR), and water in photosynthesis and allocate photosynthate to essential functions such as growth and stress resistance. These mechanisms are measured as traits that describe seedling phenology, survival, growth, and non-structural carbohydrates (NSC). Phenology traits—such as timing of emergence, bud formation, and needle burst—indicate how seedlings are attuned to environmental cues like temperature, day length, and moisture availability. These cues determine whether seedlings initiate growth during favorable periods to minimize exposure to late frosts, drought, or heat stress. Understanding phenology can help determine optimal outplanting windows to align seedling development with local conditions. Non-structural carbohydrates (NSC)—including starch, sucrose, glucose, and fructose—are products of photosynthesis that serve as critical C reserves for supporting plant function under stress. NSC play a key role in drought response by maintaining phloem transport and enabling osmoregulation and xylem embolism repair when stomatal closure limits carbon uptake (Hartmann & Trumbore, 2016). Together, traits like phenology, survival, growth, and NSC drive seedling establishment, survival, and species distributions.

Successful outplanting programs must select seedlings to plant and suitable planting locations to ensure seedling survival. Historically, efforts primarily have involved transferring seed within the same seed zone (Borgman et al., 2015; Keane et al., 2022; Tomback et al., 2022). However, given the long lifespans of PIAL and PIFL and that current climates are expected to change over the next century and beyond, family-level (local) adaptations may no longer align with current or future climate conditions (Bradley St Clair & Howe, 2007). Therefore, it is essential to consider climate requirements and local adaptation when selecting outplanting locations (Keane et al., 2022; Tomback et al., 2022). Based on results from their common garden study, Bower and Aitken (2008) proposed moving seed from cone collection sites to planting sites that are cooler by up to 1.9℃ in mean temperature of the coldest month. Planting PIAL seedlings into environments near their low-temperature limits ensures adequate survival and growth and that some adults remain within their high-temperature limits (Bower & Aitken, 2008). Given the limitations of natural dispersal and adaptation, managers may also consider assisted gene flow (seed from other populations within the species' distribution that are better suited to the new climate) or assisted migration (relocating families or populations outside their current range to align with future climates). Although managers of PIAL and PIFL have considered assisted migration and expanding elevational and geographical seed zones to accommodate future climates, models predicting new planting sites are highly uncertain and require more research to be operational (Keane et al., 2022). Therefore, current outplanting efforts include outplanting at least some seedlings from warmer aspects or lower latitudes as a bet-hedging strategy to provide resilience to climate change (Tomback et al., 2022). Priority planting locations include areas that have not yet undergone infection, have low resistance levels, have high infection rates, or have recently had a MPB outbreak (Schoettle et al., 2022; Tomback & Achuff, 2010).

Currently, seed zones for PIAL have been developed for outplanting programs, specifically to identify rust resistant 'plus' trees and suitable planting locations with modest climate mitigation (Tomback et al., 2022). Seed zones represent a larger geographic scale of adaptation than tree provenances or ecotypes (Bower et al., 2014). Seed zones began in commercial forestry to improve productivity of timber species and have since expanded to include non-commercial tree species (Johnson et al., 2004; Tomback et al., 2022). PIAL seed zones in the northern Rocky Mountains, Inland West, and Pacific Northwest (USFS Region 6; Washington and Oregon) were created by integrating the distribution of genetic variation and local adaptation, resulting in 7 seed zones in the Northern Rocky Mountains and Inland West, and 9 seed zones in Washington and Oregon (Aubry et al., 2008; Mahalovich & Hipkins, 2011). Current recommendations are to identify at least 100 'elite' or 'plus' trees within a seed zone to ensure that seed and pollen have adequate genetic diversity for cold hardiness, growth, phenology, and resistance traits to be outplanted in the same seed zone (or a different seed zone in the future) (Sniezko & Liu, 2022). PIFL has been split into 5 seed zones in the U.S. Interior Mountain West and the southwest U.S. (Borgman et al., 2015). PIAL and PIFL exhibit moderate genetic diversity—especially in growth and phenology traits (Bower & Aitken, 2008)—and show moderate to high heritability for key adaptive traits (Mahalovich et al., 2006) as well as some level of rust resistance (Keane et al., 2017), suggesting that these species may have the capacity to be transferred within seed zones and within seed zones that have similar climates. Given that current seed zone transfer guidelines may need to be updated to reflect more than 'modest' (Tomback et al., 2022) changes in future climates, further research is needed to determine the climatic requirements and adaptive capacity of the families from each seed zone being outplanted prior to transfer. Investigating climatic predictors of seedling establishment, survival, growth, and function can help identify locations for outplanting seedlings.

Common Garden Research

Identifying traits that are controlled by genetic (local, seed source, family) adaptation or by the environment (phenotypic plasticity) helps managers match seedling families and outplanting locations to ensure successful seedling establishment (Howe et al., 2003; Baughman et al., 2019). In the field, we cannot distinguish if traits are phenotypically plastic or genetically driven (de Villemereuil et al., 2016). As a result, common gardens (or common environments) are used to identify whether an individual's phenotype (trait) is a result of genetic adaptation or phenotypic plasticity. Seedlings collected from distinct groups (e.g., families, seed zones, climates, species, rust resistance levels) are grown together under controlled conditions (greenhouse, outdoor). Under a common growing environment, traits that differ between seedling groups are genetically driven. Traits that do not differ among seedling groups may be driven by phenotypic plasticity. In High-5 species, common gardens are used to determine adaptive traits for resistance, cold hardiness, and drought tolerance (Keane et al., 2017; Tomback et al., 2022).

Objective

To guide outplanting strategies for PIAL and PIFL in locations that support successful seedling establishment under current and future climates, we measured 10 phenological and survival traits, 56 growth traits, and 18 NSC traits in <1-year-old greenhouse-grown seedlings in a common garden setup. The seedlings originated from 51 PIAL families spanning a broad latitudinal (32 to 54°N) and longitudinal (–127 to –115°E) range in the U.S. (USFS Region 6) and British Columbia, and 12 PIFL families from northern Alberta. U.S. PIAL families originated from 5 seed zones in WA and 4 seed zones in OR and were categorized into rust resistance levels A–F (with A being most resistant). PIFL included 6 resistant and 6 susceptible families. We asked: Q1) Do PIAL traits relate to seed source climates of origin?, Q2) Do U.S. PIAL traits differ between U.S. seed zones?, Q3) Do U.S. PIAL traits differ between rust resistance levels?, and Q4) Do PIAL and PIFL traits differ between species and rust resistant and susceptible groups?

For Q1 and Q2, we hypothesized that early seedling phenology, survival, and growth traits will reflect seed source climate of origin and be positively related to increasing snow water equivalent (Swe), precipitation, and/or temperature. For NSC traits, we hypothesized that total NSC would be greater in seedlings from warmer climates due to longer growing seasons (Blumstein et al., 2023), while seedlings from colder, drier climates would have higher sugar to starch proportions either through starch breakdown for osmoregulation (Dickman et al., 2015; Sala et al., 2012; Sevanto et al., 2014; Thalmann & Santelia, 2017) or reduced growth leading to

NSC accumulation assuming passive storage (Fajardo et al., 2012; Hoch & Körner, 2012; Kreyling et al., 2014; Lahr & Sala, 2014; Long et al., 2021; Piper et al., 2017). For Q3, we hypothesized that PIAL traits will differ between more rust-resistant and more rust-susceptible seedlings, with higher rust resistance coinciding with traits that support greater stress tolerance (Kinloch et al., 2003; Kinloch Jr., 1992). We hypothesized that more resistant seedlings would exhibit earlier emergence, bud formation, and needle burst and traits conducive to higher cold and drought hardiness (e.g., slower growth rates, higher proportion of sugars to starch, lower total NSC) than more susceptible seedlings (Mahalovich et al., 2006; Sniezko & Liu, 2023; Vogan & Schoettle, 2015). For Q4, we hypothesized that traits of resistant and susceptible groups will differ in the same way for both PIAL and PIFL, with higher rust resistance coinciding with traits that support greater stress tolerance. Similar to PIAL and Q3, we expected that PIFL resistant (PIFL R) will exhibit greater cold and drought hardiness including faster phenological development, more conservative water use strategies (e.g., slower growth rates, greater allocation to roots than shoots) (Ulrich et al., 2023; Vogan & Schoettle, 2015), higher total NSC, higher proportion of sugars to starch, increased root growth, increased root surface area, shorter height, smaller leaf area, and thicker leaves (Dubos & Plomion, 2001; Schoettle et al., 2014). Between species, we hypothesized that PIFL would exhibit both acquisitive (e.g., higher survival to each developmental stage, larger leaf area) and conservative resource use traits (e.g., thicker leaves, higher sugar concentrations for osmoregulation and cryoprotection), contributing to PIFL's ability to inhabit a broader range of environments than PIAL (Hankin et al., 2023; Schoettle et al., 2022; Tomback et al., 2022; Ulrich et al., 2023).

METHODS

Seedling Material

We obtained whitebark pine (*Pinus albicaulis*, PIAL) seed from the Dorena Genetic Resource Center US Forest Service Nursery (Cottage Grove, OR, U.S.). We obtained 36 PIAL families (3,940 seeds total) from 9 seed zones distributed between 5 zones in Washington (WA) (zones 1, 2E, 2W, 3, 4) and 4 zones in Oregon (OR) (zones 5-8) from USFS Region 6 ("U.S. PIAL"; Appx. Table 1, Figure 1). Each seed zone contained seed from 1-3 locations (300-600 seeds per location), with each location containing 3 families (100-200 seeds per family). Each family had rust resistance summary ratings from A-F, where resistance level A indicated 'resistant' (the progeny of that parent tree had the highest level of being symptom free one year post inoculation) while resistance level F indicated 'susceptible' (95% of the progeny of that parent tree had stem symptoms one year post inoculation). A family refers to seedlings grown from seeds of the same parent tree. Seeds were collected in 2001-2016. In addition to U.S. PIAL, we also obtained 15 PIAL families (2,191 seeds total, 40-164 seeds per family) from 5 locations (3 families per location) in British Columbia, Canada (B.C.) from the B.C. Forest Service Provincial Tree Seed Centre (South Surrey, B.C., Canada) ("B.C. PIAL"). Seeds were collected in 2018. Together, U.S. PIAL and B.C. PIAL resulted in 51 total PIAL families (Figure 1).

We obtained 12 limber pine (*Pinus flexilis*, PIFL) families (1,686 seeds) from 4 locations (2-3 families per location) in Alberta, Canada (AB) from the Alberta International Tree and Seed Centre (AITSC) (Smoky Lake, AB, Canada) (Appx. Table 1, Figure 1; "AB PIFL"). 2 rust resistant and 2 rust susceptible families were obtained from location Prairie Bluff (4 total families) and from location Porcupine Hills (4 total families). 2 rust resistant families were obtained from location Highwood. 2 rust susceptible families were obtained from location Sentinel Point. This resulted in 6 total rust resistant families and 6 total rust susceptible families within a 131.83 km distance from each other. Seeds were collected in 2008-2018.

Experimental Design

The 3 groups of seed (U.S. PIAL, B.C. PIAL, AB PIFL) were processed, stratified, and sown using the following protocols (Appx. Tables 2, 3). Seed processing, stratification, and sowing protocols were based on the protocols of Coeur d'Alene US Forest Service Nursery, Dorena Genetic Resource Center US Forest Service Nursery, and the AITSC (Overton, 2016; Robb, 2020). Seed processing, stratification, germination, sowing, and transplanting occurred at Montana State University's (MSU) Plant Growth Center (PGC) (Bozeman, MT, U.S.) from 22 October 2021 to 25 May 2022. U.S. PIAL and AB PIFL were obtained 3 months earlier than B.C. PIAL seed. This resulted in U.S. PIAL and AB PIFL being processed first (batch number 1, B1) while B.C. PIAL was processed second (batch number 2, B2). See timeline for details (Appx. Tables 2, 3). PIAL seed required a 30-day warm stratification prior to a 90-day cold stratification (Overton, 2016). PIFL, on the other hand, did not require warm stratification prior to the cold stratification (Kolotelo, 2001; Robb, 2020). Since PIAL required an additional month of stratification, U.S. PIAL seed was processed a month earlier (22 October 2021) than AB PIFL (22 November 2021) so both groups could undergo a cold stratification at the same time and be sown within the same week. Despite the recommended PIAL cold stratification of 90-days and PIFL's 80-day cold stratification (Robb, 2020), seeds were cold stratified for the same amount of time to ensure that both seed groups could be processed together.

Seed processing took ~72 hours. To process the seed, 25 seeds from each family were placed into 1-8, 10.16 cm x 15.24 cm white nylon mesh bags (Nvzi). A colored zip-tie system connected to the string of the bag was used to indicate species, population, and family numbers. Using an 18.18 L square bucket (API kirk Containers), seeds were soaked in a 1% hydrogen peroxide solution (480 ml water per 240 ml 3% hydrogen peroxide) for 24 hours and then rinsed with cold tap water (~7.2℃). Seeds were then placed back into the bucket and soaked in cool running aerated tap water for 48 hours using an aquarium air pump (Aquarium Air Pump Aerator, Uniclife) (Overton, 2016). Then, mesh bags were gently pressed with a paper towel to remove excess water but not dried completely before each mesh bag was placed inside a Plymor 10.16 cm x 15.24 cm plastic bag (6 Mil industrial duty Zipper re-closable plastic bags, Plymor) to maintain moisture. 12 plastic bags (each containing a mesh bag) were placed in a single layer to fill an entire 45.72 cm x 33.02 cm x 2.54 cm stainless steel baking sheet, increasing the surface area of each seed and preventing mold.

For the warm stratification (PIAL only), the stack of baking sheets (each layered between a wooden board) was placed in a growth chamber (Conviron GR96) at 20.6℃ with no light for 30 days. On a weekly basis, mesh bags were rinsed in cold tap water for 1 minute per mesh bag in a dimly lit space. After rinsing, each mesh bag was sprayed with a 1% hydrogen peroxide solution to prevent mold. Before cold stratification (PIAL and PIFL), each mesh bag was placed in a new clean labeled Plymor plastic bag. For the cold stratification, the stack of baking sheets and wooden boards were then placed into the lab refrigerator set at 2 ℃ for approximately 90 days with no light. Seeds were then rinsed and sprayed on a weekly basis in the same way as described for the warm stratification. Plymor plastic bags were replaced for each family for every month of stratification (3 total times). Each family was then rinsed one last time and surface-dried after stratification was completed. Scarification was not necessary.

To start the germination and sowing process, seeds were removed from the nylon mesh bags and then placed into a clean labeled plastic Ziploc 10.16 cm x 15.24 cm sandwich bag. Plastic bags were again placed in a single layer on baking sheets, which were placed in a growth chamber (Conviron GR96) set at 25℃ during the 18-hour photoperiod (16,146 lux of light intensity) and 18℃ for 6 hours with no light for 4 days. On the fourth day of germination, the number of seedlings that germinated were counted out of the total number of seedlings within each family. Seedlings were considered germinated if the radicle, which emerges at the tip of the seed along the main line that divides the 2 halves of the seedcoat, was as long as the seed (Overton, 2016; Robb, 2020). We recorded if there was a break in the seedcoat in the location where the radicle protrudes (a preliminary step prior to radicle protrusion). Because emergence captures both germination and emergence (e.g., Smithers et al., 2021), all seeds from the same family were sown on the same day regardless of germination status.

Seeds were hand-sown into labeled trays that contained 200 Ray-Leach Cone-tainers™ (SC4R, 1x16.10 cm, 66 ml) (Steuwe & Sons, Tangent, OR) filled with a peat-perlite soil medium (MSU Sunshine Mix #1, Sungro, Agawam, MA, U.S.). The soil medium was mixed with water until the medium was uniformly saturated and then was used to fill the cone-tainers. PIAL and PIFL seedlings were sown (radicle side down to ensure that the radicle would eventually become the root system) to a 3.81 cm depth to replicate the depth that Clark's nutcrackers typically cache the seed (Robb, 2020). Seedlings were then gently sprayed with a garden house until saturated (water dripping out the bottom). After watering, each cone-tainer was sprinkled with a thin layer of chicken grit to help retain moisture, prevent weed growth, and to protect against fungus gnats.

No fertilizer was used.

By late April of 2022, U.S. PIAL and AB PIFL seedlings had become crowded in their trays, some roots had started showing near the bottom of the holes of the cone-tainer, and 90% of all seedlings had emerged (plant tissue visible above the soil) by this point. Therefore, U.S. PIAL seedlings were transplanted on 18 April 2022 and AB PIFL seedlings were transplanted on 13 May 2022 into bigger SC10U Ray Leach Cone-tainers^{TM} (160 ml) that fit 98 cone-tainers per tray. Once transplanting was completed, cone-tainers were watered until saturated and then a thin layer of chicken grit was added to the top of the soil. B.C. PIAL seed was directly sown into SC10U cone-tainers on 19 May 2022.

Seedling maintenance (post-sowing and post-transplanting) included watering seedlings every other day until saturated, refilling with soil and chicken grit if these materials had fallen out during watering, and weeding seedlings weekly. Trays were rotated to different locations on the greenhouse bench every 3 weeks.

The measurement period for U.S. PIAL and AB PIFL was February 2022 to February 2023. The measurement period for B.C. PIAL was May 2022 to May 2023 (Appx. Tables 1, 2). For this 15-month period (February 2022-May 2023), no supplemental lighting was provided. Greenhouse conditions were recorded from June–December 2022 when the average photosynthetically active radiation (PAR) was 145.4873 W/m^2, temperatures averaged 20.7 ℃ during the day and 16.4 ℃ during the night. Maximum temperature was 31.3 ℃ and minimum temperature was 8.7 ℃. Average relative humidity was 55.84%, with a high of 95.2% and a low of 13.4%. Below and in Table 1, we describe all traits measured.

Phenology and Survival

10 of the 84 total traits analyzed were phenology traits. Phenology traits were measured every 5 days from 0-60 days post-sowing (emergence) and then biweekly from 60-365 days (bud formation, needle burst) (Appx. Figure 1). Emergence was defined as the first time any plant tissue was visible above the soil. Bud formation was defined as the bud developing within the center of the seedling at the top of the stem. Needle burst was defined as the needle elongating out of the bud. While seed germination was monitored as the first step in the growth process, data was lost for some families and therefore germination was not analyzed. We analyzed 7 proportion (prop) traits and 3 time-to-event (TTE) traits. Prop traits represented the number of individuals to survive to each of the 3 stages (emergence, bud formation, needle burst) out of the total number of individuals sown for each family. The proportion that survived (regardless of life stage) was recorded during every monitoring period (~weekly). Colored toothpicks were also used to mark the life stage of each seedling. While monitoring continued for a year, proportions had minimal changes past day 203. The number of seedlings that died was also recorded during every monitoring period (~weekly).

The number in the phenology trait name represents the number of days post-sowing (DPS) on which the measurement was made. For prop traits, two DPS were selected for each phenology stage (emergence, bud formation, needle burst) based on time-course proportion plots (Appx. Figure 2). The first DPS had the greatest rate of change (steepest slope) in proportions over time. The second DPS had the flattest slope in the curve, which represented the lowest rate of change in proportions over time (when proportions had plateaued). These points also coincided with the highest and lowest points of variability among families, respectively. PIAL and PIFL proportions were analyzed for the first emergence day on 30 and 21 DPS (prop.emg.30.21), respectively, and for the second emergence day at 55 and 56 DPS (prop.emg.55.56), respectively. PIAL and PIFL proportions were analyzed for the first bud formation day on 30 and 35 DPS (prop.bf.30.35), respectively, and for the second bud formation day on 95 and 119 DPS (prop.bf.95.119), respectively. PIAL and PIFL proportions were analyzed for the first needle burst day on 119 DPS (both species) and for the second needle burst day on 161 and 203 DPS, respectively. PIAL and PIFL were monitored for survival (all seedlings regardless of life stage) at 95 and 91 DPS when proportion traits had plateaued and stopped changing. Seedlings were determined as dead if they had brown or yellow, desiccated tissue or alive if they had green, turgid tissue. TTE traits represented the number of days for each seedling to emergence (TTE.emg), bud formation (TTE.bf), and needle burst (TTE.nb). The number of seeds that did not undergo the full stratification process due to germinating early were removed from analysis (Appx. Table 1). Individuals lost to destructive harvests for other traits were subtracted from the total number of seeds sown for that date onward (Appx. Table 1). If all seedlings from a family had died, they received an NA value from then on. All phenology traits only included non-zero values. One reason for seedling mortality may be due to high summer temperatures in July-August 2022 (B1 = 119-194 DPS, B2 = 45-105 DPS).

Growth

56 of the 84 total traits analyzed were growth traits (28 aboveground, 20 belowground, 8 whole plant traits) measured 4 months (120 DPS; DH1) and 12 months (375 DPS; DH4) post-sowing for research questions Q1-3 and 8 months post-sowing (230 DPS; DH3) and 12 months post-sowing (365 DPS; DH4) for Q4 (Appx. Tables 1, 2). For Q4, DH3 was analyzed instead of DH1 because DH3 had the largest PIFL and PIAL sample size. 16 of the 28 aboveground traits

were leaf traits while the other 12 traits were stem traits. All growth traits were obtained from destructive harvesting (except for stem diameter, seedling height, and their growth rates). For each harvest, 8 seedlings per family were randomly selected. All trait names and descriptions are listed in Table 1.

The destructive harvesting process involved gently removing the seedling from the cone-tainer. Roots were placed into a shallow tray with type 2 deionized (DI) water (stems and leaves were kept dry) and all soil was removed with a small paintbrush. Next, the roots were separated from the stem and leaves. A top-down photo was taken of cotyledons and needles spread out next to a labeled coin envelope for scale to determine leaf area. Roots were spread out and separated into 1st and 2nd order roots (absorptive roots), and 3rd+ order roots (transport roots) (Pregitzer, 2002) using a razor blade. Roots were then scanned (Epson V600), labeled, and organized for subsequent image analysis (Seethepalli et al., 2020). After scanning, the roots were dabbed dry on both sides using a Kimwipe. Leaf, stem, and root fresh biomass were measured. To account for roots being wet during scanning and because seedlings that sat out longer lost more water, a species' specific biomass-time curve was used to quantify the fresh biomass weight that was due to water weight based on how long the seedling had been drying. This curve was obtained by weighing the roots of PIAL family 29 and PIFL family 25 at 2, 4, 8, 16, 32, and 64 minutes post-Kimwipe drying. These families were chosen because they were near the mean latitude of the dataset for their respective species and had enough seedlings to be harvested. The equations for PIAL and PIFL from these curves, respectively, were:

$$PIAL_{ww} = -0.0017x + 0.423,$$

$$PIFL_{ww} = -0.0034x + 0.698,$$

where ww represents water weight (g) and x represents time post-drying (minutes). Ww for each seedling was then removed from its fresh root biomass (FRB; g) to calculate final fresh root biomass (FFRB; g). After fresh tissues were imaged and weighed, leaf, stem, and root tissue samples were microwaved in 6 30-second intervals and oven-dried for 72 hours at 70℃. Then, tissues were weighed for dry biomass. To reduce possible enzymatic activity for non-structural carbohydrate (NSC) trait analysis, each seedling was processed from pot removal to microwaving within 30-45 minutes.

Leaf area was obtained from each image using ImageJ (Schindelin et al., 2012). Leaf area, leaf fresh biomass, and leaf dry biomass were then used to calculate specific leaf area (cm^2/g), leaf mass ratio (g), leaf dry matter content (g), leaf thickness ($(m^2/g)^{-1}$), and leaf mass area (g/m^2) (Table 1). Root scans were analyzed in Rhizovision to obtain total root length (cm), root diameter (mm), root surface area (cm^2), and root volume (cm^3) (Seethepalli et al., 2020). Rhizovision images were analyzed as broken roots at 600 DPI with the threshold level adjusted to maximize clean root borders, limiting noise in the image, and with non-root objects were filtered out at 1 mm sq. These traits in addition to fresh and dry root biomass were used to calculate specific root length (cm/g), root tissue density (g/cm^3), root dry matter content (g), and root mass ratio (g) (Table 1).

8 of the 28 aboveground traits were obtained from non-destructive (ND) measurements made monthly for 5 months (29 May-26 December 2022) on the same 10 randomly selected seedlings per family and included: stem diameter (stem.diameter.97, stem.diameter.160, stem.diameter.221), seedling height (seedling.height.97, seedling.height.160, seedling.height.221), and absolute growth rates (absolute.growth.rate.stem.diameter.221,

absolute.growth.rate.seedling.height.221) in months 3 (97 DPS), 5 (160 DPS), and 7 (221 DPS). These months were selected during this period of intense seedling change ((Dobrowski et al., 2015). Stem diameter was marked and measured from where the stem met the soil. Stem height was measured from the mark to the top of the stem. The stem diameter growth rate on day 221 (stem.diameter.growth.rate.221, SDGR, mm/day) was calculated based on (Borgman et al., 2015) as:

$$SDGR = \frac{\ln(Stem.diameter.221) - \ln(Stem.diameter.97)}{(ND5_{DPS} - ND1_{DPS})}$$

Seedling height growth rate (seedling.height.growth.rate.221, SHGR, cm/day) was calculated using the same equation shown above except for using seedling height instead of stem diameter. If 1 of the 10 selected seedlings per family died, a replacement seedling was randomly selected. We observed no significant differences in stem diameter or seedling height between groups with or without replacement seedlings at both months 3 (97 DPS) and 5 (160 DPS) (Welch's two-sample t-test). Therefore, seedling height and stem diameter included replacement seedlings to increase sample size. Because growth rate calculations were based on changes over time, only seedlings that survived the entire measurement period (no replacement seedlings) were included in growth rate measurements.

Non-structural Carbohydrate (NSC)

18 of the 84 analyzed traits were NSC traits. These included 9 leaf and 9 root NSC traits that were measured on 375 DPS and included: leaf and root glucose, fructose, glucose + fructose, sucrose, starch, total sugar (glucose, fructose, sucrose), total NSC (total sugar, starch), sugar:total NSC, and starch:total NSC (mg of compound/g of tissue dry weight, % dry weight). NSC were

measured on the families that were destructively harvested for growth traits. After fresh tissues were imaged and weighed, leaf, stem, and root tissue samples were microwaved in 6 30-second intervals, oven-dried for 72 hours at 70℃, and ground to a fine powder using an industrial sample processing grinder (Mixer/mill 8000M, SPEX CertiPrep, Metuchen, New Jersey, U.S.). Then, 30 mg of ground tissue was weighed into each 2-mL tube. To obtain enough material, ground material from 8 individual seedlings was pooled into a single tube for each PIAL family (i.e. PIAL NSC traits were pooled at the family level; 8 seedlings per tube, 1 tube per family, 3-9 families per rust resistance group (resistant, intermediate, susceptible), 3-10 families per rust resistance level (A-F)). For PIFL, due to low sample sizes, individuals were pooled in a single tube for the resistant (R) group (i.e. PIFL NSC traits were pooled at the resistance group level; n=5 seedlings per tube, 1-2 seedlings per family, 3 families per tube, 1 tube per resistant group) and a single tube for the susceptible group (n=8 seedlings per tube, 1-3 seedlings per family, 3 families per tube, 1 tube per susceptible group).

Samples were analyzed for NSC concentration using the enzyme method (Landhäusser et al., 2018). Briefly, an ethanol steam extraction released glucose, fructose, and sucrose into solution. Ethanol was then added to the sample and boiled at 90℃ for 10 minutes. After centrifugation, the supernatant was used for sugar quantification and the pellet was used for starch quantification. The supernatant was first used to quantify glucose, where glucose was converted to glucose-6-phosphate through the addition of glucose assay reagent (GHK). The concentration was then measured using a 96-well microplate spectrophotometer (μQuant™, Bio Tek Instruments, Winooski, VT, U.S.) referenced at 340 nm absorption. Sucrose was then converted to free glucose using invertase. This free glucose was converted to glucose-6-

phosphate using GHK. The total sucrose concentration was calculated as the total glucose-6-phosphate from the sucrose reaction minus the total glucose 6-phosphate from the first glucose reaction. Fructose was converted to fructose-6-phosphate using phosphoglucose isomerase (PGI). Fructose-6-phosphate was then converted to glucose-6-phosphate using GHK. The concentration of glucose-6-phosphate from this reaction was then subtracted from the first glucose reaction to determine the concentration of fructose alone. The pellet was dried at room temperature for >6 hours to evaporate residual ethanol. Starch was converted to water-soluble glycans using α-amylase. The glucans were converted to free glucose using amyloglucosidase (AMG). Free glucose was then converted to glucose-6-phosphate using GHK.

Statistical Analyses

All statistical analysis was conducted in R (R Core Team, *V.4.3.2*). We examined the following: Q1) trait-climate relationships in PIAL (U.S., B.C.), Q2) trait differences among PIAL seed zones (U.S.), Q3) trait differences among PIAL rust resistance levels (U.S.), and Q4) trait differences between PIAL (U.S.) and PIFL (AL) rust resistance groups. Q1-3 analyzed DH1 and DH4 timepoints. Q4 analyzed DH3 and DH4 timepoints and NSC were only measured at the DH4 timepoint because PIFL had the greatest sample size at DH4. Formal statistical analyses were conducted on Q1 and Q3 NSC traits but not on Q4 PIFL NSC traits due to low sample sizes (Q2 did not compare NSC traits). For all questions, grouped binomial logistic regression models (hereafter logistic regression models) (*glmmTMB*, *v.1.1.8*, (Brooks et al., 2017) with a binomial family distribution and a logit link function were used to analyze the 7 phenology proportion traits. Linear mixed effects (LME) models (*lme4, v.1.1.35.1*, (Bates et al., 2015) were used to analyze all other traits (3 phenology TTE, 56 growth, 18 NSC traits). Detailed justification for each model can be found in Appx. Section C: Statistical Background. P-values ≤ 0.05 were significant and p-values between 0.05-0.01 were marginally significant. For logistic regression models, p-values were not scale-dependent.

For logistic regression models, the response variable was the phenology proportion trait. For LME models, the response variable was a continuous variable (all other traits). The fixed effects (FE) for both model types were either continuous (Q1, selected climate variable(s)) or categorical (Q2, seed zone (SZ); Q3, rust resistance status (RR.status); Q4, species rust resistance group (SRR)). To focus the analysis on our research questions and due to singularity issues, no interactions were analyzed as FE for any question. Both model types for all questions had a nested random effects (RE) structure for all traits with family nested within location (e.g. location/family) to account for families within locations being more likely to be like each other than to be like families in other locations. U.S. PIAL locations were also nested within seed zones (9 total zones). However, when seed zone was added as part of the nested RE structure (e.g. seed zone/location/family), theta (diagnose function, *glmmTMB v.1.1.8,* (Brooks et al., 2017)) was infinite, indicating that seed zone did not explain the random effect variation because 7 of the 9 seed zones only had 1 location. As a result, seed zone was not included in any RE structure for any question. Weights were used in both model types to correct for unequal sample sizes per family (Appx. Table 1). All growth traits included N=8 (DH measurements) or N=10 (ND measurements) replicates per family. Phenology proportions and NSC traits were collected at the family level (i.e., 1 value per family). Because PIAL NSC traits were pooled at the family level (i.e., 1 value per family) and there was no within-family variation for LME to calculate an effect from, the RE structure for NSC LME models only included location. For Q4, 5 PIFL resistant seedlings and 8 PIFL susceptible seedlings were pooled at the resistance level (i.e., 1 value per resistance group) to obtain PIFL NSC trait means.

Logistic regression model assumptions were checked in the same way for Q1-Q4 and included assumptions of: dispersion (*DHARMa v.0.4.6;* (Hartig, 2015/2025) and Pearson Chi-sq statistic), normality of random effects (*performance v.0.11.0*; (Lüdecke et al., 2021), goodness of fit (*DHARMa v.0.4.6;* (Hartig, 2015/2025) and residuals vs. fitted plots), and influential points (Influence plot, *car v.3.1.2*; (Fox & Weisenberg, 2019). Pearson or deviance residuals >3 were removed. LME model assumptions were checked in the same way for Q1-Q4 and included assumptions of linearity, normality (Shapiro wilks test, QQ-plot), equal variances (res vs. fitted plot for continuous FE, Levene's test for categorical FE), and influential points (Influence plot, *car v.3.1.2*; (Fox & Weisenberg, 2019). Influential observations that had a standardized residual of ≥3 and observations that had cook's distance values >1 were removed. Only LME models used log transformations when necessary to meet assumptions. For LME models, only the original (non-log transformed) estimates were reported in figures regardless of whether a log transformation was used or not for ease of interpretation. For LME models with a continuous FE, all climate variables except for Tmax and VPD improved with a log transformation. For LME models with a categorical FE, 25 of 64 variables improved with a log transformation.

Q1) Trait- Climate Relationships in PIAL (U.S., B.C.)

Climate variables were obtained for each family over a 30-year period (1992-2021) from Oak Ridge National Laboratory (ORNL) Daymet's single pixel extraction tool (Thornton et al., 2022) and included the average daily precipitation (mm/day), incident shortwave radiation (Srad, W/m^2), snow water equivalent (SWE, (kg/m^2)), minimum and maximum surface air temperature

(Tmin, Tmax; °C), and water vapor pressure (VP, hPa). These data are produced on a 1 km x 1 km gridded surface interpolated from 2-m tall weather stations. Daily precipitation was the sum of all forms converted to the water equivalent. The daily total radiation was calculated by multiplying the shortwave radiation flux density by day length divided by 1,000,000 (Thornton et al., 2022). The incident shortwave radiation flux density (W/m^2) was taken as an average over the daylight period of the day. This represented a daily cumulative solar radiation based on day length which was then averaged over the year for the 30 years of climate period. While VP was originally in units of Pa, it was converted to hPa by multiplying by 0.01 and used to calculate cumulative daily VP for each year. The average of daily values was calculated for all other climate variables. All yearly averages were then averaged over the entire 30-year period. Climate variables were highly correlated with one another resulting in high multicollinearity (high VIF values) (*car v.3.1.2*; (Fox & Weisenberg, 2019). Srad and Tmin had correlations above 75% with latitude and VP, respectively. Because latitude is a more practical measure for land managers than Srad, because we had another temperature variable in our analysis (Tmax), and because latitude has been found to correlate with NSC traits (Blumstein et al., 2023), Srad and Tmin were excluded from our analysis.

A post-hoc Dunn's test and a Bonferroni correction (that identified that the extremes of our dataset differed) were used to determine if the 7 climate variables significantly differed between the 17 PIAL (U.S. and B.C.) locations (analyzed using Kruskal Wallis tests (ANOVA normality assumption was not met) (*FSA v.0.9.6*, (Ogle, 2025). These climate variables then were selected using dredge (*MuMIn v.1.47.5*; (Bartoń, 2025)) and then double-checked with manual forward selection. Climate variables were selected if a climate variable improved the null model

AIC by ≥4 AIC (Hankin et al., 2023). If more than 2 climate variables met this criterion, the variable with the greatest AIC improvement was selected. Singularity (*performance v0.11.0;* (Lüdecke et al., 2021) and multicollinearity (*car v.3.1.2;* (Fox & Weisenberg, 2019) were checked with each variable addition. If the added climate variable resulted in a singular fit or high multicollinearity (>5 VIF), the previous model was selected.

The Q1 dataset included all PIAL groups (U.S. and B.C.; 40-200 seeds per family, 51 families, 17 locations; Figure 1. U.S. PIAL included 1-3 locations per U.S. seed zone (12 U.S. locations total) and 4-5 seed zones per state (WA = 5 seed zones, OR = 4 seed zones) spanning 32-48˚N and -123 to -118˚W. B.C. PIAL included 3 families per location (5 B.C. locations total) spanning 51-54˚N and -115 to -127˚W. The selected climate variables were the continuous FE for the logistic regression (phenology proportion (prop) traits) and LME (all other traits) models listed below. For logistic regression for phenology proportion traits, only 1 climate variable was selected (β_0 = intercept (baseline log-odds for the event occurring when climate variable 1 (CV1) is at its mean value due to centering), β_1 = slope (change in log-odds of the event occurring per unit increase in CV1). In the equation below, the following variables are defined as: Y_{jk} = number of seedlings in family *k* within location *j* that survived to the specified life stage (i.e., the observed number of "successes"), TSS_{jk} = total seeds sown for the *kth* family in the *jth* location, $Prob_{jk}$ = model-estimated probability that a seedling in the *kth* family, in the *jth* location survived to the specified life stage, OR = odds ratio, B = fixed effects (climate coefficients), b = random effect intercepts for location (b_j) and family within location (b_{jk}), CV = climate variable, est_{LO} = log-odds estimate, N = number of family observations, alpha = standard deviation of random effects, exp = exponentiated, P_{ijk} = model-estimated probability, Var = variance, $Prop_{ijk}$ = observed proportion of seedlings that survived to the life stage).

Q1 Model 1. Logistic Regression (phenology proportion traits)

$$y_{jk} \sim Binomial\ (TSS_{jk}, Prob_{jk})$$

$$logit(p_{jk}) = \log\left(\frac{Prob_{jk}}{1 - Prob_{jk}}\right) = \beta_0 + \beta_1 CV1_{jk} + b_j + b_{jk}$$

$$OR = \exp\ (est_{LO})\ ;\ Prob_{jk} = \frac{\exp(est_{LO})}{1+\exp\ (est_{LO})}$$

$$b_j \sim N(0, \sigma^2_{location});\ b_{jk} \sim N(0, \sigma^2_{family})$$

$$Var(logit(Prob_{jk})) = \sigma^2_{location} + \sigma^2_{family} + \frac{\pi^2}{3}$$

$$Var(Prop_{ijk} | CV1,\ location, family) = TSS_{jk} * p_{ijk} * (1 - p_{ijk})$$

For the non-proportion traits, LME models were used and 1-4 climate variables were selected (β_0 = intercept (trait value centered at the mean of the first climate variable (CV1) and the second climate variable (CV2)), β_1 and β_2 = slope (change in response trait (RT) for each unit increase of CV1 and CV2, respectively while holding the other CV variables constant for the *ith* observation within the *kth* family in the *jth* location, RT = response trait, N = number of observations, mu = estimated trait mean, sigma = standard deviation of residual error, TSS = total seeds sown per family, β= fixed effect (coefficients), b = random effects for location (b_j) and family within location (b_{jk}), epsilon = residual error of each observation, Var = variance).

Q1 Model 2. Linear Mixed Effects (LME) Model (all other traits)

$$RT_{ijk} \sim N(\mu_{ijk}, \sigma^2)$$

$$\mu_{ijk} = \beta_0 + \beta_1 FE\_CV1_{ijk} + \beta_2 FE\_CV2_{ijk} + b_j + b_{jk} + \epsilon_{ijk}$$

$$b_j \sim N(0, \sigma^2_{location});\ b_{jk} \sim N(0, \sigma^2_{family})$$

$$\epsilon_{ijk} = N(0, \frac{\sigma^2}{TSS_{ijk}})$$

$$Var\left(RT_{ijk} \middle| FE\_CV1, FE\_CV2, Location, Family\right) = \sigma^2_{location} + \sigma^2_{family} + \frac{\sigma^2}{TSS_{ijk}}$$

The centered intercept, estimate with standard error, lower bound estimate, slope, p-value (≤0.05), conditional (FE + RE) R^2 (%; r.squaredGLMM function, *MuMIn v.1.47.5;* (Bartoń, 2025), and sample size (N) were determined for each selected climate variable for each response variable. Intercepts were centered at the mean value of the climate variable in the dataset. For logistic regression, estimates were determined on the log-odds scale and are followed in Results tables by the response (probability) scale estimate. The lower bound estimate of the trait is the trait calculated at the lowest climate variable value in the dataset. Trait-climate relationships were assumed to be linear for ease of interpretation.

Q2) Trait Differences between PIAL Seed Zones (U.S.)

U.S. PIAL included 100-200 seeds per family for 36 families in 12 locations and 9 U.S. seed zones (SZ, USFS region 6; OR, WA) numbered 1, 2E, 2W, … 8, where 2W = Zone 2 West, 2E = Zone 2 East (Figure 1). Each location had 3 families, each seed zone contained 1–3 locations, and each state included 4–5 seed zones (WA = 15 families in 5 locations across 5 seed zones, OR = 21 families in 7 locations across 4 seed zones). Seed zone (SZ) was the categorical FE for logistic regression and LME models (β_0 = intercept (baseline log-odds for the event occurring for the reference level seed zone, zone 1), β_1 = difference in the log-odds of the event occurring between seed zone 1 and the next zone number, zone 2W. In the equation below, the following variables are defined as: y_{jk} = number of seedlings in *kth* family within the *jth* location that survived to the specified life stage (i.e., the observed number of "successes"), TSS_{jk} = total seeds sown for the *kth* family in the *jth* location, $Prob_{jk}$ = model-estimated probability that a seedling in *kth* family in the *jth* location survived to the specified life stage, OR = odds ratio, β = fixed effects (categorical coefficient), b = random effect intercepts for location (b_j) and family within location (b_{jk}), est_{LO} = log-odds estimate, N = number of family observations, alpha = standard deviation of random effects, exp = exponentiated, P_{jk} = model-estimated probability, Var = variance, $Prop_{jk}$ = observed proportion of seedlings that survived to the life stage). Each β_x represented the difference between seed zone 1 and the zone of interest (Harrell, 2015; Ramsey & Schafer, 2013).

<u>Q2 Model 1. Logistic Regression (phenology proportion traits)</u>

$$y_{jk} \sim Binomial\ (TSS_{jk}, Prob_{jk})$$

$$logit(p_{jk}) = \log\left(\frac{Prob_{jk}}{1 - Prob_{jk}}\right)$$
$$= \beta_0 + \beta_1 SZ2W_{jk} + \beta_2 SZ2E_{jk} + \cdots + \beta_8 SZ8_{jk}\ b_j + b_{jk}$$

$$OR = \exp\ (est_{LO})\ ;\ Prob_{jk} = \frac{\exp(est_{LO})}{1+\exp\ (est_{LO})}$$

$$b_j \sim N(0, \sigma^2_{location});\ b_{jk} \sim N(0, \sigma^2_{family})$$

$$Var(logit(Prob_{jk})) = \sigma^2_{location} + \sigma^2_{family} + \frac{\pi^2}{3}$$

$$Var\left(Prop_{jk} \middle| Seed\ zone, location, family\right) = TSS_{jk} * Prob_{jk} * (1 - Prob_{jk})$$

LME models were used to analyze all other traits (β_0 = intercept (trait mean for the reference level seed zone (zone 1)), β_1 = difference in the trait mean between seed zone 1 and the next seed zone, zone 2W, RT = response trait, N = number of observations, mu = estimated trait mean, sigma = standard deviation of residual error, TSS = total seeds sown per family, β= fixed effect (coefficients), b = random effects for location (b_j) and family within location (b_{jk}), epsilon = residual error of each observation, Var = variance). Each β_x represent the difference between seed zone 1 and the zone of interest (Bates et al., 2015; Ramsey & Schafer, 2013). NSC traits were not analyzed due to low sample sizes.

Q2 Model 2. Linear Mixed Effects (LME) Model (all other traits)

$$RT_{ijk} \sim N(\mu_{ijk}, \sigma^2)$$

$$\mu_{ijk} = \beta_0 + \beta_1 SZ2E_{ijk} + \beta_2 SZ2W_{ijk} + \cdots + \beta_2 SZ8_{ijk}\, b_j + b_{jk} + \epsilon_{ijk}$$
$$b_j \sim N(0, \sigma^2_{location});\ b_{jk} \sim N(0, \sigma^2_{family})$$
$$\epsilon_{ijk} = N(0, \frac{\sigma^2}{TSS_{ijk}})$$
$$Var\left(RT_{ijk} \middle| Seed\ Zone, Location, Family\right) = \sigma^2_{location} + \sigma^2_{family} + \frac{\sigma^2}{TSS_{ijk}}$$

The intercept, estimates (on log-odds scale followed by probabilities for logistic regression) for each seed zone with standard errors, p-values (≤0.05), and sample size (N) are reported. To identify if seed zone (FE) significantly affected the response variable, analysis of deviance tests (type 2, *car v3.1.2;* Fox and Weisberg, 2019) were used on the logistic regression and LME models. To determine marginal mean differences between specific seed zones, *post-hoc* linear contrasts (*lme4 v.1.1.35.1*, (Bates et al., 2015); *emmeans, v.1.10.0;* (Lenth et al., 2025) were used.

Q3) Trait Differences between PIAL
Rust Resistance Levels (U.S.)

U.S. PIAL included 100-200 seeds per family for 36 families (same as Q2) across 6 rust resistance levels (RR.status) (Figure 1) from A-F, where A= highest resistance and F = lowest resistance. RR.status was the categorical FE for logistic regression and LME models (β_0 = intercept (baseline log-odds for the event occurring for the reference level RR.status level, level A), β_1 = difference in the log-odds of the event occurring between level A and the next resistance level, level B. In the equation below, the following variables are defined as: Y_{jk} = number of seedlings in *kth* family within the *jth* location that survived to the specified life stage (i.e., the observed number of "successes"), TSS_{jk} = total seeds sown for the *kth* family in the *jth* location, $Prob_{jk}$ = model-estimated probability that a seedling in the *kth* family in the *jth* location survived to the specified life stage, OR = odds ratio, β = fixed effects (categorical coefficient), b = random effect intercepts for location (b_j) and family within location (b_{jk}), est_{LO} = log-odds estimate, N = number of family observations, alpha = standard deviation of random effects, exp = exponentiated, P_{jk} = model-estimated probability, Var = variance, $Prop_{jk}$ = observed proportion of seedlings that survived to the life stage). Each β_x represent the difference between level A and the level of interest.

<u>Q3 Model 1. Logistic Regression (phenology proportion traits)</u>

$$y_{jk} \sim Binomial\left(TSS_{jk}, Prob_{jk}\right)$$

$$logit\left(Prob_{jk}\right) = \log\left(\frac{Prob_{jk}}{1 - Prob_{jk}}\right)$$
$$= \beta_0 + \beta_1 RR.status\_A_{jk} + \beta_2 RR.status\_B_{jk} + \cdots + \beta_5 RR.status\_F_{jk}\ b_j + b_{jk}$$

$$OR = \exp\left(est_{LO}\right) ; Prob_{jk} = \frac{\exp(est_{LO})}{1 + \exp\left(est_{LO}\right)}$$

$$b_j \sim N(0, \sigma^2_{location}); b_{jk} \sim N(0, \sigma^2_{family})$$

$$Var(logit\left(Prob_{jk}\right)) = \sigma^2_{location} + \sigma^2_{family} + \frac{\pi^2}{3}$$

$$Var\left(Prob_{jk} \middle| RR.status,\ location, family\right) = TSS_{jk} * Prob_{jk} * (1 - Prob_{jk})$$

LME models were used to analyze all other traits (β_0 = trait mean for the reference level RR.status level (level A), β_1 = difference in the trait mean between level A and the next level, level B, RT = response trait, N = number of observations, mu = estimated trait mean, sigma =

standard deviation of residual error, TSS = total seeds sown per family, β= fixed effect (coefficients), b = random effects for location (b_j) and family within location (b_{jk}), epsilon = residual error of each observation, Var = variance). Each β_x represent the difference between RR.status level A and the RR.status level of interest.

Q3 Model 2. Linear Mixed Effects (LME) Model (all other traits)

$$RT_{ijk} \sim N(\mu_{ijk}, \sigma^2)$$

$$\mu_{ijk} = \beta_0 + \beta_1 RR.status\_A_{ijk} + \beta_2 RR.status\_B_{ijk} + \cdots + \beta_2 RR.status\_F_{ijk}\ b_j + b_{jk} + \epsilon_{ijk}$$
$$\sim N(0, \sigma^2_{location});\ b_{jk} \sim N(0, \sigma^2_{family})$$
$$\epsilon_{ijk} = N(0, \frac{\sigma^2}{TSS_{ijk}})$$
$$Var(RT_{ijk} | RR.status, Location, Family) = \sigma^2_{location} + \sigma^2_{family} + \frac{\sigma^2}{TSS_{ijk}}$$

The intercept, estimates (on the log-odds scale followed by probabilities for logistic regression) for each RR.status level with standard errors, p-values (≤0.05), and sample size (N) are reported. To identify significant differences between RR.status levels, analysis of deviance tests (type 2, *car v3.1.2;* (Fox & Weisenberg, 2019)) were used. To determine marginal mean differences between specific RR.status levels, *post-hoc* linear contrasts (*lme4 v.1.1.35.1*, (Bates et al., 2015); *emmeans, v.1.10.0* (Lenth et al., 2025)) were used. For NSC traits, each A-F rust resistance level contained 3-10 families (1 NSC value per family).

Q4) Trait Differences between PIAL and
PIFL Rust Resistance Groups (U.S. AL)

Data for Q4 included U.S. PIAL (same as Q2, Q3) and AB PIFL because we had RR.status levels for U.S. PIAL and not for B.C. PIAL. For PIAL, Q3 RR.status levels from A-F (A= highest resistance and F = lowest resistance) were grouped into 3 rust resistance groups:

PIAL R (A-B), PIAL I (C-D), and PIAL S (E-F) (Figure 1). The PIFL data included 100-200 seeds per family for 12 PIFL families from 4 locations (3 families per location) within a 131.83 km distance from each other. 2 rust resistant (R) and two rust susceptible (S) families were obtained from Prairie Bluff (4 total families) and from Porcupine Hills (4 total families). 2 R families were obtained from Highwood, and 2 S families were obtained from Sentinel Point, which were ~2.07 km apart. Together, PIFL R had N=6 R families and PIFL S had N = 6 S families.

We tested for differences in climate between PIFL locations using ANOVA tests on models that tested for differences in latitude or longitude (due to meeting ANOVA assumptions). Kruskal-Wallis tests were performed on all other climate variables. While we observed no significant differences between PIFL locations in latitude, longitude, elevation, precipitation, Srad, Tmin, and Tmax, we observed significant differences in SWE between Porcupine Hills and Prairie Bluff (PH < PB) and in VP between Prairie Bluff and Sentinel Point (PB > SP). PIFL climate variables were obtained from ORNL Daymet.

Species rust resistance (SRR) group (PIFL R, PIFL S, PIAL R, PIAL I, PIAL S) was the categorical FE for logistic regression and LME models (β_0 = intercept (baseline log-odds for the event occurring for the reference level species rust resistance group, PIAL R), β_1 = difference in the log-odds of the event occurring between PIAL R and the next group, PIAL I. In the equation below, the following variables are defined as: Y_{jk} = number of seedlings in the *kth* family within the *jth* location that survived to the specified life stage (i.e., the observed number of "successes"), TSS_{jk} = total seeds sown for the *kth* family in the *jth* location, $Prob_{jk}$ = model-estimated probability that a seedling in the *kth* family in the *jth* location survived to the specified life stage, OR = odds ratio, β = fixed effects (categorical coefficient), b = random effect intercepts for location (b_j) and family within location (b_{jk}), est_{LO} = log-odds estimate, N = number of family observations, alpha = standard deviation of random effects, exp = exponentiated, P_{jk} = model-estimated probability, Var = variance, $Prop_{jk}$ = observed proportion of seedlings that survived to the life stage). Each β_x represent the difference between PIAL R and the group of interest.

<u>Q4. Model 1. Logistic Regression (phenology proportion traits)</u>

$$y_{jk} \sim Binomial\ (TSS_{jk}, Prob_{jk})$$

$$logit(p_{jk}) = \log\left(\frac{Prob_{jk}}{1 - Prob_{jk}}\right)$$
$$= \beta_0 + \beta_1 SSR\_PIAL\_R_{jk} + \beta_2 SSR\_PIAL\_I_{jk} + \cdots + \beta_4 SSR_{PIFLs_{jk}} + b_j + b_{jk}$$

$$OR = \exp\ (est_{LO})\ ;\ Prob_{jk} = \frac{\exp(est_{LO})}{1+\exp\ (est_{LO})}$$

$$b_j \sim N(0, \sigma^2_{location});\ b_{jk} \sim N(0, \sigma^2_{family})$$

$$Var(logit(Prob_{jk})) = \sigma^2_{location} + \sigma^2_{family} + \frac{\pi^2}{3}$$

$$Var(Prob_{jk} | SSR,\ location, family) = TSS_{jk} * Prob_{jk} * (1 - Prob_{jk})$$

LME models were used to analyze all other traits (β_0 = intercept (trait mean for the SRR reference level (PIAL R)), β_1 = difference in the trait mean between PIAL R and the next group, PIAL I, RT = response trait, N = number of observations, mu = estimated trait mean, sigma = standard deviation of residual error, TSS = total seeds sown per family, beta = fixed effect (coefficients), b = random effects for location (b_j) and family within location (b_{jk}), epsilon = residual error of each observation, Var = variance). Each β_x represents the difference between PIAL resistant and the group of interest.

Q4. Model 2. Linear Mixed Effects (LME) Model (all other traits)

$$RT_{ijk} \sim N\left(\mu_{ijk}, \sigma^2\right)$$

$$\mu_{ijk} = \beta_0 + \beta_1 SSR\_PIAL\_R_{ijk} + \beta_2 SSR\_PIAL\_I_{ijk} + \cdots + \beta_2 SSR\_PIFL\_S_{ijk}\, b_j + b_{jk} + \epsilon_{ijk}$$
$$b_j \sim N(0, \sigma^2_{location});\; b_{jk} \sim N(0, \sigma^2_{family})$$
$$\epsilon_{ijk} = N(0, \frac{\sigma^2}{TSS_{ijk}})$$
$$Var\left(RT_{ijk} \middle| SRR, Location, Family\right) = \sigma^2_{location} + \sigma^2_{family} + \frac{\sigma^2}{TSS_{ijk}}$$

Q4 was unique from Q1-Q3 because growth traits were analyzed for DH3 and DH4 timepoints instead of DH1 and DH4 time-points. The reason for this is because PIFL had the highest sample size at the DH3 timepoint. Another unique aspect for Q4 was that NSC traits were not formally analyzed as they were for Q1 and Q3. The reason for this is because PIFL did not have a high enough sample size to analyze at the family level at the DH4 timepoint. Instead, seedlings had to be analyzed at the resistance level. Because of this, NSC trait raw means were compared (instead of estimated means). For PIAL, we homogenized 8 seedlings per family to result in 1 NSC value per family and 3-9 families per SRR group (N of $PIAL_R$ = 9 families, N of $PIAL_I$ = 4 families, N of $PIAL_S$ = 3 families). We had low PIFL survival at timepoint DH4 so this resulted in the PIFL S group containing n=8 seedlings, 1-3 seedlings per family, 3 families per tube, and 1 tube (and NSC value) per susceptible group. The PIFL R group contained n=5 seedlings, 1-2 seedlings per family, 3 families per tube, and 1 tube (and NSC value) per resistant group We analyzed NSC samples in triplicates (replicates of 3) so that we were able to determine standard error of each of those NSC absorbance values to be ±2.36-4.49 for leaves, ±0.33-9.45 for roots and ±2.05-6.43 for leaves, ±4.37-11.17 for roots for PIFL R and PIFL S, respectively from glucose, fructose, sucrose, and starch concentrations.

The intercept, estimates (on the log-odds scale followed by probabilities for logistic regression) for each SRR group with standard errors, p-values (≤0.05), and sample size (N) are reported. To identify significant differences between SRR groups, analysis of deviance tests (type 2, *car v3.1.2;* (Fox & Weisenberg, 2019) were used. To determine marginal mean differences between specific SRR groups, *post-hoc* linear contrasts (*lme4 v.1.1.35.1*, (Bates et al., 2015); *emmeans, v.1.10.0;* (Lenth et al., 2025) were used. Traits that had a significant ($p \leq 0.05$), bolded Anova p-value indicated that at least 2 of the 5 SRR groups differed from each other. A 'complete' species difference occurred when all 3 PIAL groups shared one post-hoc letter, both PIFL groups shared another letter, but no letters were shared between PIAL and PIFL. A 'strong' species difference occurred when only 1 PIAL group and 1 PIFL group shared the same post-hoc letter. While statistical analyses could not be completed on the 5 SRR groups for NSC traits, post-hoc differences that were completed on PIAL NSC traits in Q3 are shown for PIAL raw data means in Q4. Due to PIFL's N=1 value per resistance group, standard error values are not presented for PIFL.

RESULTS

Q1. PIAL Trait-Climate Relationships

We observed significant differences among the 17 PIAL locations in all climate variables except for snow water equivalent (Swe) (Kruskal Wallis test, $p<0.001$, Appx. Table 1). Climate variables improved the null model for 8 of the 10 (80%) phenology traits, 11 of the 28 (39.3%) aboveground growth traits, 9 of the 20 (45%) belowground traits, 2 of the 8 (25%) whole plant traits, and 4 of the 18 (22.2%) NSC traits for a total of 34 out of 84 traits (40.5% of all analyzed traits) having a significant improvement (≥4 AIC) when a climate variable was added to the null model.

Null (random effects only) models for 8 out of the 10 phenology traits significantly improved (≥4 AIC) when a climate variable was added (Table 2). Generally, models of phenology proportion traits improved with the addition of latitude while those of phenology TTE traits improved with the addition of latitude and longitude. Specifically, latitude was the first selected variable to improve model AIC for 7 of the 8 phenology traits and elevation was the first selected variable to improve the model for the eighth phenology trait (prop.bf.30). All 3 phenology TTE (time-to-event) traits had an additional improvement when longitude was added to the model (in addition to latitude). Only 2 traits improved with the addition of elevation (prop.bf.30, TTE.nb)(Figure 2). The proportion of seedlings to survive to each life stage significantly increased with increasing latitude for 4 traits (prop.emg.30, prop.emg.55, prop.bf.95, prop.surv.95)(Figure 2) and decreased with increasing elevation for 1 trait (prop.bf.30). The 3 phenology TTE traits decreased with increasing latitude, indicating that seedlings reached each phenology life stage (emergence, bud formation, needle burst) faster with increasing latitude.

Models for 11 of the 28 aboveground traits significantly improved (≥4 AIC) when a climate variable was added (Table 2). Generally, models of aboveground traits improved with the addition of latitude or longitude as a first or second variable and some traits improved with the addition of elevation, VPD, and precipitation as a second or third variable. Specifically, latitude was the first selected variable to improve model AIC for 4 of the 11 aboveground traits (leaf.mass.area.375, seedling.height.221, fresh.stem.biomass.150, dry.stem.biomass.150). Longitude was the first selected variable to improve model AIC for 7 of the 11 aboveground traits (leaf.area.150, leaf.area.375, specific.leaf.area.150, specific.leaf.area.375, leaf.thickness.375, leaf.mass.area.150, leaf.mass.area.375). 6 of the 11 aboveground traits improved with the addition of both latitude and longitude (leaf.area.375, specific.leaf.area.150, specific.leaf.area.375, leaf.thickness.375, leaf.mass.area.150, leaf.mass.area.375). 3 of the 11 traits improved with the addition of either elevation (leaf.area.150), VP (specific.leaf.area.150), or precipitation (leaf.thickness.150) as a second variable. Only 1 trait significantly improved when precipitation was added as a third variable (leaf.mass.area.150). Though latitude improved model AIC for 10 of the 11 aboveground traits, latitude only had significant (and negative) relationships with 3 traits (seedling.height.221, fresh.stem.biomass.150, dry.stem.biomass.150)(Figure 2). Longitude improved model AIC for 7 of the 11 aboveground traits, but only had a significant, positive relationship with 1 trait (leaf.thickness.150). Precipitation improved model AIC for 2 of the 11 traits and had significant positive relationships with both traits (leaf.thickness.150, leaf.mass.area.150). VP improved the model for 1 trait and had a significant, negative relationship with this trait (specific.leaf.area.150).

Models for 9 of the 20 belowground traits significantly improved (difference ≥4 AIC) when a climate variable was added (Table 2). Generally, belowground traits improved with the addition of latitude or longitude as first and second variables, while some traits measured on day 375 improved with the addition of SWE and Tmax as third and fourth variables. Latitude was the first selected variable to improve the model AIC for 2 of the 9 belowground traits (specific.root.length.150, root.mass.ratio.150). Longitude was the first selected variable to improve model AIC for 6 of the 9 traits (total.root.length.150, total.root.length.375, root.surface.area.150, root.surface.area.375, root.volume.150, root.volume.375). Precipitation was the first selected variable to improve model AIC for 1 of the 9 traits (specific.root.length.375). Latitude and longitude improved the model AIC as first and second variables for 7 of the 9 traits (total.root.length.150, total.root.length.375, root.surface.area.150, root.surface.area.375, root.volume.150, root.volume.375, specific.root.length.150). Longitude and latitude improved the model AIC as second and third selected variables for 1 of the 9 traits (specific.root.length.375) which was in addition to precipitation. SWE improved the model AIC as a third variable for 3 of the 9 traits (total.root.length.375, root.surface.area.375, root.volume.375) which was in addition to latitude and longitude. Tmax improved the model AIC as a fourth variable for 1 trait (root.volume.375) which was in addition to latitude, longitude, and SWE. Latitude improved model AIC for all 9 belowground traits but only had significant (negative and positive, respectively) relationships with 2 traits (root.volume.375, root.mass.ratio.150). Longitude improved model AIC for 8 of the 9 traits but only had a significant, negative relationship with 1 trait (root.surface.area.375). SWE improved model AIC for 3 of the 9 traits and had significant, negative relationships with all 3 traits (total.root.length.375, root.surface.area.375, root.volume.375). Precipitation improved the model AIC for 1 of the 9 traits (specific.root.length.375) and had a significant, negative relationship with this trait.

Models for 2 of the 8 whole plant growth traits significantly improved (difference ≥4 AIC) when a climate variable was added (Table 2). Whole plant traits generally improved with the addition of latitude and longitude as first selected variables. Latitude and longitude were the first selected variables to improve model AIC for root:shoot.ratio.150 (Figure 2) and root:stem+leaves.ratio.150, respectively. Only latitude (not longitude) had a significant positive relationship with root:shoot.ratio.150.

Models for 4 of the 18 NSC traits significantly improved (difference ≥4 AIC) when a climate variable was added (Table 2). Latitude was the first selected variable for 3 significant non-structural carbohydrate (NSC) sugar traits (leaf.suc.375, leaf.total.sugar.375, and root.suc.375) (Figure 2) while longitude was the first selected variable for leaf.starch.375. Latitude had a significant, negative relationship with 2 of these 3 NSC sugar traits (leaf.suc.375, root.suc.375).

Q2. PIAL Seed Zones

The average precipitation (mm/day) among seed zones increased in the following order: 8, 2E, 3, 6, 2W, 7, 5, 1, and 4. The average solar radiation ($MJ/m^2/day$) among seed zones increased in the following order: 3, 2W, 1, 4, 2E, 5, 6, 8, and 7. The average Swe (Kg/m^2) among seed zones increased in the following order: 8, 3, 2W, 2E, 6, 5, 1, 7, and 4. The average Tmax (°C) among seed zones increased in the following order: 4, 2E, 6, 3, 1, 2W, 5, 7, and 8. The average Tmin (°C) among seed zones increased in the following order: 2E, 7, 6, 8, 4, 3, 5, 1, and 2W. The average vapor pressure (VP; hPa) among seed zones increased in the following order: 8, 7, 2E, 6, 4, 2W, 5, 3, and 1.

7 of the 10 phenology traits significantly differed among seed zones (Table 3). These 7 traits included all proportion traits (but no TTE traits). For 5 of these 7 traits (prop.emg.30, prop.emg.55, prop.bf.30, prop.bf.95, prop.surv.95), proportions were the lowest in zone 8 and the highest in zone 5 (prop.emg.30, prop.emg.55, prop.bf.95, prop.surv.95)(Figure 3) or zone 4 (prop.bf.30). These differences observed on the first measurement day (day 30) became more pronounced by the second measurement day (days 55 and 95). For the remaining 2 of the 7

proportion traits (prop.nb.119, prop.nb.161)(Figure 3), zone 3 always had the highest proportion and zones 2E and 7 always had the lowest proportion. For all 7 proportion traits (prop.emg.30, prop.emg.55, prop.bf.30, prop.bf.95, prop.nb.119, prop.nb.161, prop.surv.95), proportions generally increased from zones 1-2E and 7-8 towards zones 3-5.

5 of the 28 aboveground traits significantly differed among seed zones (Table 3). For traits on day 150, leaf.mass.ratio.150 and leaf.thickness.150 were the highest in zone 4 and were lowest in zone 2W. For traits on day 375, specific.leaf.area.375 (Figure 3) was the highest in zone 3 and lowest in zone 1 while leaf.thickness.375 and leaf.mass.area.375 were lowest in zone 3 and highest in zone 1. Leaf thickness was the only trait that significantly differed among seed zones on both days 150 and 375. While aboveground trait differences on day 150 focused primarily on zones 4 (highest) and 2W (lowest), differences on day 375 focused primarily on zones 1 (highest) and 3 (lowest).

9 out of the 20 belowground traits significantly differed among seed zones (Table 3). For 5 of these 9 traits (total.root.length.150, root.diameter.150, root.surface.area.150, root.volume.150, specific.root.length.150), seed zone 8 had the highest value while seed zone 6 had the lowest value. For 1 of these 9 traits (root.tissue.density.150), zone 8 had the lowest value while zone 6 had the highest value. For 6 of these traits on day 150, zone 6 was generally lower (total.root.length.150, root.diameter.150, root.surface.area.150, root.volume.150, specific.root.length.150) or higher (root.tissue.density.150) than zone 2W and zone 3. Zone 6 also had a lower total.root.length.150 than zones 5, 7, and 8, and a lower root.surface.area.150 than zones 7-8, and had a higher root.tissue.density.150 than zone 5. For the other 3 of the 9 traits, root.dry.matter.content.150 was highest in zone 8 and lowest in zone 4,

specific.root.length.375 (Figure 3) was highest in zone 6 and lowest in zone 1, and root.mass.ratio.375 was highest in zone 1 and 2W (tied) and lowest in zones 6 and 7 (tied). Specific root length was also the only root trait that significantly differed among seed zones on both days (150 and 375). While belowground trait differences on day 150 focused primarily on zone 8 (highest) and 6 (lowest), differences on day 375 focused primarily on zones 6 (highest) and 1 (lowest).

Only 1 of the 8 whole plant traits (root:stem+leaves.ratio.150) significantly differed among seed zones. Root:stem+leaves.150 were highest in zone 2W and lowest in zone 4.

Q3. PIAL Rust Resistance Levels

4 out of the 10 phenology traits significantly differed among rust resistance levels (Table 4). Generally, 3 of these 4 traits (prop.bf.30, prop.nb.119, prop.nb.161) decreased with decreasing rust resistance (A to F), while 1 of these traits (TTE.nb)(Figure 4) increased with decreasing rust resistance.

13 out of the 28 aboveground growth traits significantly differed among rust resistance levels (Table 4). The 13 traits showed the following general patterns. 3 of the 13 traits (leaf.dry.matter.content.150, leaf.area.375, leaf.mass.ratio.375) (Figure 4), decreased with decreasing rust resistance (A to F). For 9 of these 13 traits (leaf.thickness.150, leaf.thickness.375, leaf.mass.area.150, leaf.mass.area.375, fresh.leaf.biomass.150, fresh.leaf.biomass.375, dry.leaf.biomass.375, fresh.stem.biomass.375, dry. stem.biomass.375), we observed u-shaped trends with decreasing rust resistance where levels C-D were lower than levels A-B and E-F. For 1 of these 13 traits (specific.leaf.area.375), we observed a hump-shaped trend where levels C-D were greater than levels A-B and E-F.

5 of the 20 belowground traits significantly differed among rust resistance levels (Table 4). Generally, 1 of these 5 traits (root.mass.ratio.375) increased with decreasing rust resistance. For 2 of these traits (root.dry.matter.content.150, specific.root.length.375), we observed hump-shaped trends with decreasing rust resistance where levels C-D were relatively higher than levels A-B and E-F. For 2 of these 5 traits (root.tissue.density.375, dry.root.biomass.375), we observed significant u-shaped trend where levels C-D were relatively lower than levels A-B and E-F.

3 out of the 8 whole plant traits significantly differed among rust resistance levels-(Table 4). Generally, 1 of these 3 traits (root:stem+leaves.375) increased with decreasing rust resistance. For 2 of these 3 traits (total.dry.biomass.375, root:shoot.ratio.375), we observed u-shaped trends with decreasing rust resistance where levels C-D were relatively lower than levels A-B and E-F.

12 of the 18 NSC traits significantly differed among rust resistance groups (resistant = A-B, intermediate = C-D, and susceptible = E-F) (Table 4). Generally, 2 of these 12 traits (leaf.starch.375, leaf.starch:NSC.375), increased with decreasing rust resistance while 1 of these 12 traits (leaf.sugar:NSC.ratio.375)(Figure 4) decreased with decreasing rust resistance. For 7 of these 12 traits (leaf.fru.375, leaf.glu.fru.375, root.fru.375, root.glu.fru.375, root.total.sugar.375, root.total.NSC.375, root.sugar:NSC.ratio.375), we observed hump-shaped trends with decreasing rust resistance where levels C-D were relatively higher than levels A-B and E-F. For 2 traits (root.starch.375, root.starch:NSC.ratio.375), we observed u-shaped trends where levels C-D were relatively lower than levels A-B and E-F.

Q4. PIAL and PIFL Rust Resistance Groups

A) Trait Differences among PIFL R, PIFL S, PIAL R, PIAL I, and PIAL S

To examine trait differences between rust resistance and susceptibility groups within PIFL (limber pine) and between species (PIFL vs. PIAL (whitebark pine)), we compared 5 species resistance groups: PIFL resistant (PIFL R), PIFL susceptible (PIFL S), PIAL resistant (PIAL R), PIAL intermediate (PIAL I), and PIAL susceptible (PIAL S). 38 traits out of the 66 total traits analyzed (excluding NSC traits) significantly differed among the 5 resistance groups (Table 5; Figure 5). These traits included: 8 of the 10 phenology traits (prop.emg.30, prop.emg.55, prop.bf.30, prop.bf.95, prop.nb.119, prop.nb.161, prop.surv.95, TTE.nb), 17 of the 28 aboveground growth traits (leaf.area.245, specific.leaf.area.245, specific.leaf.area.375, leaf.mass.ratio.245, leaf.mass.ratio.375, leaf.dry.matter.content.375, leaf.thickness.245, leaf.mass.area.245, leaf.mass.area.375, fresh.leaf.biomass.245, fresh.leaf.biomass.375, dry.leaf.biomass.245, dry.leaf.biomass.375, stem.diameter.160, stem.diameter.221, fresh.stem.biomass.375, dry.stem.biomass.375), 7 of the 20 belowground growth traits (specific.root.length.375, root.tissue.density.375, root.dry.matter.content.375, fresh.root.biomass.375, dry.root.biomass.375, root.mass.ratio.245, and root.mass.ratio.375), and 6 of the 8 whole plant traits (total.dry.biomass.375, total.fresh.biomass.375, root:shoot.ratio.245, root:shoot.ratio.375, root:stem+leaves.ratio.375, root:stem+leaves.ratio.245). Only the 38 traits that significantly differed between species were considered when defining a 'complete' species difference and a 'strong' species difference. A 'complete' species difference occurred when all 3 PIAL groups shared one post-hoc letter, both PIFL groups shared another letter, but no letters were shared between PIAL and PIFL. A 'strong' species difference occurred when only 1 PIAL group and 1 PIFL group shared the same post-hoc letter.

B) Trait Differences between PIFL R and PIFL S

Only 1 of the 38 traits that significantly differed among the 5 groups (excluding NSC traits) showed a ‘complete’ difference between PIFL R and PIFL S. PIFL S had a higher root.mass.ratio.245 than PIFL R (Table 5; Figure 5). PIFL S had a higher mean than PIFL R for 8 of the 9 leaf NSC traits (leaf.glu.375, leaf.fru.375, leaf.glu.fru.375, leaf.suc.375, leaf.starch.375, leaf.total.sugar.375, leaf.total.NSC.375, leaf.sugar:NSC.375) and a lower mean for 1 of the 9 leaf NSC traits (leaf.sugar.NSC.ratio.375). For 3 of these 8 leaf NSC traits (leaf.suc.375, leaf.total.sugar.375, leaf.total.NSC.375), PIFL S had 2x the concentration of PIFL R. In contrast to the leaf NSC traits, PIFL S had a lower mean than PIFL R for 6 root NSC traits (root.fru.375, root.glu.fru.375, root.suc.375, root.total.sugar.375, root.total.NSC.375, root.sugar:NSC.375), and a higher mean for 3 root NSC traits (root.glu.375, root.starch.375, root.starch:NSC.375).

C) Trait Differences between Species (PIFL, PIAL)

Only 2 of the 38 traits that significantly differed between species (excluding NSC traits) showed ‘complete’ species differences (leaf.mass.ratio.375, root:stem+leaves.ratio.375 (Figure 5) and 6 of the 30 traits showed ‘strong’ species differences (prop.emg.30, prop.emg.55, prop.nb.119.119, TTE.nb, leaf.mass.ratio.245, root:stem+leaves.245) (Table 5; Figure 5). For complete species differences, leaf.mass.ratio.375 was higher in PIFL than in PIAL while root:stem+leaves.ratio.375 was higher in PIAL than in PIFL. For strong species differences, all 3 PIAL groups were higher than PIFL S groups for 2 traits (prop.emg.30, prop.emg.55) while PIAL R and PIAL intermediate (PIAL I) were higher than both PIFL groups for the one trait (prop.nb.119.119) but were lower than both PIFL groups for another trait (TTE.nb)(Figure 5). Both PIFL groups had a higher leaf.mass.ratio.245 than PIAL I and PIAL S and all 3 PIAL groups had a higher root:stem+leaves.ratio.245 than PIFL R.

Although formal statistical comparisons were not conducted on NSC traits, 6 of the 18 NSC trait means exhibited patterns consistent with a ‘complete’ species difference (leaf.suc.375, leaf.total.sugar.375, leaf.sugar:NSC.ratio.375, root.glu.375, root.glu.fru.375, leaf.starch:NSC.ratio.375) and 4 of the 18 exhibited patterns consistent with a ‘strong’ species difference (leaf.glu.375, leaf.fru.375, leaf.glu.fru.375, leaf.starch.375). Generally, PIFL had higher NSC concentrations than PIAL. Specifically, for 5 of the 6 traits that showed complete species differences (leaf.suc.375, leaf.total.sugar.375, leaf.sugar:NSC.ratio.375, root.glu.375, root.glu.fru.375), PIFL was higher than PIAL. For 3 of these 5 traits (leaf.suc.375, leaf.total.sugar.375, leaf.total.NSC.375), PIFL S was ~twice as large as the concentration of all 3 PIAL groups. In contrast, 1 of these 6 NSC traits (leaf.starch:NSC.ratio.375) was higher in PIAL than PIFL. For the 4 traits that showed a ‘strong’ species difference, PIAL I and PIAL S were higher than both PIFL groups for 3 traits (leaf.glu.375, leaf.fru.375, leaf.glu.fru.375) while all 3 PIAL groups were higher than PIFL R for one trait (leaf.starch.375). These 4 NSC traits (leaf.glu.375, leaf.fru.375, leaf.glu.fru.375, leaf.starch.375) were also ~2x higher in all 3 PIAL groups than in PIFL R.

D) Comparing PIAL and PIFL Within-Species Differences between R and S

We did not detect significant differences in phenology and growth traits between within-species R and S groups that were the same direction in both species (e.g., R < S in both PIAL and PIFL)(Table 5). However, we detected significant trait differences between R and S groups that differed between species where PIAL differed between R and S groups while PIFL R and S groups did not. For phenology traits, PIAL R was greater than PIAL S for prop.nb.119.119 and prop.nb.161.203 and PIAL R was lower than PIAL S for TTE.nb (Figure 5), while PIFL R and S groups did not differ for these three traits. For growth traits, PIAL R was greater than PIAL S for leaf.mass.ratio.375 (Figure 5), leaf.thickness.245, and specific.root.length.375, while PIFL R and S groups did not differ. PIAL R was lower than PIAL S for specific.leaf.area.245, leaf.dry.matter.content.375, dry.leaf.biomass.375, fresh.stem.biomass.375, dry.stem.biomass.375, root.mass.ratio.375, dry.root.biomass.375, total.dry.biomass.375, root:shoot.ratio.375, and root:stem+leaves.ratio.375(Figure 5), while PIFL R and S groups did not differ. In contrast to PIAL, only root.mass.ratio.245 differed between PIFL R and S where PIFL R had lower root.mass.ratio.245 than PIFL S (Figure 5). Considering only the NSC traits that showed within-PIAL differences, PIAL R and PIFL R had lower leaf.starch.375 and leaf.starch:NSC.375 and higher leaf.sugar:NSC.375 than PIAL S and PIFL S, respectively

DISCUSSION

Q1. PIAL Trait-Climate Relationships

We hypothesized that PIAL early seedling phenology, survival, and growth traits will reflect seed source climate of origin and be positively related to increasing water availability and/or temperature. Somewhat consistent with our hypothesis, latitude (followed by longitude) was commonly the first selected climate variable for all traits, indicating its importance as the top predictor of the variation in our measured traits. Latitude was selected the most out of all climate variables and improved the null models for 7 of the 8 phenology traits, 10 of the 11 aboveground traits, 9 of the 9 belowground traits, 1 of the 2 whole plant traits, and 3 of the 4 NSC traits, showing that latitude improved the null model for 30 of the 34 traits (88% of all traits). Out of these 30 traits, latitude was selected as the first climate variable for 16 traits (53%). Latitude significantly related to 15 of the 30 traits that selected latitude.

Although previous studies have observed significant effects of temperature, elevation, and water availability on PIAL seedling traits (Bower & Aitken, 2008; Hamlin et al., 2011; Hankin et al., 2023; Hankin & Bisbing, 2021; McLane & Aitken, 2012), latitude negatively correlated with Srad ($r = -0.88$; this high correlation resulted in Srad not being included in model selection), Tmax (maximum temperature ˚C) ($r = -0.71$) and elevation (m) ($r = -0.65$) in our study, indicating that latitude may serve as a proxy for Srad (Ruddiman, 2013), Tmax, and elevation, and that families from higher latitudes were found at lower elevations and at locations with shorter daily photoperiods and annual growing seasons, and colder temperatures. In contrast, water-related variables, including precipitation, SWE, and VP (vapor pressure), did not significantly relate to latitude in our dataset. Considering that PIAL is a snow-dependent species

(Tomback et al., 2011) and the important role of snow for PIAL regeneration (Hankin et al., 2023; Hankin & Bisbing, 2021; Lett & Dorrepaal, 2018; Pansing & Tomback, 2019), it may not be surprising that SWE of our PIAL seed source climates of origin did not significantly relate to latitude.

Notably, seed source latitude was positively related to prop.emg.30, prop.emg.55, prop.bf.95, and prop.surv.95 and negatively related to all three phenology time-to-event (TTE) traits (TTE.emg, TTE.bf, TTE.nb), indicating that seedling survival to each stage was higher and that seedlings reached each stage faster at more northern latitudes. The prop traits' models also only improved with latitude, indicating that latitude was the primary predictor for early seedling establishment. This latitudinal increase in rate to each phenological stage became more pronounced across life stages: seedlings emerged 2.36 (±0.94) days sooner, reached bud formation 2.98 (±1.04) days sooner, and reached needle burst 12.65 (±3.22) days sooner with each degree increase in latitude. Colder temperatures found at higher latitudes with shorter days and growing seasons requires that seedlings maximize the short growing season by initiating each life stage immediately upon adequate growing conditions, and have greater cold tolerance (Bower & Aitken, 2008; Keane et al., 2017; McLane & Aitken, 2012). In a broader common garden study spanning a large latitudinal gradient of 48 PIAL populations from the western U.S. to western Canada, Bower and Aitken (2008) found that seedlings from populations originating from colder climates had less overall growth, earlier needle flush in the spring, and less cold injury in the fall than seedlings originating from milder climates. Moreover, needle flush and cold injury were strongly associated with latitude, temperature, and the frost-free period. At high-elevation environments, the rate of snowmelt can determine the growing season length and survival (Hagedorn et al. 2014). Lower maximum temperatures and shorter days can also increase snowpack retention, prolong soil moisture availability, and promote gradual seedling transition into the next life stage by insulating seedlings from extreme temperatures, wind, and ice abrasion (Hagedorn et al., 2014; Hankin & Bisbing, 2021). Colder temperatures at higher latitudes may also promote the necessary temperatures for seed stratification (Bower & Aitken, 2008; McLane & Aitken, 2012). Although heavy snowpack can delay germination and emergence by covering seedlings in snow and preventing seeds from obtaining sunlight (McLane & Aitken, 2012), not enough snow can prevent germination and emergence and can leave recently emerged seedlings in extremely hot, dry soils (Brodersen et al., 2019).

Latitude was also negatively related to 3 of the 4 aboveground growth traits that improved when latitude was added to the model (lower seedling.height.221, fresh.stem.biomass.150, dry stem.biomass.150), indicating that seedlings originating from higher latitudes were shorter and smaller than those originating from lower latitudes. Consistently, other studies have found that more cold-tolerant seedlings tend to be shorter which may be due to the trade-off between cold tolerance and growth with strong selection influencing the length of active growth (Monson et al., 2022). Cold temperatures can inhibit photosynthesis and cell growth (Hoch & Körner, 2009) and increase seedling mortality through mechanisms such as photoinhibition and freeze-thaw-induced xylem embolism (Moyes et al., 2015). A rust resistance screening study of PIAL seedlings from the U.S. interior mountain west found that seedling height decreased with increased cold hardiness (Mahalovich et al., 2006). In a second study that aimed to test the capacity of PIAL to germinate, establish, survive, and grow north of its current range, (McLane & Aitken, 2012) planted seeds from 7 populations in 8 locations spanning from

600 km southeast to 800 km northwest of the northern boundary of PIAL's species' range. In addition to having increased germination, establishment, and survival capacity, growth and height also decreased for populations from colder provenances. In a common garden study spanning a broad latitudinal gradient of 48 PIAL families, higher latitude seedlings were shorter than lower latitude seedlings (Bower & Aitken, 2008). A previous common garden study on USFS Region 6 PIAL seed zones found that seedling height also decreased with elevation in seed zone 6, which coincided with colder temperatures (Hamlin et al. 2011). Under colder temperatures, shorter seedling height can reduce low temperature photoinhibition by reducing convective heat dissipation from foliage (Germino & Smith, 1999). A shorter growing season and cold temperatures may also limit the amount of time available for stem growth (Moyes et al., 2015).

Consistent with our observed shorter aboveground stems in higher latitude seedlings, we also observed that belowground biomass allocation traits (root.mass.ratio.150, root:shoot.ratio.150) positively related to latitude, indicating that seedlings originating from higher latitudes allocated more biomass belowground to roots than aboveground tissue. Increased root biomass allocation can limit water loss by reducing the amount of aboveground tissue through which water can be lost and limit the risk of frost-induced xylem cavitation or plant collapse through aboveground exposure to wind and snow. Increased root biomass allocation also is a strategy to increase water and nutrient uptake, increase structural support especially in rocky, poorly developed soils at alpine treeline, and serve as a location for NSC storage to support over-wintering and insulate roots from frost damage (Brunner et al., 2015; Comas et al., 2013; Poorter et al., 2009). Consistently, seedlings of PIFL, Englemann spruce, and lodgepole pine in heated plots had lower root mass and shorter roots (Kueppers et al. 2017, Lazarus et al. 2018). Additionally, greater investment in roots has been linked to enhanced drought resistance and seedling survival in drought-prone ecosystems. A common garden study found that PIFL seedlings from drier seed sources had a higher root:shoot ratio (Hankin et al., 2023). Hankin et al. (2023) reported a similar root:shoot ratio (~2 (g) for 3-month old greenhouse grown PIAL) to that observed in our study (root:stem+leaves.ratio.375 was 2.06 g/g for our lowest latitude family). In a latitudinal study in the Southern Rockies, PIFL seedlings from drier, colder regions had a higher root:shoot ratio 2 months post-germination and a higher root length 4 months post-germination than seedlings from the warmer, wetter regions (Borgman et al., 2015). Another study on recently germinated *Pinus ponderosa* Douglas ex C. Lawson seedlings from dry and mesic climates in the Oregon Cascade mountains found that seedlings from the drier climate allocated more resources towards larger root systems in the first year of growth to prioritize drought tolerance (Kerr et al., 2015).

Latitude was negatively related to leaf and root sucrose non-structural carbohydrate (NSC) traits (leaf.suc.375, root.suc.375; marginally significant negative relationship with total leaf sugar), indicating that leaf and root sucrose concentrations were lower in seedlings originating from higher latitudes. Given that higher latitudes are associated with shorter days and growing seasons and colder temperatures, leaf sucrose may have declined with increasing seed source latitude due to shorter growing seasons, smaller plants, and slower growth rates (Blumstein et al., 2023). This is only partially consistent with our hypothesis because we would have expected to see the same trend in total NSC. NSC are primarily soluble sugars (sucrose, fructose, glucose) and starch that can be allocated to transport, energy metabolism, osmoregulation, reproduction, and stress resistance (Hartmann & Trumbore, 2016). Starch is a compact, insoluble long-term storage molecule, while soluble sugars provide immediate energy, function in signaling and osmoregulation, and support metabolic demands (Blumstein et al., 2023; Martínez-Vilalta et al., 2016). Sucrose is a disaccharide that can be hydrolyzed to smaller carbohydrates, and it is the most common transport sugar in plants (Hartmann & Trumbore, 2016).

NSC reserves buffer plants against freezing, cold, and drought stress by supplying energy or acting as osmoprotectants. Studies have shown that NSC levels increase with latitude and elevation in pine species, likely as an adaptation to cold and drought stress (Fajardo et al., 2012; Hoch & Körner, 2012; Kreyling et al., 2014; Lahr & Sala, 2014; Long et al., 2021; Piper et al., 2017), and with increasing cold and drought stress (Dickman et al., 2015; Sala et al., 2012; Sevanto et al., 2014). Soluble sugars may accumulate in colder environments for cryoprotection or due to reduced growth or sink activity (Körner, 2003). As a result, we had also hypothesized that the proportion of total NSC that are sugars will increase in seedlings from colder climates. However, given we sampled NSC in a common garden setup across families at the same temperature, it appeared that genetic adaptation to higher latitude including shorter growing season (i.e. lower sucrose) may have outweighed the increase in sugars with increasing temperature. Moreover, increases in sugar proportions typically increase seasonally and relative to dormant season concentrations. However, we used annual rather than seasonal climate data so we did not determine how seasonal climates influence NSC traits. Blumstein et al. (2022) found that sugars increased with decreasing temperature at the time of sampling (growing or dormant seasons) and decreased with decreasing climate of origin temperature (Blumstein et al., 2023).

Also, we may have observed leaf and root sucrose decreasing with latitude because sucrose could be depleted due to conversion to compounds not measured in this study (e.g., lipids) since glucose, fructose, and starch did not exhibit a relationship with latitude.

Taken together, while temperature can provide insight on fine-scale processes and microsites, latitude may be a useful variable and first step for selecting seed sources and outplanting locations because latitude may serve as a proxy for Srad, Tmax, and elevation, and can describe broad climatic trends in addition to other factors like topography, plant distributions, and gene flow. Latitude is also easier to obtain than other climate variables and can be useful when other climate data is not available. In addition, seed zones are created from broad-scale genetic differentiation and local adaptation (Borgman et al., 2015) which often span large latitudinal and longitudinal gradients. Latitude and growing season length have also been identified as a climatic predictor of WPBR infection where WPBR infection is greatest near 49-50˚latitude but decreases north and south of this point (Burns et al., 2023; Shepherd et al., 2025; Thoma et al., 2019). Studies have used temperature and latitude as guidelines for outplanting PIAL seedlings (Bower & Aitken, 2008). For B.C., Canada, Bower and Aitken, 2008 proposed moving seed from cone collection sites to planting sites that differ by up to 1.9℃ (4.6˚ latitude or 505 km) in mean temperature of the coldest month. In the Rocky Mountain region in the U.S., the climatic transfer maximum was reduced to 1.0℃ (320 km). To enhance survival, climate mitigation strategies include planting genetically diverse seedlings in moist microsites within their range, favoring cooler slopes, northern aspects at low latitudes, and higher elevations near snow retention or watershed areas (Keane et al., 2022; Schoettle et al., 2022; Tomback et al., 2022). Using these current outplanting practices in conjunction with latitude may be helpful for identifying outplanting locations.

Q2. PIAL Seed Zones

We observed significant variation among seed zones in 7 of 10 (70%) phenology traits, 5 of 28 (17.9%) aboveground growth traits, 9 of 20 (45%) belowground growth traits, and 1 of 8 (12.5%) whole plant growth traits. Of the traits that significantly differed among seed zones, seed zones 3 and 5 consistently stood out in several traits that promoted a resource acquisitive life history strategy (Brunner et al., 2015; Ulrich et al., 2023; Wright et al., 2004). Zone 4 also stood out but had traits that promoted a more conservative life history strategy. These results generally supported our hypothesis that seed zone traits reflect climate of origin, discussed below.

Seed zones 3, 4, and 5 had the highest proportion of seedlings that survived to each phenological stage. Zone 5 had the first (prop.emg.30, prop.emg.55, prop.bf.95, prop.surv.95), second (prop.bf.30, prop.nb.161) and third highest (prop.nb.119) phenology proportions. Zone 3 had the first (prop.nb.119,prop.nb.161), second (prop.emg.30, prop.bf.95, prop.surv.95), and third highest (prop.emg.55, prop.bf.30) proportions. Zone 4 had the second (prop.bf.30), third (prop.emg.30, prop.nb.119, prop.nb.161), and fourth highest (prop.emg.55) proportions. Notably, zone 3 had a 2-3x higher proportion of seedlings survive to needle burst than all other zones. Interestingly, zones 3-4 have stood out in other studies for having high survivorship and zone 3 for needle burst (Hamlin et al., 2011) making them promising zones for future studies and outplanting. Specifically, the families from Warm Springs and Mt. Hood from seed zone 5 consistently had the highest proportion of seedlings for each of the seven proportion traits (prop.emg.30, prop.emg.55, prop.bf.35, prop.bf.95, prop.nb.119, prop.nb.161, and prop.surv.95). In addition, families from Colville (seed zone 3) had the first to second highest proportions for prop.nb.119 and prop.nb.161.

Compared to the other seed zones, zones 3 and 5 had relatively high specific.leaf.area.375 and low leaf.thickness.150, leaf.thickness.375, and leaf.mass.area.375. These traits indicate that seedlings in these zones produced large, thin leaves with a greater surface area per unit mass, a characteristic often associated with fast-growing species in resource-rich environments (Reich, 2014). Zone 3 also had a high leaf.mass.ratio.150, suggesting greater aboveground investment in leaf tissue. While not statistically significant, both zones also had the highest estimates for leaf.area.150, which may further reflect greater photosynthetic allocation or leaf expansion. These leaf traits promote efficient light capture and photosynthesis, supporting early seedling growth (Poorter et al., 2009). In contrast, zone 4 exhibited a low specific.leaf.area.150 and high leaf.mass.ratio.150 and leaf.thickness.150, indicating thicker leaves and a more conservative investment strategy. Although not statistically different, zone 4 also had the second-highest leaf thickness estimate on day 375. Thicker leaves can reduce water loss, increase cold tolerance, and protect against photoinhibition through enhanced structural and optical properties (Lusk et al., 2018; Niinemets, 2016), and may boost photosynthesis under high light by increasing chloroplast layering (W. Liu et al., 2020). Together, these findings suggest that fast, photosynthetically efficient leaf growth (zones 3 and 5) and durable, stress-tolerant leaves (zone 4) may support survival to early phenological stages through divergent strategies.

Zones 3 and 5 expressed belowground traits associated with a resource-acquisitive strategy (Wright et al., 2004, p. 200), including higher total.root.length.150, root.surface.area.150, root.volume.150, specific.root.length.150, and lower root.tissue.density.150. These traits reflect thin, extensive, loosely packed root systems with greater absorptive capacity (Comas et al., 2013; Zhang et al., 2024). Zone 5 additionally showed high root water content, indicated by low root.dry.matter.content.150, which may be advantageous in warm, moist environments by allowing for short-lived, inexpensive roots that capitalize on transient water pulses and store water internally. These characteristics align with a high-foraging resource-acquisitive approach, in contrast to reliance on mycorrhizal outsourcing (Zhang et al., 2024). In contrast, zone 4 had shorter (lower total.root.length.150), more localized (lower root.volume.150), densely packed (higher root.tissue.density.150) roots, and high root water content (low root.dry.matter.content.150). These traits support a stress-tolerant, more conservative resource use strategy that emphasizes mechanical support, cold protection, and internal water storage over rapid uptake (Brunner et al., 2015). In cold, rocky soils with shorter growing seasons, such root systems may confer an advantage by increasing resilience to frost and mechanical stress. These contrasting root strategies—extensive absorptive high-foraging systems in zones 3 and 5, and dense, conservative systems in zone 4—demonstrate how different root architectures can promote seedling survival.

Traits supporting either resource-acquisitive (zones 3 and 5) or resource-conservative (zone 4) strategies appear to reflect the distinct climates of these seed zones and likely contributed to high early seedling survivorship (emergence, budburst, needle formation, survival). In zone 3, moderate temperatures, low precipitation, high vapor pressure, and low Srad may have promoted traits that support rapid early-season leaf expansion, high photosynthetic efficiency, and fine root systems optimized for nutrient and water uptake. Zone 5, characterized by warm temperatures, high precipitation, and moderate to high Srad, fostered the development of large, thin leaves, fast phenological transitions, and extensive root systems—traits aligned with rapid growth in moist, energy-rich environments, supporting high survival to each phenological stage. In contrast, zone 4's colder, wetter, and snowier climate—with high Srad and VP—resulted in conservative traits such as thick leaves and dense, localized roots that may enhance cold tolerance and structural protection yet still supported strong emergence and bud formation. Together, these patterns suggest that zones 3–5 may represent a climatic Sweet spot for seedling establishment, where intermediate elevations, moderate temperatures, and high atmospheric moisture promote survival through either acquisitive or conservative strategies depending on local conditions.

In contrast to zones 3–5, seedlings in zones 1 and 2W had low to intermediate survivorship but developed thick, dense leaves characterized by higher leaf thickness (leaf.thickness.375), higher leaf mass per area (leaf.mass.area.375), and lower specific leaf area (specific.leaf.area.375), particularly evident on day 375. While both zones 1 and 4 had thick leaves, zone 4 experienced greater Srad than zone 1. This suggests that Srad may be a key climatic factor influencing functional trait expression underlying seedling survival. Seedlings from zones 1 and 2W also developed denser root systems with higher root tissue density (root.tissue.density.150) and lower root volume (root.volume.150), reflecting more localized root structures, suggesting that high-foraging roots in early stages of life may be critical for survival to early developmental stages.

In addition to climate other factors may play a role in our observed variation in early survivorship and growth traits. The highest WPBR resistance (indicated by low early stem infection) is found in seed zones 3, 4, and 5 from the Cascade Mountains of Oregon and Washington, while the lowest rust resistance is found in seed zones 1, 2E, 6, and 8 from eastern Oregon, the Interior West, California, and British Columbia (Sniezko et al., 2018; Sniezko & Liu, 2023). Consistently, inoculation trials showed that PIAL seedlings from seed zones 3–5 exhibited the highest levels of resistance, with zone 3 having the greatest proportion of resistant (A) families (>40% of seedlings cankered) followed by zones 4 and then 5 (Sniezko & Liu, 2022). In contrast, zones 1, 2E, 6, and 8 had the highest proportions of susceptible (F) families, with many showing disease symptoms (>95–100% of seedlings cankered). Rust resistance frequency in the field aligns with our results, with zones 3-5 having both the highest natural rust resistance frequency and the highest survivorship to each life stage in our study. From our dataset, seed zones with the highest proportion of resistant (A) families (listed highest to lowest resistance) were zones 4, 7, 5, and 3 and seed zones with the highest proportion of susceptible (F) families were 8, 2W, 2E, 1 (highest to lowest resistance). Therefore, survivorship in zones 3-5 could be associated with rust resistance. While future research is needed to confidently identify what may have caused the geographic trends we observed in early seedling survivorship (e.g., climate, rust resistance, WPBR incidence, gene flow, glacial movement), there seems to be consistent patterns in our study and others (Hamlin et al., 2011; Sniezko & Liu, 2023) that zones 3-5 may be the sweet spot for early seedling PIAL survivorship and rust resistance.

Q3. PIAL Rust Resistance Levels

We observed support for our hypothesis that more resistant seedlings would exhibit faster phenological timing and traits conducive to higher cold and drought hardiness such as higher sugar concentrations. We unexpectedly observed that more resistant seedlings exhibited larger leaves and less allocation belowground. The proportions of seedlings that survived to bud formation and needle burst (prop.bf.30, prop.nb.119, prop.nb.161) were highest for seedlings with high rust resistance and generally declined with decreasing rust resistance (A to F). Consistently, the time to needle burst (TTE.nb) increased with decreasing rust resistance with levels A-D reaching needle burst ~15 days earlier than levels E-F. Together, these results indicate that more rust resistant seedlings reached and survived to these critical stages sooner than less resistant seedlings. Bud formation initiates the growing season and needle burst (commonly called budburst) is when seedlings first obtain true leaves, marking the stage where plants fully rely on photosynthesis (not seed reserves) for autotrophic functioning (Martínez-Berdeja et al., 2019). Species vary in their thermal and moisture thresholds for bud formation and needle burst, with temperature, photoperiod, and water availability determining the timing of these developmental transitions (Basler & Körner, 2012; D. M. Johnson et al., 2011; Martínez-Berdeja et al., 2019).

Exhibiting earlier and more successful bud formation and needle burst may indicate increased cold hardiness to tolerate early season cold temperatures (Martínez-Berdeja et al., 2019). In a broad-scale regional study among northern (British Columbia, Canada), Rocky Mountains (Montana, Wyoming), and southern (Oregon and California) regions, Bower and Aitken (2008) found that PIAL seedlings from colder, drier climates exhibited earlier budburst and greater cold hardiness, while those from milder provenances delayed growth cessation but were more vulnerable to cold injury (Bower & Aitken, 2008). Similarly, Hamlin et al. (2011) found distinct differences in PIAL phenology among seed zones in Washington and Oregon, U.S. (USFS Region 6). Zone 6 in the Blue Mountains (central east Oregon) initiated and completed growth earliest—likely due to its high elevation and cold temperatures—while Cascadian seed zones 4, 5, and 7 had later growth initiation (Hamlin et al., 2011). Consistently, higher rust resistance has been observed in colder locations. In the interior mountain west, PIAL rust resistance was higher in the colder, wetter northwest than the warmer, drier southeast (Mahalovich et al., 2006). In sugar pine, the R gene, *Cr1,* occurs at a much greater frequency above 1700 m in the Sierra Nevada, and when used in a transplant study, these provenances displayed substantial cold hardiness (Kinloch Jr., 1992). The highest frequency of *Cr2* in western white pine also is found in high elevations of the southern Sierra Nevada and correlates with increased cold hardiness (Kinloch et al., 2003). Earlier needle burst also may allow resistant individuals to complete early seedling life stages before the late spring when WPBR aeciospores are present (Thoma et al., 2019).

Higher cold resistance coinciding with increasing rust resistance may occur because Pathogenesis Related family 10 (PR-10) genes that are induced for rust resistance likely increase cold and drought tolerance (Zamani et al., 2003). R genes have leucine-rich repeats (LCCs) which have antifreeze capabilities (Ekramoddoullah & Liu, 2008), and the overexpression of the PR10 gene has been shown to trigger the upregulation of cold-responsive genes (Liu et al., 2013). In a common garden experiment, Vogan and Schoettle (2015) found that after cold hardening, 3-year-old resistant PIFL families had greater cold hardiness than those without the R gene (Vogan & Schoettle, 2015). In a study that overexpressed a PR10 protein from western white pine in *Arabidopsis thaliana*, seedlings had improved survival under cold stress, maintained higher chlorophyll content, and exhibited stronger membrane stability under cold stress (measured as reduced electrolyte leakage). In contrast, Mahalovich et al. (2006) found no statistically significant difference in cold hardiness between rust resistant and susceptible PIAL in the US intermountain west (Mahalovich et al., 2006). In addition to cold tolerance, pathogen resistance likely has some cross-over with drought tolerance possibly due to PR proteins observed to increase in response to drought in pines (Dubos & Plomion, 2001). The upregulation of PR proteins increases chitinase and glucanase concentrations, which increase cell wall stability and subsequently drought and salinity tolerance (J.-J. Liu et al., 2013; Zamani et al., 2003). In addition to higher cold hardiness, resistant PIFL seedlings had lower stomatal conductance than susceptible families during moderate drought, which may protect from xylem embolism (Vogan & Schoettle, 2015). R families may be anatomically inclined to maintain lower stomatal conductance through smaller stomatal pore size. Smaller pore size also may serve as a smaller entry point for fungal hyphae as suggested by the finding that western white pine had both lower WPBR-induced needle lesion frequency and smaller stomatal size than susceptible families (Woo et al., 2001).

Consistent with earlier and more successful phenology indicating possible higher cold tolerance, seedlings with higher rust resistance had greater biomass allocation to tough, large leaves (higher leaf.area.375, leaf.dry.matter.content.150, leaf.mass.ratio.375) and lower allocation to belowground biomass (root.mass.ratio.375, root:stem+leaves.ratio.375) than more susceptible seedlings. Resistant seedlings' greater allocation aboveground increases resource (light, CO_2) acquisition through larger leaves and may increase tolerance to stressors such as cold through higher leaf dry matter content. Higher leaf dry matter content increases structural biomass (cellulose, lignin) compared to water saturated biomass, resulting in thicker, stronger, expensive, and long-lived cell walls that increase cell wall stability (Poorter et al., 2009; Wright et al., 2004), resistance to mechanical stress such as wind or snow cover, and cold tolerance (Markesteijn et al. 2011). Consistently, Mahalovich et al. (2006) found that more resistant PIAL seedlings were taller than susceptible seedlings and Vogan and Schoettle (2016) observed greater A_{sat} (maximum rate of photosynthesis when exposed to saturating light levels) in resistant PIFL families compared to susceptible families (Mahalovich & Hipkins, 2011; Vogan & Schoettle, 2016).

With decreasing rust resistance (A-F), starch and the proportion of total NSC to starch (leaf.starch.375, leaf.starch:NSC.375) increased and the proportion of total NSC to sugars (leaf.sugar:NSC.ratio.375) decreased, indicating that leaves of more resistant seedlings had lower starch and higher sugar concentrations than susceptible seedlings. Starch is an osmotically inactive molecule for C storage and can be converted to other forms, such as sucrose, fructose, and glucose, for transport, energy growth, metabolism, reproduction, and stress resistance (Hartmann & Trumbore, 2016). Conversion from starch to sugars can decrease osmotic potentials to maintain cell turgor during drought and serve as a cryoprotectant by lowering the freezing temperature of water and stabilizing cell walls (Thalmann & Santelia, 2017). Conifer species sampled in colder temperatures increased the proportion of sugars relative to total NSC, likely due to the need for cryoprotective compounds (Blumstein et al., 2023; Fajardo et al., 2012; Hoch & Körner, 2012). Additionally, soluble sugars increased in boreal and temperate forest species originating from higher latitudes (Kreyling et al., 2014) and elevation (Long et al., 2021), and in response to experimentally induced cold shock (Hoermiller et al., 2017). Leaf starch also was observed to decrease during cold stress coinciding with increased sugar accumulation in common crops and model plant species (Thalmann & Santelia, 2017). Maintaining a higher proportion of sugars may support PR10 proteins in increasing cold tolerance. The higher soluble sugar concentrations observed in resistant seedlings may reflect a proactive or constitutive strategy that enhances tolerance to environmental stress. While it is clear there is a correlation between rust resistance and abiotic stress tolerance, more research is required to understand how these mechanisms interact.

While we observed several traits increasing or decreasing with decreasing rust resistance, most of our traits exhibited u-shaped and hump-shaped trends with decreasing resistance where the intermediate rust resistance levels (C-D) had higher or lower values than the most resistant (A-B) and least resistant (E-F) groups. In general, intermediate seedlings had low overall biomass, small thin leaves, thin, low-volume root system, and high leaf and root fructose, and overall high root sugar concentrations. We may have observed these non-linear patterns because PIAL resistance is quantitative and controlled by multiple genes, which challenges our understanding of how PIAL's rust resistance interacts with other traits. Our observed strong trait differences among all rust resistance levels highlights the value of maintaining genetic diversity in outplanting and management efforts (Mahalovich & Hipkins, 2011). For example, the intermediate resistance group may express traits that are more advantageous than those of the other resistance groups under certain conditions. Therefore, we recommend more research on the full range of rust resistance levels to improve our understanding and management and conservation efforts.

Q4. PIAL and PIFL Rust Resistance Groups

To examine trait differences between PIFL (limber pine) rust resistance groups (R (resistant), S (susceptible)) and between species (PIFL, PIAL (whitebark pine)), we compared 5 species resistance groups: PIFL resistant (PIFL R), PIFL susceptible (PIFL S), PIAL resistant (PIAL R), PIAL intermediate (PIAL I), and PIAL susceptible (PIAL S). 38 of 64 (59.4%) of the analyzed traits (excluding NSC trait means) significantly differed among the 5 groups (8 of the 10 (80%) phenology traits, 17 of the 28 (60.7%) of the aboveground growth traits, 7 of the 20 (35%) of the belowground growth traits, and 6 of the 8 (75%) whole plant traits). For these 38 traits, we discuss within-species R and S differences within PIFL, species differences between PIAL and PIFL, and species differences in within-species R and S differences between PIAL and PIFL.

PIFL S Allocated More Biomass Belowground than PIFL R

Unexpectedly, only 1 of the 38 traits significantly differed between PIFL R and PIFL S, which is consistent with other studies that observed few significant differences between PIFL R and S in seedling (2 months to 2 years old) growth (height, annual shoot growth rate) and leaf-level gas exchange (net photosynthesis, stomatal conductance, respiration, leaf N, CO2 compensation point) between PIFL R and PIFL S (Schoettle et al., 2014; Vogan & Schoettle, 2016). PIFL R had significantly lower root.mass.ratio.245 than PIFL S, indicating that PIFL R allocated relatively less biomass belowground to its root system and presumably more biomass aboveground (although not significantly). This pattern was consistent with our observation that resistant PIAL seedlings allocated relatively less biomass to roots and more biomass aboveground than susceptible seedlings (Q3), but unexpected based on our hypothesis that R groups will exhibit more stress tolerant traits that S groups (e.g., more belowground root growth). Consistent with our observations, PIFL R has been observed to have greater maximum light-saturated photosynthetic rate (Asat) than PIFL S (Vogan & Schoettle, 2016), suggesting that PIFL R has greater photosynthetic capacity that can support rapid growth for successful establishment (Reinhardt et al., 2015). One-year-old PIFL R seedlings also have been observed to have higher cold tolerance and drought resistance (more sensitive stomatal control than PIFL S where stomata closed sooner during moderate drought) (Vogan & Schoettle, 2015). We observed that PIFL R had lower total NSC, sugars, and starch in leaves and higher total NSC and sugars in roots than PIFL S, suggesting that more NSC were allocated to leaf growth than leaf NSC, and to root NSC than root growth. PIFL R may rely on stored NSC reserves in roots during drought and/or cold stress-induced reductions in gas exchange (Brunner et al., 2015; Comas et al., 2013). Both leaves and roots of PIFL R had higher sugar proportions than PIFL S. Given that sugars typically accumulate during environmental stress (Nägele et al., 2022), a higher proportion of sugars in PIFL R may support higher cold and drought resistance through cryoprotection and osmoregulation to maintain turgor and function, as well as increase water and nutrient uptake. Specifically, PIFL R had greater root fructose and root sucrose than PIFL S. Fructose may help lower water potential, protect against oxidative damage, maintain membrane integrity, and stabilize proteins (Nägele et al., 2022). Compared to glucose, which is the primary sugar used in metabolic processes, fructose has greater osmotic pressure because it is smaller and more soluble (Hartmann & Trumbore, 2016; Nägele et al., 2022). Moreover, glucose may be utilized sooner than fructose in metabolic activities, allowing fructose to accumulate in higher quantities. Sucrose is primarily used in transport from source to sink and plays a role in gene signaling (Hartmann & Trumbore, 2016).

PIFL had Lower Survival and Allocated More Biomass Aboveground and Less Biomass Belowground than PIAL

Compared to PIAL, we found that PIFL had greater aboveground biomass allocation, lower belowground biomass allocation, a lower proportion of seedlings surviving to emergence and needle burst, later needle burst timing, greater leaf sugars, and lower leaf starch, providing support for our hypothesis that PIFL may exhibit both resource acquisitive and conservative traits promoting a generalist strategy. In previous comparisons of the two morphologically and ecologically similar species, PIAL and PIFL have been viewed as specialist and generalist species, respectively (Hankin et al., 2023; Reich, 2014; Ulrich et al., 2023). Specialist species like PIAL inhabit a narrower range of environments and display traits on either the acquisitive ("fast") or conservative ("slow") extremes of the resource use continuum (Reich, 2014; Ulrich et al., 2023; Wright et al., 2004). In contrast, generalist species like PIFL inhabit a broader range of environments and display both acquisitive and conservative resource use traits (Sanaphre-Villanueva et al., 2017; Ulrich et al., 2023). However, to our knowledge, only one other study to our knowledge (Hankin et al., 2023) has compared phenology, morphology, and physiological traits between 1-year old PIAL and PIFL with no studies comparing 1-year old PIAL and PIFL seedling NSC. In support of our hypothesis, allocating more biomass aboveground to photosynthetic tissue and less belowground to roots may indicate both acquisitive and conservative resource use, supporting PIFL's generalist strategy. For example, higher aboveground biomass allocation supports faster growth rates and establishment, which can increase PIFL's competitive ability (Smithers et al., 2018). Consistently, previous studies have found that PIFL had greater aboveground biomass allocation (root:shoot ratio), higher SLA, greater leaf area, and faster growth rates than PIAL (Hankin et al., 2023; Ulrich et al., 2023). In a greenhouse common garden study that compared the physiological and morphological traits of 5-

year old PIAL and PIFL juveniles, Ulrich et al. (2023) observed PIFL having increased needle biomass and a reduced sunlit leaf area to total leaf area ratio, which can increase PIFL's high-light tolerance and prevent low temperature photoinhibition by reducing convective heat dissipation foliage (Germino & Smith, 1999). Our first-year germinant PIFL seedlings' higher aboveground biomass ratios may support and predispose PIFL to have continued aboveground biomass allocation after establishment through 5 years old, where PIFL was observed to have thicker and shorter stems, which increase PIFL's mechanical resistance to wind and snow cover (Gerrish, 1990; Read & Stokes, 2006; Ulrich et al., 2023). While not statistically significant, but consistent with Ulrich et al. (2023), PIFL generally had larger leaf area and shorter seedling height.

It was surprising that PIFL generally had a lower proportion of seedlings survive to emergence and needle burst, considering the infamously low germination and emergence rates that PIAL is known for, possibly due to PIAL's requirement for an additional warm stratification period, a longer cold stratification period, and greater moisture to break seed dormancy (Overton, 2016; Pansing & Tomback, 2019). In contrast to our findings, in a fully reciprocal common garden study that examined early seedling (<1-year-old) traits from 2 PIAL populations and 4 PIFL populations from the Great Basin, U.S., Hankin et al. (2023) found that PIFL had higher proportions of seedlings survive to emergence and PIFL reached emergence faster than PIAL (Hankin et al., 2023). Consistently, 5-year-old PIFL had earlier needle burst than PIAL (Ulrich et al., 2023). Hankin et al. (2023) hypothesized this high emergence was part of a "live fast, die young" strategy where PIFL invests heavily in early seedling survival and rapid growth but may have a lower chance of long-term survival (Hankin et al., 2023; Smithers et al., 2021). Ulrich et al. (2023) hypothesized the earlier needle burst to be part of a drought avoidance strategy and being active early season when soil moisture is available (Letts et al., 2009).

Several factors may influence why we observed later phenology and lower survival in PIFL compared to PIAL, in contrast to Hankin et al. (2023) and Ulrich et al. (2023). First, both studies compared PIAL and PIFL from similar latitudes and elevations and used PIFL populations from lower latitudes and higher elevations (45-48˚N, 1646-2225 m for Ulrich et al. 2023, 36-41˚N, 2788-3195 m for Hankin et al. 2023). In our study, we compared 4 PIFL populations from Alberta, Canada (49-50˚N, 1450-1804 m) and 36 PIAL families (42-48˚N, 1359-2405 m) which includes a wider latitudinal and elevational range. PIAL seedlings from colder climates and higher elevations initiated budburst and completed growth earlier than those from milder climates and lower elevations, respectively (Bower & Aitken, 2008; Hamlin et al., 2011). Therefore, it is possible that PIFL had delayed needle burst because our PIFL seedlings originated from lower elevations that also are relatively dry and warm. Additionally, low PIFL seedling survival to each life stage could be representative of Alberta PIFL seedlings, which may differ from other PIFL populations. Notably, Ulrich et al. (2023) also measured 5-year-old juveniles that are larger and likely have different requirements than first-year-germinant seedlings in our study. PIFL's low survival also may be related to seed quality. While our BC PIAL seed had an "A" class vitality rating implying that the seeds had healthy, large reserves, we had no vitality ratings for U.S. PIAL or PIFL seed. PIFL seed was noted to have a possible vitality rating of ~30% if it was poor seed or ~50-70% if it was high quality seed (personal communication). Therefore, we may have had lower quality seed. PIFL's lower survival also may be due to our seed processing. We stratified our seed for 88 days when current practices recommend 80 days (Robb, 2020), and PIFL had a higher proportion of early germinants.

PIFL had Higher Leaf NSC Concentrations than PIAL

Although formal statistical comparisons were not conducted on NSC traits, we observed that 1-year-old PIFL had higher leaf total soluble sugars, total NSC, and sugar proportion primarily due to high sucrose concentrations (PIFL had twice as much leaf sucrose, total sugar, and total NSC as PIAL) while PIAL had higher leaf glucose, fructose, starch, and starch proportion (PIAL had twice as much glucose, fructose, and starch as PIFL). We observed no differences in root NSC between species. Higher concentrations of leaf sucrose, and therefore total sugars and total NSC in 1-year-old seedlings may contribute to PIFL's ability to inhabit a broader range of elevations including warmer, lower-elevation environments than PIAL (Ulrich et al., 2023), providing support for our hypothesis. PIFL may maintain higher sucrose and total sugars (from starch conversion) for long-distance transport of C and water as sucrose is the most chemically stable non-reducing sugar compared to glucose and fructose (Taiz et al., 2014). Sucrose is also used for rapid stress response including osmoprotection and cryoprotection under drought and cold stress, and stress signaling (Hartmann & Trumbore, 2016; Thalmann & Santelia, 2017). PIFL's increased sucrose and decreased glucose and fructose could indicate that glucose and fructose had been used for metabolism or for synthesis of sucrose (Taiz et al., 2014). Soluble sugars have been observed to accumulate in colder or drier environments for stress resistance (Dickman et al., 2015; Sala et al., 2012; Sevanto et al., 2014) or due to reduced sink (growth) activity due to cold or drought (Hoch & Körner, 2009; Woodruff et al., 2015). Many studies have shown that total starch levels increase with latitude and elevation, likely as an adaptation to cold and drought stress (Fajardo et al., 2012; Hoch & Körner, 2012; Kreyling et al., 2014; Lahr & Sala, 2014; Long et al., 2021; Piper et al., 2017). Additionally, higher total NSC has been linked to greater growth capacity and aboveground biomass (Blumstein et al., 2023), which aligns with our observed increased aboveground biomass allocation in PIFL seedlings, though we observed no complete or strong difference in total dry and wet biomass between species in our study.

In contrast to PIFL, PIAL appears to store more C as starch, which may indicate slower mobilization or conversion to sugars, reflecting a more conservative strategy that prioritizes long-term storage over short-term responsiveness, consistent with our hypothesis. Starch is an osmotically inactive, primary C reserve that plays a key role in plant responses to environmental stress, where higher starch concentrations have been linked to greater long-term survival (O'Brien et al., 2014; Woodruff et al., 2015) and leaf starch decreased with abiotic stress especially during cold or high salinity stress (Thalmann & Santelia, 2017). PIAL also had higher glucose and fructose (and lower sucrose and total soluble sugars and total NSC) than PIFL. Glucose, the primary substrate for cellular respiration, energy metabolism, biosynthesis, and hormone signaling, and fructose contributes to energy supply, osmoregulation, and the synthesis of amino acids and cell wall component (Taiz et al., 2014). Although starch and sugars have distinct functions, they are part of a dynamic pool, constantly interconverted based on developmental stage and environmental cues, highlighting the importance of measuring multiple and total NSC components rather than individual components in isolation.

To our knowledge, no studies have compared first-year germinant seedling NSC between PIAL and PIFL. Our NSC values were low (leaf starch: 0.48-0.60 mg/g for PIAL, 0.19-0.52

mg/g for PIFL; leaf sugars: 2.11-2.5 mg/g for PIAL, 2.65-4.79 mg/g for PIFL) but within range of NSC values measured in PIAL and PIFL. Reinhardt et al. (2015) measured NSC in 60 day-post-emergence PIFL seedlings in the field and measured 7.2% dry mass of soluble leaf sugars and 3.5% dry mass leaf starch (Reinhardt et al., 2015). Ulrich et al. (2023) found that 5-year-old PIFL juveniles had a lower concentration and proportion of glucose (0.14 mg/g dry weight, 0.75) and higher concentration and proportion of starch (no concentration reported but 0.25% proportion) than PIAL (Ulrich et al., 2023). Consistently, we observed that PIFL had lower leaf glucose than PIAL. However, in contrast, we found that PIFL had a higher proportion of sucrose rather than starch compared to PIAL. Several factors may contribute to these contrasting findings. First, 1-year-old PIFL seedlings are more sensitive to environmental stress and accumulate sucrose more rapidly than 5-year-old juveniles. Second, 1-year-old seedlings prioritize C allocation to rapid growth for successful establishment over stress tolerance and starch stores (Reinhardt et al., 2015). Third, juveniles are larger with higher capacity to store NSC than 1-year-old seedlings. Fourth, we had a small sample size for our PIFL NSC samples (n=5-8 seedlings per tube, 1 tube per resistance level) and we compared PIAL and PIFL from different latitudes and longitudes.

<u>Traits in R and S Differed within PIAL but not PIFL</u>

We observed 16 growth and phenology trait differences between R and S groups for PIAL but only one trait difference between R and S groups for PIFL (root.mass.ratio.245), where PIFL R had lower root.mass.ratio.245 than PIFL S. This pattern was observed on day 375 for PIAL (but not day 245). Our results suggested that in first year-germinant seedlings of PIAL, rust resistance may be associated with earlier and more successful phenology, greater biomass allocation to tough, large leaves and lower allocation to belowground biomass. PIFL only had lower belowground biomass allocation, suggesting PIFL resistance may be decoupled from most of our measured growth and phenology traits. In other studies, PIFL R and S have been found to not differ in growth traits and instead to rely on physiological differences (not measured in this study) to promote resistance and survival (Vogan & Schoettle, 2015, 2016). Our observed multiple PIAL and few PIFL within-species trait differences between R and S groups may occur due to differences between PIAL's quantitative resistance (polygenic, controlled by multiple genes) and PIFL's qualitative resistance (controlled by a single gene). Having a polygenic basis for resistance may increase the variation in traits and stress response because resistance depends on the suite of genes each seedling has, while a single gene may have fewer cascading impacts on traits. Additionally, WPBR has been more prominent in PIAL populations for a longer time than PIFL populations (Schoettle et al., 2022), which could result in PIAL R having a more developed response to WPBR, increasing the number of other traits affected by rust resistance level.

In contrast to growth and phenology traits, PIAL R and PIFL R had lower leaf.starch.375 and leaf.starch:NSC.375 and higher leaf.sugar:NSC.375 than PIAL S and PIFL S, respectively. This consistent pattern across both species may indicate a stronger relationship between rust resistance and increased investment in soluble sugars, which are more readily mobilized for stress response, osmotic regulation, and metabolic needs. In contrast, higher starch allocation in susceptible seedlings may reflect a higher priority towards storage and recovery after stress, potentially at the cost of short-term rapid responsiveness to environmental stress.

Limitations

This study had several limitations. For Q1, we used annual climate variables that provided information about broad-scale trends but did not provide finer-scale climatic insight like growing or dormant season climate variables. This may have contributed to low R^2 values (0.06-1.89%) for all traits (except for phenology proportion traits, 33.35-37.98%). Additionally, it was challenging to find a more extensive list of climate variables that included data for both the U.S. and Canada. For Q2, DH1 and DH4 harvest dates had different sample sizes, affecting how well DH1 (150 DPS) measurements related to DH4 (375 DPS) measurements. The DH1 harvest was more representative of the entire US Region 6 (OR, WA), with 25 families of 8 seedlings each while DH4 had 17 families with 4-8 seedlings each. We had selected DH4 to relate traits to NSC traits which were only obtained on day 375. However, we only had 1-2 families sampled per zone (N=1 value per family) for NSC at day 375 which prevented us from statistically analyzing NSC traits among seed zones.

For Q3, we measured traits under ambient, non-stressed conditions. However, physiological differences between R and S families may be more evident under stress or WPBR inoculation (Vogan & Schoettle, 2016). Additionally, we had a small sample size for rust resistance levels E-F. For A-F levels, our sample sizes were 9, 7, 6, 6, 3, and 4 families, respectively, resulting in 16 resistant (A-B) families, 12 intermediate (C-D) families, and 7 susceptible (E-F) families. This also resulted in declining harvested sample sizes from A-F. For example, on day 150 (DH1), this included 6, 6, 4, 4, 2, and 2 families for levels A-F, respectively. For day 375 (DH4), this included 6, 4, 2, 2, 2 families and 1 family for levels A-F, respectively. Also we did not have all A-F levels represented for each seed zone so that our results may not be representative of all seed zones.

For Q4, we compared PIFL and PIFL from different locations with different climates. Specifically, the 4 PIFL populations from Alberta, Canada (49-50˚N, 1450-1804 m) had a higher latitude, lower elevation, and smaller elevational range than the 36 US PIAL families (42-48˚N, 1359-2405 m), which could have influenced trait differences between species. Also, we had a smaller PIFL sample size than PIAL which may have occurred due to low quality seed although seed quality information was not available. PIFL seed was noted to have a possible vitality rating of ~30% if it was poor seed or ~50-70% if it was high quality seed (personal communication).

Methodologically, first, the study had some inconsistency in cold stratification timing across seedling groups. Due to logistical constraints, U.S. PIAL was sown first, resulting in PIFL and B.C. PIAL undergoing longer cold stratification periods. Ideally, PIFL would have been sown first, as it requires the shortest stratification period among the three groups. PIFL seeds were stratified for 88 days, slightly longer than the 80 days recommended in current protocols (Robb, 2020). Moreover, the high proportion of early germinants in PIFL may indicate that our stratification temperature (set at 2 °C) was too high, despite aligning with published recommendations. Second, we were unable to stagger sowing based on germination timing due to time and resource constraints so that seeds were planted simultaneously regardless of germination status. While we assume that seedlings that emerged had already germinated (Smithers et al., 2021), this approach may have negatively affected families with more sensitive or delayed germination cues. Additionally, because sowing and transplanting occurred over multiple weeks, there was some variation in the number of days post-sowing among seedlings, depending on how quickly they were processed. Staggered sowing also resulted in B.C. PIAL being planted in May while U.S. PIAL and AB PIFL were sown in February. However, early sowing (February–March) is standard practice for PIAL and PIFL at facilities such as the Dorena Genetic Resource Center (Overton, 2016), which reduces concern that this timing was inappropriate.

Statistically, our study had several limitations. First, we had low statistical power for analyzing phenology proportion traits, primarily due to the lack of replication at the family level. Ideally, we would have sown an equal number of seeds per family and organized them into multiple replicate blocks (e.g., 20 seedlings per block) to improve model robustness and allow for testing interaction effects. Second, traits were measured at varying hierarchical levels, which complicated analysis. PIAL phenology time-to-event (TTE) traits were measured at the seed level (based on all seeds sown), whereas growth traits were recorded at the individual seedling level (eight seedlings per family), and phenology proportion and NSC traits were analyzed at the family level (one value per family). This inconsistency limited our ability to integrate all traits into a unified analytical framework (e.g., correlation matrix) because they were not always measured comparable scales of replication. Third, PIFL traits were measured at the rust resistance group level (PIFL R = 5 seedlings; PIFL S = 8 seedlings) due to low survival by day 375, while PIAL traits were measured at the family level (8 seedlings per family). As a result, this precluded formal statistical comparisons between species beyond descriptive statistics, limiting our scope of inference when interpreting NSC trait differences between species.

More broadly, while the common greenhouse experimental design allows for trait comparisons under controlled settings, it does not represent field conditions with variation in soil, microclimate, or mycorrhizal associations, limiting our study's scope of inference to controlled conditions. For example, soil-filled cone-tainers offer a different environment than field soil, which may have affected the expression of our measured traits. Finally, while this study captured key phenological, growth, and NSC traits, incorporating additional physiological measurements would have provided a more comprehensive understanding of species responses to environmental change.

Future studies should incorporate PIAL's lower latitudinal families (e.g. Great Basin) in addition to PIAL's northern range limit. Studies on <1-year-old seedlings should measure physiology like gas exchange, high-light tolerance, A-Ci curves, and stomatal and hydraulic traits to improve our understanding of how families differ among climates and resistance levels, and with other species like PIFL. In addition to incorporating a higher family sample size, monitoring these traits on the same families into the juvenile stage could improve our understanding of how these traits change with age and inform seedling selection to improve outplanting success. Future studies could also induce cold drought, and/or WPBR inoculation treatments to elucidate the relationship between growth, rust resistance and NSC. Lastly, since there is a predicted probability of ~30% of the most resistant PIAL families surviving in high infection sites (Sniezko & Liu, 2023), outplanting locations should ideally have low future WPBR infection (Schoettle et al., 2022) and be in areas where surrounding trees are also resistant to propagate more resistant seedlings (Sniezko & Liu, 2023). Therefore, future outplanting research should focus on incorporating current and future geographic distributions of WPBR infection and climate when selecting seedlings and identifying outplanting locations.

Conclusions

For Q1, we observed support for our hypothesis that traits reflect seed source climate of origin. Specifically, we observed that latitude was the most important trait predictor, improving model fit for 88% of the 34 traits tested, and serving as the first-selected variable in >half of them. Seedlings originating from higher latitudes exhibited adaptations to colder and shorter days and growing seasons including higher survival to each phenological stage, reaching each stage faster, shorter height, allocating more biomass belowground to roots than aboveground tissue, and having lower leaf and root sucrose concentrations than those originating from lower latitudes. Our results suggest that latitude may serve as a practical first step in selecting seed sources and outplanting sites, especially when climate data are limited. Additionally, our results highlight the management value of both latitude-based transfer guidelines for outplanting and local adaptation especially because seed zones span large geographic regions and multiple latitudes.

For Q2, while our hypothesis that our measured traits would reflect seed zone climate was largely supported, we observed that seed zones 3, 4, and 5 had the highest proportion of seedlings that survived to each phenological stage, which unexpectedly appeared to be due to divergent resource use strategies. Seed zones 3 and 5 consistently had traits that promoted a resource acquisitive life history strategy, while zone 4 had traits that promoted a conservative resource use strategy. Seed zones 3 and 5 had large, thin leaves and thin, extensive, loosely packed, highly absorptive root systems, characteristics of fast-growing species in resource-rich environments such as warm, moist climates. In contrast, zone 4 exhibited a resource conservative strategy, characterized by thicker leaves and dense, localized roots to tolerate stress in cold, snowy environments. Notably, zones 3–5 also had the highest frequency of rust-resistant families in both inoculation trials and field samples, suggesting that climate and resistance may jointly influence geographic patterns in seedling success. These zones may therefore represent a “sweet spot" for outplanting, employing either acquisitive or conservative trait combinations to promote survival under varying environmental pressures.

For Q3, our hypothesis that more resistant seedlings will have higher survival and stress tolerance (resource conservative) traits was partially supported by more rust resistant seedlings having higher survival but also had a mix of resource acquisitive and conservative traits. More resistant seedlings reached and survived to each phenological stage faster, had greater biomass allocation to tough, large leaves, had lower allocation to belowground biomass, and had lower starch and higher sugar concentrations than less resistant seedlings. Together, these traits may be related to higher cold, drought, or high-light tolerance. Interestingly, while some traits increased or decreased with resistance level, many exhibited non-linear (u- or hump-shaped) relationships, with intermediate resistance groups (C-D) having distinct trait combinations, emphasizing the potential adaptive value of maintaining a full spectrum of resistance classes in conservation efforts, especially given the quantitative, polygenic basis of PIAL resistance and the possibility that intermediate group traits may be advantageous under specific environmental conditions.

For Q4, unexpectedly, PIFL R and S only differed in 1 trait, while PIAL R and S differed in 16 traits. Consistent with our hypothesis, we observed that compared to PIAL, PIFL exhibited a mix of resource acquisitive and conservative traits including greater aboveground biomass allocation, lower belowground biomass allocation, a lower proportion of seedlings surviving to emergence and needle burst, later needle burst timing, higher leaf sugars, and lower leaf starch which may support a generalist life history strategy. Future research should include a greater range of PIAL and PIFL families spanning the full species' distributions, measuring physiological traits (e.g., gas exchange, high-light tolerance, cold tolerance), and implement stress treatments (e.g., drought, cold, WPBR) to improve our understanding of the physiological drivers of early seedling establishment and enhance the conservation of two ecologically critical species in western North American subalpine ecosystems.

TABLES AND FIGURES

Tables

Table 1: Trait category (phenology, growth, NSC)-subcategory (phenology (proportions, TTE), growth (aboveground, belowground, whole plant), NSC (leaf, root)), full trait name, abbreviated trait name, units, and description (calculation, primary method). The numbers in the trait name represent the day post-sowing (DPS) on which the measurement occurred.

Category	Full trait name	Abbreviated trait name	Units	Description
Phenology - proportion	proportion emerged by day 30 (PIAL) or 21 (PIFL)	prop.emg.30.21		number of individuals emerged by day 30 or 21 / total seeds sown
	proportion emerged by day 55 (PIAL) or 56 (PIFL)	prop.emg.55.56		number of individuals emerged by day 55 or 56 / total seeds sown
	proportion with bud formation by day 30 (PIAL) or 35 (PIFL)	prop.bf.30.35		number of individuals with bud formation by day 30 or 35 / total seeds sown
	proportion with bud formation by day 95 (PIAL) or 115 (PIFL)	prop.bf.95.115		number of individuals with bud formation by day 95 or 119 /total seeds sown
	proportion with needle burst by day 119 (PIAL) or 119 (PIFL)	prop.nb.119.119		number of individuals with needle burst by day 119 / total seeds sown
	proportion with needle burst by day 161 (PIAL) or 203 (PIFL)	prop.nb.161.203		number of individuals with needle burst by day 161 or 203 / total seeds sown
	proportion survived by day 95 (PIAL) or 91 (PIFL)	prop.surv.95.91		number of individuals survived by day 95 or 91 / total seeds sown
Phenology - TTE	time-to-event for emergence	TTE.emg	days	number of days for a seedling to emerge
	time-to-event for bud formation	TTE.bf		number of days for a seedling to have bud formation
	time-to-event for needle burst	TTE.nb		number of days for a seedling to have needle burst
Growth - aboveground	leaf area on day 150	leaf.area.150	cm²	obtained via ImageJ analysis
	leaf area on day 245	leaf.area.245		
	leaf area on day 375	leaf.area.375		
	specific leaf area on day 150	specific.leaf.area.150	cm²/g	leaf area (cm²) / leaf dry mass (g)
	specific leaf area on day 151	specific.leaf.area.245		
	specific leaf area on day 152	specific.leaf.area.375		
	leaf mass ratio on day 150	leaf.mass.ratio.150		Leaf dry mass (g)/ total plant biomass (g)
	leaf mass ratio on day 245	leaf.mass.ratio.245		

Table 1 Continued

	leaf mass ratio on day 375	leaf.mass.ratio.375		
	leaf dry matter content on day 150 leaf dry matter content on day 245 leaf dry matter content on day 375	leaf.dry.matter.content.150 leaf.dry.matter.content.245 leaf.dry.matter.content.375		leaf dry mass (g) / leaf fresh mass (g)
	leaf thickness on day 150 leaf thickness on day 245 leaf thickness on day 375	leaf.thickness.150 leaf.thickness.245 leaf.thickness.375	cm^2/g	1 / (specific leaf area (cm^2/g) * Leaf dry matter content (g/g))
	leaf mass area on day 150 leaf mass area on day 245 leaf mass area on day 375	leaf.mass.area.150 leaf.mass.area.245 leaf.mass.area.375	g/cm^2	leaf dry mass (g) / leaf area (cm^2)
	fresh leaf biomass on day 150 fresh leaf biomass on day 245 fresh leaf biomass on day 375	fresh.leaf.biomass.150 fresh.leaf.biomass.245 fresh.leaf.biomass.375	g	obtained via analytical scale
	dry leaf biomass on day 150 dry leaf biomass on day 245 dry leaf biomass on day 375	dry.leaf.biomass.150 dry.leaf.biomass.245 dry.leaf.biomass.375	g	obtained via analytical scale
	stem diameter on day 97 stem diameter on day 160 stem diameter on day 221	stem.diameter.97 stem.diameter.160 stem.diameter.221	mm	calipers
	seedling height on day 97 seedling height on day 160 seedling height on day 221	seedling.height.97 seedling.height.160 seedling.height.221	cm	ruler
	stem diameter growth rate on day 221 seedling height growth rate on day 221	stem.diameter.growth.rate.221 seedling.height.growth.rate.221	mm/day cm/day	ln(SD_ND5) - ln(SD_ND1) / (ND5_dps - ND1_dps) ln(SH_ND5) - ln(SH_ND1) / (ND5_dps - ND1_dps)
	fresh stem biomass on day 150 fresh stem biomass on day 245 fresh stem biomass on day 375	fresh.stem.biomass.150 fresh.stem.biomass.245 fresh.stem.biomass.375	g	obtained via analytical scale
	dry stem biomass on day 150 dry stem biomass on day 245	dry.stem.biomass.150 dry.stem.biomass.245	g	obtained via analytical scale

Table 1 Continued

	dry stem biomass on day 375	dry.stem.biomass.375		
Growth - belowground	total root length on day 150 total root length on day 245 total root length on day 375	total.root.length.150 total.root.length.245 total.root.length.375	cm	obtained via Rhizovision image analysis
	root diameter on day 150 root diameter on day 245 root diameter on day 375	root.diameter.150 root.diameter.245 root.diameter.375	mm	obtained via Rhizovision image analysis
	root surface area on day 150 root surface area on day 245 root surface area on day 375	root.surface.area.150 root.surface.area.245 root.surface.area.375	cm^2	obtained via Rhizovision image analysis
	root volume on day 150 root volume on day 245 root volume on day 375	root.volume.150 root.volume.245 root.volume.375	cm^3	obtained via Rhizovision image analysis
	specific root length on day 150 specific root length on day 245 specific root length on day 375	specific.root.length.150 specific.root.length.245 specific.root.length.375	cm/g	root length (cm) / dry root biomass (g)
	root tissue density on day 150 root tissue density on day 245 root tissue density on day 375	root.tissue.density.150 root.tissue.density.245 root.tissue.density.375	g/cm^3	dry root biomass (g) / root volume (cm^2)
	root dry matter content on day 150 root dry matter content on day 245 root dry matter content on day 375	root.dry.matter.content.150 root.dry.matter.content.245 root.dry.matter.content.375	g	dry root biomass (g) / fresh root biomass (g)
	root mass ratio on day 150 root mass ratio on day 245 root mass ratio on day 375	root.mass.ratio.150 root.mass.ratio.245 root.mass.ratio.375		root dry biomass (g) / total dry biomass (g)
	fresh root biomass on day 150 fresh root biomass on day 245 fresh root biomass on day 375	fresh.root.biomass.150 fresh.root.biomass.245 fresh.root.biomass.375	g	obtained via analytical scale
	dry root biomass on day 150 dry root biomass on day 245 dry root biomass on day 375	dry.root.biomass.150 dry.root.biomass.245 dry.root.biomass.375	g	obtained via analytical scale

Table 1 Continued

Growth -whole plant	total fresh biomass on day 150	total.fresh.biomass.150	g	obtained via analytical scale
	total fresh biomass on day 245	total.fresh.biomass.245		
	total fresh biomass on day 375	total.fresh.biomass.375		
	total dry biomass on day 150	total.dry.biomass.150	g	obtained via analytical scale
	total dry biomass on day 245	total.dry.biomass.245		
	total dry biomass on day 375	total.dry.biomass.375		
	root:shoot ratio on day 150	root:shoot.ratio.150		root biomass (g) / leaf biomass (g)
	root:shoot ratio on day 245	root:shoot.ratio.245		
	root:shoot ratio on day 375	root:shoot.ratio.375		
	root:(stem+leaves) on day 150	root:stem+leaves.ratio.150		root biomass (g) / (stem + leaf) biomass (g)
	root:(stem+leaves) on day 245	root:stem+leaves.ratio.245		
	root:(stem+leaves) on day 375	root:stem+leaves.ratio.375		
NSC - leaf	leaf glucose on day 375	leaf.glu.375	mg/g	obtained via enzyme method and spectrophotometer
	leaf fructose on day 375	leaf.fru.375		
	leaf (glucose + fructose) on day 375	leaf.glu.fru.375		
	leaf sucrose on day 375	leaf.suc.375		
	leaf starch on day 375	leaf.starch.375		
	leaf total sugar on day 375	leaf.total.sugar.375		
	leaf total NSC on day 375	leaf.total.NSC.375		
	leaf sugar:NSC ratio on day 375	leaf.sugar:NSC.375		
	leaf starch:NSC ratio on day 375	leaf.starch:NSC.375		
NSC - root	root glucose on day 375	root.glu.375	mg/g	
	root fructose on day 375	root.fru.375		
	root (glucose + fructose) on day 375	root.glu.fru.375		
	root sucrose on day 375	root.suc.375		
	root starch on day 375	root.starch.375		
	root total sugar on day 375	root.total.sugar.375		
	root total NSC on day 375	root.total.NSC.375		
	root sugar:NSC ratio on day 375	root.sugar:NSC.375		
	root starch:NSC ratio on day 375	root.starch:NSC.375		

Table 2: Climate variables (selected using manual forward selection that improved the null model by ≥4 AIC) and estimated means (from logistic regression and linear mixed effects models) for intercept (dataset mean for each climate variable), lower bound of the trait calculated at the lowest climate variable value in the dataset (± standard errors in gray), slope, p-value (significant p-values ($p \leq 0.05$) are bolded, marginal p-values are underlined), conditional R^2 (fixed + random), and sample size (N, note: phenology prop (proportion) and NSC (non-structural carbohydrate) traits were measured at the family level, phenology TTE (time-to-event) and growth traits were measured at the individual level) for U.S. and B.C. PIAL (whitebark pine) and the following traits: phenology (prop, TTE), growth (aboveground, belowground, whole plant) traits, and NSC traits. Climate variables include latitude (degrees), longitude (degrees), elevation (m), precipitation (mm/day), snow water equivalent (SWE, kg/m2), maximum temperature (Tmax °C), and vapor pressure deficit (hPa). For the prop variables, the intercept and lower bound estimates are presented on the log-odds scale (probability estimate follows the lower bound log-odds estimate). Model estimates that required log transformations show the non-transformed model estimate. The number in each trait name indicates the day post sowing (DPS) on which the trait was measured. Units are listed below each trait name. Emg = emerged, bf = bud formation, nb = needle burst, surv = survived.

		Climate variable	Intercept	Lower Bound	Slope	p-value	R^2 (%)	N
Phenology	Prop.emg.30	Latitude	-1.23	-2.24, 0.10 ± 0.06	0.21	**<0.001**	37.98	50 families
	Prop.emg.55	Latitude	-0.39	-1.20, 0.23 ± 0.05	0.17	**<0.001**	33.35	51 families
	Prop.bf.30	Elevation	-1.79	0.41, 0.60 ± 0.0005	-0.002	**<0.001**	34.10	49 families
	Prop.bf.95	Latitude	-0.50	1.41, 0.20 ± 0.06	0.19	**<0.001**	36.11	50 families
	Prop.surv.95	Latitude	-0.42	-1.25, 0.22 ± 0.06	0.18	**0.002**	35.08	50 families
	TTE.emg days	Latitude	31.65	45.80 ± 0.94	-2.36	**0.04**	0.43	1-102
		Longitude	31.65	26.12 ± 1.05	0.88	0.27		
	TTE.bf days	Latitude	37.41	55.41 ± 1.04	-2.98	**0.01**	0.59	1-99
		Longitude	37.41	31.14 ± 1.19	1.05	0.21		
	TTE.nb days	Latitude	109.11	173.59 ± 3.22	-12.65	**0.005**	1.46	1-46

Table 2 Continued

		Longitude	109.11	130.13 ± 3.73	-3.09	0.25		
		Elevation	109.11	73.21 ± 3.56	0.04	0.36		
Growth - aboveground	Leaf.area.150 cm²	Longitude	22.84	22.53 ± 0.33	0.05	0.79	0.22	312
		Elevation	22.84	26.13 ± 0.003	-0.005	0.20		
	Leaf.area.375 cm²	Longitude	20.26	22.23 ± 0.43	-0.31	0.51	0.49	189
		Latitude	20.26	20.63 ± 0.41	-0.07	0.83		
	Specific.leaf.area.150 cm²/g	Longitude	377.48	411.25 ± 2.35	-5.33	0.06	0.06	309
		VPD	377.48	327.42 ± 9.49	-27.96	**0.02**		
		Latitude	377.48	362.63 ± 2.22	2.83	0.23		
	Specific.leaf.area.375 cm²/g	Longitude	236.87	224.13 ± 5.52	2.01	0.72	0.50	188
		Latitude	236.87	237.76 ± 5.23	-0.17	0.93		
	Leaf.thickness.150 $(m^2/g)^{-1}$	Longitude	70.26	60.05 ± 0.50	1.61	**0.001**	0.06	300
		Precipitation	70.26	61.57 ± 0.002	0.01	**<0.001**		
		Latitude	70.26	70.41 ± 0.46	-0.03	0.91		
	Leaf.thickness.375 $(m^2/g)^{-1}$	Longitude	106.25	120.20 ± 2.67	-2.20	0.44	0.88	190
		Latitude	106.25	104.57 ± 2.52	0.32	0.94		
	Leaf.mass.area.150 g/m²	Latitude	27.85	29.26 ± 0.16	-0.27	0.18	0.08	306
		Longitude	27.85	24.77 ± 0.18	0.49	0.07		
		Precipitation	27.85	25.25 ± 0.001	0.003	**0.04**	0.08	306

Table 2 Continued

	Leaf.mass.area.375 g/m²	Longitude	47.05	54.12 ± 1.27	-1.04	0.75	1.04	188
		Latitude	47.05	49.18 ± 1.19	-0.47	0.45		
	Seedling.height.221 cm	Latitude	2.93	3.18 ± 0.02	-0.05	**0.03**	0.35	391
	Fresh.stem.biomass.150 g	Latitude	0.07	0.10 ± 0.002	-0.01	**<0.001**	1.89	299
	Dry.stem.biomass.150 g	Latitude	0.02	0.03 ± 0.0003	-0.001	**<0.001**	1.55	315
Growth - belowground	Total.root.length.150 cm	Longitude	173.03	185.91 ± 3.56	-2.05	0.54	0.12	319
		Latitude	173.03	144.92 ± 3.29	5.29	0.14		
	Total.root.length.375 cm	Longitude	230.77	244.16 ± 4.87	-1.98	0.65	0.72	194
		Latitude	230.77	266.03 ± 4.84	-7.28	0.11		
		SWE	230.77	267.82 ± 0.17	-0.39	**0.01**		
	Root.surface.area.150 cm²	Longitude	81.70	80.13 ± 2.20	0.25	0.92	0.07	317
		Latitude	81.70	79.91 ± 2.05	0.34	0.89		
	Root.surface.area.375 cm²	Longitude	79.11	81.07 ±1.96	-0.29	**0.01**	0.50	195
		Latitude	79.11	98.39 ± 1.97	-4.23	0.86		
		SWE	79.11	94.34 ± 0.07	-0.16	**0.002**		
	Root.volume.150 cm³	Longitude	8.28	7.55 ± 0.27	0.12	0.67	0.09	313
		Latitude	8.28	8.84 ± 0.25	-0.10	0.67		
	Root.volume.375 cm³	Longitude	6.05	5.92 ± 0.25	0.02	0.13	0.36	195
		Latitude	6.05	7.42 ± 0.33	-0.30	**0.003**		

Table 2 Continued

		SWE	6.05	6.91 ± 0.01	-0.01	**<0.001**		
		Tmax	6.05	5.79 ± 0.53	0.07	**0.05**		
	Specific.root.length.150 cm/g	Latitude	1781.76	1721.26 ± 33.32	11.35	0.78	0.08	313
		Longitude	1781.76	1477.22 ± 31.15	48.74	0.15		
	Specific.root.length.375 cm/g	Precipitation	1043.23	1361.27 ± 0.11	-0.33	**<0.001**	0.81	193
		Longitude	1043.23	1123.40 ± 24.32	-11.89	0.47		
		Latitude	1043.23	1127.75 ± 21.76	-18.49	0.22		
	Root.mass.ratio.150 g	Latitude	0.51	0.44 ± 0.002	0.01	**<0.001**	1.15	309
Growth – whole Plant	Root:shoot.ratio.150 g	Latitude	1.09	0.77 ± 0.01	0.06	**<0.001**	1.22	315
	Root:stem+leaves.ratio.150 g	Longitude	1.81	2.06 ± 0.02	-0.04	0.09	0.61	318
NSC	Leaf.suc.375 mg/g	Latitude	1.37	1.59 ± 0.02	-0.05	**0.02**	0.24	24 families
	Leaf.starch.375 mg/g	Longitude	0.58	0.78 ± 0.02	-0.03	0.07	0.16	24 families
	Total.leaf.sugar.375 mg/g	Latitude	2.19	2.40 ± 0.02	-0.05	0.05	0.19	22 families
	Root.suc.375 mg/g	Latitude	1.43	1.65 ± 0.02	-0.05	**0.03**	0.40	23 families

Table 3: Estimated means (from logistic regression and linear mixed effects models), ± standard errors (in gray), p-values (significant p-values (p≤0.05) are bolded, marginal p-values are underlined), and sample sizes (N, note: phenology prop (proportion) traits were measured at the family level and phenology TTE (time-to-event) and growth traits were measured at the individual level) for U.S. PIAL (whitebark pine) for phenology (prop, TTE) and growth (aboveground, belowground, whole plant) traits. For traits with significant p-values, lowercase letters distinguish significant differences in estimated means among seed zones. The locations within each seed zone include zone 1 (Olympic NP), 2E (Okanogan Wenatchee NF – East), 2W (Okanogan Wenatchee NF – West), 3 (Colville), 4 (Gifford Pinchot NF), 5 (Deschutes NF, Mt. Hood, and Warm Springs), 6 (Wallowa-Whitman NF), 7 (Umpqua NF, Crater Lake NP), and 8 (Fremont-Winema NF). The number in each trait name indicates the day post sowing (DPS) on which the trait was measured. NA is listed for seed zones that did not have any available material to sample at 375 DPS. Units are listed below each trait name. Emg = emerged, bf = bud formation, nb = needle burst, surv = survived.

		Seed zone									p-value	N
		1	2E	2W	3	4	5	6	7	8		
Phenology	Prop.emg.30	0.07 a ± 0.02	0.09 ab ± 0.09	0.22 bc ± 0.06	0.25 c ± 0.05	0.24 c ± 0.05	0.33 c ± 0.03	0.21 bc ± 0.06	0.05 a ± 0.09	0.03 a ± 0.11	**<0.001**	2-6 families
	Prop.emg.55	0.15 ab ± 0.04	0.25 bc ± 0.11	0.40 bc ± 0.08	0.52 cd ± 0.06	0.49 cd ± 0.06	0.69 d ± 0.03	0.54 cd ± 0.05	0.19 b ± 0.10	0.04 a ± 0.09	**<0.001**	2-6 families
	Prop.bf.30	0.04 ab ± 0.02	0.04 ab ± 0.14	0.12 abc ± 0.09	0.13 bc ± 0.09	0.25 c ± 0.05	0.24 c ± 0.05	0.12 bc ± 0.09	0.04 ab ± 0.12	0.02 a ± 0.14	**<0.001**	2-8 families
	Prop.bf.95	0.15 abc ± 0.06	0.26 abcd ± 0.15	0.39 bcd ± 0.12	0.52 cd ± 0.08	0.26 abcd ± 0.16	0.57 d ± 0.06	0.37 bcd ± 0.12	0.11 ab ± 0.15	0.03 a ± 0.10	**<0.001**	2-6 families
	Prop.nb.119	0.07 a ± 0.02	0.04 a ± 0.12	0.05 a ± 0.11	0.27 b ± 0.06	0.11 ab ± 0.11	0.10 a ± 0.09	0.08 a ± 0.12	0.06 a ± 0.11	0.09 a ± 0.12	**<0.001**	2-9 families
	Prop.nb.161	0.08 ab ± 0.02	0.07 ab ± 0.11	0.14 ab ± 0.09	0.30 c ± 0.05	0.14 ab ± 0.10	0.15 b ± 0.08	0.11 ab ± 0.11	0.07 a ± 0.11	0.09 ab ± 0.11	**<0.001**	2-9 families
	Prop.surv.95	0.16 abc ± 0.06	0.26 abcd ± 0.15	0.39 bcd ± 0.11	0.53 cd ± 0.08	0.25 abcd ± 0.15	0.59 d ± 0.06	0.39 bcd ± 0.11	0.14 ab ± 0.14	0.03 a ± 0.10	**<0.001**	2-6 families
	TTE.emg days	35.41 ± 4.86	36.96 ± 6.85	33.67 ± 6.76	33.90 ± 6.77	34.99 ± 6.93	32.04 ± 5.57	34.15 ± 6.83	39.61 ± 5.98	31.84 ± 7.07	0.75	49-515

Table 3 Continued

	TTE.bf days	43.83 ± 5.71	43.45 ± 8.08	40.10 ± 7.99	41.81 ± 8.00	36.87 ± 8.18	41.63 ± 6.57	41.72 ± 8.04	42.19 ± 7.03	38.53 ± 8.25	0.99	46-487
	TTE.nb days	106.68 ± 8.65	133.64 ± 10.63	124.07 ± 10.40	111.27 ± 10.15	116.29 ± 12.71	122.51 ± 9.24	119.46 ± 10.83	129.37 ± 9.97	113.20 ± 11.99	0.07	15-159
Growth - aboveground	Leaf.area.150 cm²	19.76 ± 3.93	18.90 ± 6.26	22.93 ± 5.31	25.82 ± 5.41	16.91 ± 6.15	26.37 ± 4.47	19.41 ± 5.60	22.90 ± 4.98	28.20 ± 6.78	0.30	8-71
	Leaf.area.375 cm²	14.75 ± 5.37	NA	18.12 ± 6.81	25.05 ± 6.69	15.49 ± 7.59	24.36 ± 5.90	13.82 ± 7.59	20.80 ± 6.96	NA	0.29	8-55
	Specific.leaf. area.150 cm²/g	339.00 ± 29.79	406.27 ± 52.75	360.25 ± 38.46	292.50 ± 39.92	254.20 ± 50.64	373.43 ± 33.48	362.61 ± 42.88	377.63 ± 38.66	404.82 ± 62.58	0.06	8-71
	Specific.leaf. area.375 cm²/g	111.27 a ± 35.06	NA	152.96 a ± 40.66	284.24 b ± 41.33	181.40 ab ± 49.30	271.92 b ± 37.82	275.35 b ± 49.30	215.73 ab ± 44.48	NA	**<0.001**	8-56
	Leaf.mass. ratio.150 g	0.40 ab ± 0.02	0.37 ab ± 0.04	0.31 a ± 0.03	0.40 b ± 0.03	0.42 b ± 0.04	0.36 ab ± 0.03	0.40 ab ± 0.03	0.39 ab ± 0.03	0.37 ab ± 0.04	**0.008**	8-72
	Leaf.mass. ratio.375 g	0.22 ± 0.02	NA	0.24 ± 0.02	0.27 ± 0.02	0.27 ± 0.02	0.26 ± 0.02	0.27 ± 0.02	0.27 ± 0.02	NA	0.05	7-55
	Leaf.dry.matter. content.150 g	0.42 ± 0.03	0.44 ± 0.05	0.40 ± 0.04	0.39 ± 0.04	0.35 ± 0.05	0.37 ± 0.03	0.41 ± 0.04	0.39 ± 0.04	0.42 ± 0.05	0.66	6-64
	Leaf.dry.matter. content.375 g	0.44 ± 0.06	NA	0.60 ± 0.08	0.43 ± 0.07	0.44 ± 0.09	0.43 ± 0.07	0.44 ± 0.09	0.44 ± 0.08	NA	0.10	5-53
	Leaf.thickness.150 $(m^2/g)^{-1}$	68.38 a ± 7.29	59.11 a ± 12.85	57.61 a ± 9.26	66.09 a ± 9.58	114.90 b ± 11.91	72.39 a ± 8.18	69.94 a ± 10.26	74.31 a ± 9.27	64.25 a ± 14.50	**<0.001**	7-66
	Leaf.thickness.375 $(m^2/g)^{-1}$	198.23 b ± 22.59	NA	96.73 a ± 26.86	84.80 a ± 25.93	137.89 ab ± 31.88	91.45 a ± 24.07	86.83 a ± 31.57	122.04 ab ± 27.66	NA	**<0.001**	7-56
	Leaf.mass. area.150 g/m²	32.42 ± 2.43	26.62 ± 4.55	30.01 ± 3.01	29.83 ± 3.19	41.85 ± 4.33	28.95 ± 2.71	28.97 ± 3.52	28.56 ± 3.20	26.66 ± 5.53	0.14	8-71

Table 3 Continued

	Leaf.mass. area.375 g/m²	103.61 b ± 14.45	NA	59.40 ab ± 17.33	36.19 a ± 16.69	66.71 ab ± 20.41	40.64 a ± 15.44	38.34 ab ± 20.41	53.55 ab ± 17.81	NA	**0.03**	8-56
	Fresh.leaf. biomass.150 g	0.14 ± 0.03	0.11 ± 0.05	0.14 ± 0.04	0.17 ± 0.04	0.19 ± 0.05	0.19 ± 0.04	0.13 ± 0.04	0.17 ± 0.04	0.17 ± 0.05	0.67	7-70
	Fresh.leaf. biomass.375 g	0.32 ± 0.08	NA	0.23 ± 0.10	0.22 ± 0.10	0.22 ± 0.11	0.23 ± 0.09	0.12 ± 0.11	0.23 ± 0.10	NA	0.77	7-55
	Dry.leaf. biomass.150 g	0.06 ± 0.01	0.05 ± 0.02	0.06 ± 0.02	0.07 ± 0.02	0.06 ± 0.02	0.07 ± 0.02	0.06 ± 0.02	0.06 ± 0.02	0.07 ± 0.02	0.95	7-71
	Dry.leaf. biomass.375 g	0.15 ± 0.04	NA	0.14 ± 0.05	0.09 ± 0.04	0.10 ± 0.05	0.10 ± 0.04	0.05 ± 0.05	0.10 ± 0.05	NA	0.49	8-56
	Stem.diameter.97 mm	0.92 ± 0.15	1.08 ± 0.21	1.15 ± 0.21	1.16 ± 0.21	1.12 ± 0.17	1.13 ± 0.17	1.00 ± 0.21	0.92 ± 0.18	0.95 ± 0.22	0.79	12-90
	Stem.diameter.160 mm	1.22 ± 0.11	1.30 ± 0.15	1.45 ± 0.15	1.38 ± 0.15	1.37 ± 0.16	1.36 ± 0.12	1.27 ± 0.15	1.33 ± 0.13	1.27 ± 0.16	0.89	12-90
	Stem.diameter.221 mm	1.43 ± 0.13	1.51 ± 0.18	1.64 ± 0.18	1.59 ± 0.18	1.58 ± 0.19	1.56 ± 0.15	1.52 ± 0.18	1.62 ± 0.16	1.52 ± 0.20	0.97	12-90
	Seedling.height.97 cm	2.27 ± 0.27	2.40 ± 0.38	2.42 ± 0.37	2.47 ± 0.38	2.15 ± 0.42	2.40 ± 0.31	2.49 ± 0.38	2.25 ± 0.34	2.24 ± 0.42	0.99	12-90
	Seedling.height.160 cm	2.49 ± 0.25	2.78 ± 0.34	2.72 ± 0.34	2.85 ± 0.38	2.66 ± 0.38	2.76 ± 0.28	2.70 ± 0.35	2.65 ± 0.31	2.55 ± 0.39	0.99	12-84
	Seedling.height.221 cm	2.90 ± 0.22	3.14 ± 0.30	3.06 ± 0.29	3.42 ± 0.29	3.18 ± 0.35	3.23 ± 0.25	3.12 ± 0.30	3.00 ± 0.27	2.85 ± 0.37	0.71	12-84
	Stem.diameter. growth.rate.221 mm/day	0.004 ± 0.0007	0.003 ± 0.001	0.002 ± 0.001	0.002 ± 0.001	0.003 ± 0.001	0.003 ± 0.0008	0.003 ± 0.0001	0.005 ± 0.0009	0.004 ± 0.001	0.11	11-89
	Seedling.height. growth.rate.221 cm/day	0.002 0.0006	0.002 ± 0.0009	0.002 ± 0.0008	0.003 ± 0.0009	0.003 ± 0.0009	0.003 ± 0.0007	0.002 ± 0.0009	0.002 ± 0.0008	0.002 ± 0.0009	0.76	12-82
	Fresh.stem. biomass.150 g	0.08 ± 0.03	0.04 ± 0.05	0.08 ± 0.04	0.07 ± 0.04	0.05 ± 0.04	0.08 ± 0.03	0.08 ± 0.04	0.09 ± 0.03	0.06 ± 0.05	0.74	8-70

Table 3 Continued

	Fresh.stem. biomass.375 g	0.08 ± 0.02	NA	0.09 ± 0.02	0.07 ± 0.02	0.07 ± 0.03	0.07 ± 0.02	0.05 ± 0.03	0.10 ± 0.02	NA	0.40	8-54
	Dry.stem. biomass.150 g	0.02 ± 0.006	0.02 ± 0.01	0.03 ± 0.008	0.02 ± 0.009	0.02 ± 0.01	0.03 ± 0.007	0.03 ± 0.009	0.03 ± 0.008	0.03 ± 0.01	0.84	8-72
	Dry.stem. biomass.375 g	0.05 ± 0.008	NA	0.04 ± 0.009	0.03 ± 0.009	0.04 ± 0.01	0.03 ± 0.008	0.03 ± 0.01	0.04 ± 0.009	NA	<u>0.06</u>	7-56
Growth - belowground	Total.root. length.150 cm	120.66 ab ± 27.38	88.95 abc ± 51.19	222.30 c ± 33.23	199.37 bc ± 34.47	116.5 abc ± 48.75	172.94 bc ± 30.47	38.66 a ± 39.64	157.10 bc ± 36.00	237.01 bc ± 62.28	**<0.001**	8-72
	Total.root. length.375 cm	209.43 ± 43.87	NA	284.97 ± 54.78	291.50 ± 54.48	163.19 ± 61.87	269.23 ± 48.26	186.58 ± 61.87	220.07 ± 57.08	NA	<u>0.09</u>	8-53
	Root.diameter.150 mm	0.82 ab ± 0.23	0.74 ab ± 0.40	1.42 b ± 0.29	1.45 b ± 0.30	0.92 ab ± 0.38	1.24 ab ± 0.26	0.48 a ± 0.33	0.98 ab ± 0.30	1.74 ab ± 0.47	**0.007**	8-72
	Root.diameter.375 mm	1.31 ± 0.17	NA	1.23 ± 0.20	1.19 ± 0.20	1.47 ± 0.25	1.15 ± 0.18	1.35 ± 0.24	1.29 ± 0.23	NA	0.57	5-48
	Root.surface. area.150 cm^2	56.03 ab ± 19.24	32.98 abc ± 30.07	108.77 c ± 23.08	107.66 bc ± 23.91	57.69 abc ± 33.43	93.31 bc ± 21.26	12.26 a ± 27.34	76.5 abc ± 25.14	139.99 bc ± 42.52	**<0.001**	8-72
	Root.surface. area.375 cm^2	91.47 ± 15.74	NA	105.38 ± 17.24	110.60 ± 17.48	68.33 ± 21.42	87.54 ± 16.65	91.27 ± 22.11	74.64 ± 19.15	NA	0.12	7-56
	Root.volume.150 cm^3	3.59 ab ± 2.62	2.87 ab ± 4.48	11.42 b ± 3.17	11.46 b ± 3.26	5.78 ab ± 4.30	10.47 b ± 2.89	1.16 a ± 3.63	7.80 ab ± 3.36	15.97 ab ± 5.32	**0.001**	8-71
	Root.volume.375 cm^3	8.58 ± 1.73	NA	8.54 ± 1.87	9.13 ± 1.90	5.77 ± 2.28	6.90 ± 1.82	7.74 ± 2.34	6.08 ± 2.08	NA	0.16	6-56
	Specific.root. length.150 cm/g	1543.99 ab ± 288.97	1091.55 ab ± 538.99	2095.11 b ± 357.84	2115.33 b ± 364.29	1367.89 ab ± 513.53	1759.57 b ± 321.71	593.11 a ± 418.26	1669.93 ab ± 383.17	2632.65 ab ± 655.19	**0.001**	8-72

Table 3 Continued

	Specific.root. length.375 cm/g	528.29 ab ± 178.10	NA	654.15 a ± 200.30	1378.36 c ± 198.90	684.41 ab ± 250.20	1062.21 bc ± 189.80	1597.31 c ± 250.20	950.59 abc ± 221.70	NA	**<0.001**	8-56
	Root.tissue. density.150 g/cm^3	1.16 ab ± 0.23	1.15 ab ± 0.42	0.28 a ± 0.27	0.49 a ± 0.29	1.03 ab ± 0.40	0.88 a ± 0.25	1.78 b ± 0.33	0.84 ab ± 0.30	0.25 ab ± 0.51	**<0.001**	8-72
	Root.tissue. density.375 g/cm^3	0.08 ± 0.02	NA	0.05 ± 0.02	0.03 ± 0.02	0.05 ± 0.03	0.05 ± 0.02	0.02 ± 0.03	0.04 ± 0.02	NA	0.33	5-51
	Root.dry.matter. content.150 g	0.52 b ± 0.05	0.61 b ± 0.08	0.38 ab ± 0.07	0.40 ab ± 0.07	0.24 a ± 0.08	0.34 a ± 0.06	0.36 ab ± 0.07	0.38 ab ± 0.07	0.62 b ± 0.09	**<0.001**	8-71
	Root.dry.matter. content.375 g	0.48 ± 0.12	NA	0.49 ± 0.14	0.27 ± 0.13	0.33 ± 0.16	0.27 ± 0.12	0.21 ± 0.16	0.30 ± 0.14	NA	0.26	5-55
	Root.mass. ratio.150 g	0.47 ± 0.04	0.51 ± 0.07	0.53 ± 0.06	0.47 ± 0.06	0.47 ± 0.07	0.49 ± 0.05	0.43 ± 0.06	0.43 ± 0.06	0.49 ± 0.07	0.72	7-72
	Root.mass. ratio.375 g	0.69 cd ± 0.02	NA	0.69 d ± 0.02	0.63 ab ± 0.02	0.62 abc ± 0.03	0.66 bcd ± 0.02	0.61 ab ± 0.03	0.61 a ± 0.02	NA	**<0.001**	8-54
	Fresh.root. biomass.150 g	0.14 ± 0.09	0.13 ± 0.11	0.35 ± 0.11	0.29 ± 0.11	0.33 ± 0.15	0.35 ± 0.10	0.18 ± 0.12	0.28 ± 0.11	0.15 ± 0.16	0.17	7-72
	Fresh.root. biomass.375 g	0.95 ± 0.21	NA	1.02 ± 0.25	0.82 ± 0.25	0.60 ± 0.30	0.96 ± 0.23	0.58 ± 0.30	0.78 ± 0.26	NA	0.27	8-54
	Dry.root. biomass.150 g	0.07 ± 0.02	0.07 ± 0.03	0.10 ± 0.03	0.09 ± 0.03	0.08 ± 0.03	0.10 ± 0.02	0.06 ± 0.03	0.08 ± 0.03	0.09 ± 0.04	0.75	8-72
	Dry.root. biomass.375 g	0.49 ± 0.15	NA	0.48 ± 0.18	0.22 ± 0.17	0.34 ± 0.21	0.25 ± 0.16	0.12 ± 0.11	0.23 ± 0.18	NA	0.18	7-54
	Total.fresh. biomass.150 g	0.39 ± 0.12	0.33 ± 0.21	0.52 ± 0.16	0.53 ± 0.16	0.57 ± 0.21	0.61 ± 0.14	0.39 ± 0.18	0.51 ± 0.16	0.38 ± 0.22	0.61	8-70

Table 3 Continued

Growth – whole plant	Total.fresh. biomass.375 g	1.35 ± 0.30	NA	1.36 ± 0.36	1.11 ± 0.35	0.96 ± 0.42	1.24 ± 0.32	0.76 ± 0.42	1.11 ± 0.37	NA	0.65	8-56
	Total.dry. biomass.150 g	0.15 ± 0.04	0.13 ± 0.06	0.19 ± 0.05	0.19 ± 0.05	0.16 ± 0.06	0.20 ± 0.04	0.15 ± 0.05	0.17 ± 0.05	0.19 ± 0.06	0.75	8-71
	Total.dry. biomass.375 g	0.69 ± 0.19	NA	0.67 ± 0.23	0.35 ± 0.22	0.50 ± 0.27	0.38 ± 0.21	0.20 ± 0.27	0.38 ± 0.24	NA	0.29	7-54
	Root:shoot. ratio.150 g	0.83 ± 0.15	1.06 ± 0.24	1.16 ± 0.20	0.91 ± 0.20	0.90 ± 0.23	1.01 ± 0.17	0.75 ± 0.21	0.79 ± 0.19	0.96 ± 0.25	0.46	7-72
	Root:shoot. ratio.375 g	2.36 ± 0.27	NA	2.34 ± 0.33	1.80 ± 0.31	1.71 ± 0.39	2.00 ± 0.29	1.60 ± 0.38	1.63 ± 0.34	NA	<u>0.05</u>	7-54
	Root:stem+leaves. ratio.150 g	1.59 ab ± 0.17	1.77 ab ± 0.29	2.28 b ± 0.23	1.58 a ± 0.23	1.39 a ± 0.28	1.86 ab ± 0.19	1.58 ab ± 0.24	1.62 a ± 0.22	1.73 ab ± 0.31	**0.007**	8-72
	Root:stem+leaves. ratio.375 g	3.67 ± 0.29	NA	3.33 ± 0.35	2.72 ± 0.35	2.82 ± 0.41	2.98 ± 0.31	2.79 ± 0.41	2.76 ± 0.37	NA	<u>0.07</u>	7-55

Table 4: Estimated means (from logistic regression and linear mixed effects models), ± standard errors (in gray), p-values (significant p-values ($p \leq 0.05$) are bolded, marginal p-values are underlined), and sample sizes (N, note: phenology prop (proportion) traits were measured at the family level, phenology TTE (time-to-event) and growth traits were measured at the individual level) for U.S. PIAL (whitebark pine) rust resistance levels A-F for phenology (prop, TTE) and growth traits (aboveground, belowground, whole plant), and for combined rust resistance groups (Resistant = A-B, Intermediate = C-D, and Susceptible – E-F) for NSC (non-structural carbohydrate) traits. A is the highest and F is the lowest resistance level. A significant p-value indicated that at least 2 of the 6 groups resistance levels differed from each other. For traits with significant p-values, lowercase letters distinguish significant differences in estimated means among rust resistance levels (phenology, growth traits) or combined rust resistance groups (NSC traits). Model estimates that required log transformations show the non-transformed estimate. The number in each trait name indicates the day post sowing (DPS) on which the trait was measured. Units are listed below each trait name. Emg = emerged, bf = bud formation, nb = needle burst, surv = survived.

		Rust Resistance Level						p-value	N
		A	B	C	D	E	F		
Phenology	Prop.emg.30	0.14 ± 0.06	0.23 ± 0.09	0.12 ± 0.10	0.12 ± 0.09	0.09 ± 0.08	0.14 ± 0.11	0.87	3-9 families
	Prop.emg.55	0.35 ± 0.08	0.47 ± 0.11	0.27 ± 0.12	0.30 ± 0.12	0.20 ± 0.16	0.25 ± 0.14	0.66	3-9 families
	Prop.bf.30	0.11 b ± 0.04	0.09 b ± 0.05	0.14 b ± 0.06	0.04 a ± 0.03	0.07 ab ± 0.06	0.11 b ± 0.07	**<0.001**	3-8 families
	Prop.bf.95	0.32 ± 0.08	0.41 ± 0.10	0.29 ± 0.10	0.19 ± 0.11	0.24 ± 0.15	0.20 ± 0.13	0.64	3-9 families
	Prop.nb.119	0.14 c ± 0.03	0.14 c ± 0.05	0.07 b ± 0.05	0.05 ab ± 0.04	0.01 ab ± 0.01	0.03 a ± 0.02	**<0.001**	3-9 families
	Prop.nb.161	0.16 c ± 0.04	0.09 b ± 0.04	0.10 abc ± 0.05	0.05 a ± 0.03	0.03 ab ± 0.02	0.13 bc ± 0.06	**<0.001**	3-9 families
	Prop.surv.95	0.35 ± 0.08	0.46 ± 0.11	0.30 ± 0.11	0.21 ± 0.12	0.23 ± 0.16	0.21 ± 0.13	0.53	3-9 families
	TTE.emg days	33.27 ± 2.38	35.45 ± 3.39	35.98 ± 3.51	34.61 ± 3.60	36.77 ± 4.61	32.54 ± 4.18	0.92	56-395

Table 4 Continued

	TTE.bf days	37.34 ± 2.64	43.67 ± 3.75	39.37 ± 3.86	40.18 ± 4.00	46.77 ± 5.07	40.67 ± 4.60	0.53	50-367
	TTE.nb days	114.98 a ± 3.67	119.24 ab ± 4.83	119.89 ab ± 5.13	120.38 ab ± 4.91	142.08 b ± 8.94	131.01 ab ± 6.25	**0.02**	14-175
Growth - aboveground	Leaf.area.150 cm²	24.73 ± 1.88	22.47 ± 2.70	19.94 ± 2.78	26.68 ± 2.88	17.38 ± 3.8	23.71 ± 3.62	0.12	15-48
	Leaf.area.375 cm²	20.97 ab ± 2.31	22.16 ab ± 2.56	21.74 ab ± 3.48	15.07 a ± 2.74	14.75 a ± 6.35	24.77 b ± 3.05	**0.005**	8-48
	Specific.leaf.area.150 cm²/g	331.38 ± 24.97	332.09 ± 35.14	375.94 ± 36.13	407.99 ± 36.65	343.25 ± 49.86	380.98 ± 47.22	0.27	15-48
	Specific.leaf.area.375 cm²/g	226.85 ab ± 23.82	289.30 b ± 37.75	297.07 b ± 48.00	308.16 b ± 44.12	111.27 a ± 62.72	208.54 ab ± 45.45	**0.006**	8-48
	Leaf.mass.ratio.150 g	0.39 ± 0.02	0.37 ± 0.02	0.36 ± 0.02	0.37 ± 0.02	0.39 ± 0.03	0.32 ± 0.03	0.38	16-48
	Leaf.mass.ratio.375 g	0.27 b ± 0.01	0.25 ab ± 0.01	0.26 ab ± 0.01	0.26 ab ± 0.01	0.22 a ± 0.02	0.24 ab ± 0.01	**0.004**	8-47
	Leaf.dry.matter.content.150 g	0.42 b ± 0.01	0.41 b ± 0.01	0.40 b ± 0.01	0.42 b ± 0.01	0.35 a ± 0.02	0.34 a ± 0.01	**<0.001**	12-42
	Leaf.dry.matter.content.375 g	0.44 ± 0.03	0.44 ± 0.04	0.45 ± 0.05	0.43 ± 0.05	0.49 ± 0.07	0.57 ± 0.05	0.13	4-42
	Leaf.thickness.150 $(m^2/g)^{-1}$	85.63 c ± 4.76	75.92 bc ± 6.70	66.21 ab ± 6.55	55.22 a ± 6.00	84.77 bc ± 9.45	74.10 abc ± 8.02	**<0.001**	15-45
	Leaf.thickness.375 $(m^2/g)^{-1}$	112.83 a ± 9.81	91.02 a ± 15.21	78.96 a ± 19.22	83.14 a ± 17.40	222.87 b ± 25.53	103.06 a ± 18.36	**0.001**	8-47
	Leaf.mass.area.150 g/m²	33.23 b ± 1.82	30.32 ab ± 2.65	28.58 ab ± 2.66	26.20 a ± 2.69	33.04 ab ± 3.68	28.08 ab ± 3.4	**0.04**	16-48
	Leaf.mass.area.375 g/m²	51.36 ab ± 6.03	41.71 a ± 9.22	34.94 a ± 11.62	35.02 a ± 10.73	103.61 b ± 15.69	62.09 ab ± 11.23	**0.01**	8-48
	Fresh.leaf.biomass.150 g	0.20 b ± 0.01	0.18 ab ± 0.02	0.13 a ± 0.02	0.14 a ± 0.02	0.13 ab ± 0.03	0.16 ab ± 0.02	**0.002**	15-47

Table 4 Continued

	Fresh.leaf.biomass.375 g	0.23 bc ± 0.02	0.26 c ± 0.03	0.12 a ± 0.04	0.17 ab ± 0.03	0.32 abc ± 0.06	0.29 c ± 0.03	**<0.001**	8-47
	Dry.leaf.biomass.150 g	0.08 ± 0.01	0.07 ± 0.02	0.06 ± 0.02	0.06 ± 0.02	0.05 ± 0.03	0.07 + 0.03	0.09	15-48
	Dry.leaf.biomass.375 g	0.11 ab ± 0.01	0.11 ab ± 0.02	0.06 a ± 0.02	0.06 a ± 0.02	0.15 ab ± 0.03	0.15 b ± 0.02	**<0.001**	8-48
	Stem.diameter.97 mm	1.13 ± 0.06	1.05 ± 0.08	1.01 ± 0.08	0.99 ± 0.08	1.05 ± 0.11	1.01 ± 0.10	0.54	27-71
	Stem.diameter.160 mm	1.43 ± 0.03	1.29 ± 0.04	1.34 ± 0.04	1.34 ± 0.04	1.30 ± 0.06	1.26 ± 0.05	0.12	26-68
	Stem.diameter.221 mm	1.67 b ± 0.04	1.50 ab ± 0.06	1.56 ab ± 0.06	1.58 ab ± 0.06	1.48 ab ± 0.08	1.47 a ± 0.07	0.05	26-66
	Seedling.height.97 cm	2.34 ± 0.11	2.37 ± 0.16	2.29 ± 0.16	2.38 ± 0.16	2.34 ± 0.20	2.51 ± 0.17	0.94	27-72
	Seedling.height.160 cm	2.78 ± 0.11	2.77 ± 0.15	2.62 ± 0.16	2.70 ± 0.16	2.61 ± 0.20	2.82 ± 0.19	0.86	24-66
	Seedling.height.221 cm	3.23 ± 0.10	3.26 ± 0.14	3.06 ± 0.14	2.99 ± 0.13	2.95 ± 0.18	3.23 ± 0.16	0.09	24-66
	Absolute.growth.rate. stem diameter.221 cm/day	0.003 ± 0.0005	0.003 ± 0.0006	0.004 ± 0.007	0.003 ± 0.0007	0.003 ± 0.0009	0.003 ± 0.0008	0.49	25-65
	Absolute.growth.rate. Seedling. height.221 cm/day	0.003 ± 0.0003	0.003 ± 0.0003	0.002 ± 0.0003	0.002 ± 0.0003	0.002 ± 0.0005	0.002 ± 0.0004	0.19	23-64
	Fresh.stem.biomass.150 g	0.07 ± 0.01	0.07 ± 0.01	0.07 ± 0.01	0.06 ± 0.01	0.04 ± 0.01	0.07 ± 0.01	0.24	10-47
	Fresh.stem.biomass.375 g	0.08 ab ± 0.01	0.08 a ± 0.01	0.05 a ± 0.01	0.06 a ± 0.01	0.08 ab ± 0.02	0.11 b ± 0.01	**<0.001**	8-46
	Dry.stem.biomass.150 g	0.03 ± 0.003	0.03 ± 0.004	0.03 ± 0.004	0.03 ± 0.004	0.02 ± 0.005	0.03 ± 0.005	0.49	15-48
	Dry.stem.biomass.375 g	0.04 ab ± 0.004	0.03 a ± 0.01	0.03 a ± 0.01	0.03 a ± 0.01	0.05 ab ± 0.01	0.05 b ± 0.01	**<0.001**	8-48

Table 4 Continued

Growth - belowground	Total.root.length.150 cm	188.62 ± 27.9	170.63 ± 39.37	103.39 ± 40.84	139.19 ± 41.44	114.87 ± 55.75	234.92 ± 53.44	0.12	16-48
	Total.root.length.375 cm	239.76 ± 21.69	286.26 ± 28.81	185.30 ± 37.66	250.45 ± 30.32	209.43 ± 57.72	285.09 ± 33.63	0.22	8-48
	Root.diameter.150 mm	1.29 ± 0.20	1.24 ± 0.29	0.83 ± 0.30	1.21 ± 0.31	0.93 ± 0.40	1.52 ± 0.39	0.46	16-48
	Root.diameter.375 mm	1.12 ± 0.06	1.07 ± 0.09	1.39 ± 0.12	1.34 ± 0.09	1.31 ± 0.16	1.36 ± 0.10	0.06	8-48
	Root.surface.area.150 cm²	104.02 ± 17.84	88.02 ± 25.57	49.09 ± 26.55	79.53 ± 27.66	61.45 ± 36.03	126.44 ± 34.46	0.31	16-48
	Root.surface.area.375 cm²	83.19 ± 6.88	86.71 ± 10.80	80.15 ± 14.03	106.82 ± 10.86	80.18 ± 18.10	109.32 ± 11.79	0.11	8-48
	Root.volume.150 cm³	12.27 ± 2.16	8.88 ± 3.12	5.19 ± 3.23	9.23 ± 3.37	6.00 ± 4.42	14.57 ± 4.18	0.35	15-48
	Root.volume.375 cm³	6.52 ± 0.66	6.44 ± 1.06	6.60 ± 1.39	9.15 ± 1.11	6.44 ± 1.76	8.44 ± 1.19	0.12	8-48
	Specific.root.length.150 cm/g	1916.77 ± 305.26	1753.03 ± 435.33	1449.65 ± 448.40	1814.10 ± 459.54	1527.78 ± 614.38	2286.33 ± 582.58	0.74	16-48
	Specific.root.length.375 cm/g	1011.35 bc ± 91.93	1071.63 bc ± 133.78	1572.19 c ± 181.37	1543.68 c ± 139.92	494.08 a ± 268.15	616.68 ab ± 155.21	**<0.001**	5-47
	Root.tissue.density.150 g/cm³	0.63 ± 0.26	0.77 ± 0.36	1.11 ± 0.38	0.91 ± 0.39	1.04 ± 0.51	0.33 ± 0.50	0.66	16-48
	Root.tissue.density.375 g/cm³	0.05 c ± 0.01	0.05 bc ± 0.01	0.02 ab ± 0.01	0.02 a ± 0.01	0.08 bc ± 0.02	0.06 bc ± 0.01	**<0.001**	6-43
	Root.dry.matter.content.150 g	0.40 a ± 0.05	0.40 ab ± 0.04	0.42 ab ± 0.04	0.49 b ± 0.03	0.29 a ± 0.06	0.36 a ± 0.04	**<0.001**	16-48
	Root.dry.matter.content.375 g	0.30 ± 0.05	0.32 ± 0.07	0.22 ± 0.09	0.22 ± 0.09	0.41 ± 0.13	0.48 ± 0.09	0.17	6-43
	Root.mass.ratio.150 g	0.46 ± 0.02	0.49 ± 0.03	0.48 ± 0.03	0.48 ± 0.03	0.50 ± 0.04	0.54 ± 0.04	0.60	14-48

Table 4 Continued

	Root.mass.ratio.375 g	0.64 a ± 0.01	0.67 ab ± 0.02	0.62 a ± 0.02	0.64 a ± 0.02	0.70 ab ± 0.03	0.71 b ± 0.02	**<0.001**	8-48
	Fresh.root.biomass.150 g	0.30 ± 0.04	0.29 ± 0.06	0.21 ± 0.06	0.22 ± 0.07	0.14 ± 0.09	0.36 ± 0.08	0.19	13-47
	Fresh.root.biomass.375 g	0.87 ± 0.08	0.93 ± 0.12	0.70 ± 0.16	0.72 ± 0.14	0.95 ± 0.21	1.17 ± 0.15	0.11	8-48
	Dry.root.biomass.150 g	0.09 ± 0.01	0.10 ± 0.01	0.07 ± 0.01	0.07 ± 0.01	0.07 ± 0.02	0.11 ± 0.02	<u>0.05</u>	16-48
	Dry.root.biomass.375 g	0.27 ab ± 0.06	0.31 ab ± 0.08	0.15 a ± 0.10	0.15 a ± 0.09	0.49 ab ± 0.14	0.52 b ± 0.10	**<0.001**	8-47
Growth – whole plant	Total.fresh.biomass.150 g	0.62 ± 0.06	0.57 ± 0.09	0.47 ± 0.09	0.46 ± 0.09	0.34 ± 0.12	0.77 ± 0.12	<u>0.05</u>	16-48
	Total.fresh.biomass.375 g	1.22 ± 0.10	1.14 ± 0.15	0.89 ± 0.20	0.95 ± 0.17	1.35 ± 0.26	1.54 ± 0.18	<u>0.06</u>	8-48
	Total.dry.biomass.150 g	0.20 ± 0.02	0.19 ± 0.02	0.16 ± 0.02	0.16 ± 0.02	0.14 ± 0.03	0.21 ± 0.03	<u>0.08</u>	14-48
	Total.dry.biomass.375 g	0.42 ab ± 0.07	0.46 ab ± 0.10	0.24 a ± 0.13	0.23 a ± 0.11	0.69 ab ± 0.19	0.72 b ± 0.12	**<0.001**	8-47
	Root:shoot.ratio.150 g	0.88 ± 0.07	1.01 ± 0.10	0.85 ± 0.10	0.94 ± 0.10	0.98 ± 0.14	1.20 ± 0.13	0.14	15-48
	Root:shoot.ratio.375 g	1.79 a ± 0.10	2.06 ab ± 0.14	1.68 a ± 0.18	1.68 a ± 0.16	2.36 ab ± 0.25	2.43 b ± 0.17	**<0.001**	8-47
	Root:stem+leaves.ratio.150 g	1.64 ± 0.11	1.75 ± 0.15	1.79 ± 0.15	1.75 ± 0.15	1.67 ± 0.21	2.12 ± 0.20	0.26	16-48
	Root:stem+leaves.ratio.375 g	2.73 a ± 0.08	2.98 a ± 0.13	2.87 a ± 0.17	2.98 a ± 0.13	3.67 b ± 0.22	3.14 ab ± 0.15	**0.003**	8-45
		Resistant (A-B)		Intermediate (C-D)		Susceptible (E-F)			
	Leaf.glu.375 mg/g	0.43 ± 0.02		0.44 ± 0.02		0.45 ± 0.02		0.60	3-8 families

Table 4 Continued

NSC	Leaf.fru.375 mg/g	0.30 a ± 0.04	0.48 b ± 0.06	0.24 a ± 0.09	**0.009**	2-9 families
	Leaf.glu.fru.375 mg/g	0.69 a ± 0.05	0.90 b ± 0.07	0.73 a ± 0.09	**0.02**	2-9 families
	Leaf.suc.375 mg/g	1.33 ± 0.15	1.64 ± 0.21	1.45 ± 0.24	0.32	3-10 families
	Leaf.starch.375 mg/g	0.43 a ± 0.02	0.37 a ± 0.04	0.62 b ± 0.04	**<0.001**	2-9 families
	Leaf.total.sugar.375 mg/g	2.11 ± 0.13	2.43 ± 0.20	2.30 ± 0.23	0.28	3-9 families
	Leaf.total.NSC.375 mg/g	2.56 ± 0.16	3.07 ± 0.23	2.92 ± 0.26	<u>0.08</u>	3-9 families
	Leaf.sugar:NSC.375 mg/g	0.84 b ± 0.01	0.84 b ± 0.02	0.79 a ± 0.02	**0.02**	3-8 families
	Leaf.starch:NSC.375 mg/g	0.17 a ± 0.01	0.16 a ± 0.02	0.21 b ± 0.02	**0.02**	3-8 families
	Root.glu.375 mg/g	0.38 ± 0.02	0.36 ± 0.04	0.44 ± 0.05	0.30	2-8 families
	Root.fru.375 mg/g	0.14 a ± 0.03	0.30 b ± 0.04	0.21 ab ± 0.06	**0.003**	2-7 families
	Root.glu.fru.375 mg/g	0.51 a ± 0.03	0.66 b ± 0.06	0.48 ab ± 0.06	**0.04**	1-6 families
	Root.suc.375 mg/g	1.52 ± 0.11	1.79 ± 0.19	1.46 ± 0.19	0.28	3-9 families
	Root.starch.375 mg/g	0.91 b ± 0.04	0.72 a ± 0.06	0.93 b ± 0.06	**0.001**	3-7 families
	Root.total.sugar.375 mg/g	2.03 a ± 0.13	2.51 b ± 0.20	2.24 ab ± 0.25	**0.04**	2-8 families
	Root.total.NSC.375 mg/g	2.73 a ± 0.09	3.15 b ± 0.15	3.14 ab ± 0.20	**0.01**	2-7 families

Table 4 Continued

	Root.sugar:NSC.375 mg/g	0.70 a ± 0.01	0.77 b ± 0.01	0.70 a ± 0.01	**<0.001**	2-5 families
	Root.starch:NSC.375 mg/g	0.30 b ± 0.01	0.23 a ± 0.01	0.30 b ± 0.01	**<0.001**	2-5 families

Table 5: Estimated means (from logistic regression and linear mixed effects models), ± standard errors (in gray), p-values (significant p-values (p≤0.05) are bolded; marginal p-values are underlined), and sample sizes (N, note: phenology prop (proportion) and NSC traits were measured at the family level and phenology TTE (time-to-event) and growth traits were measured at the individual level; top value = U.S. PIAL (whitebark pine) N, bottom value = PIFL (limber pine) N) for PIAL and PIFL species rust resistance groups (PIAL resistant, intermediate, susceptible; PIFL resistant, susceptible) of phenology (prop, TTE) and growth (aboveground, belowground, whole plant) traits. PIAL rust resistance groups were obtained from A-F resistance levels, where A = highest and F = lowest resistance (PIAL resistant = A-B, PIAL intermediate = C-D, and PIAL susceptible = E-F). PIAL NSC samples were pooled to the family level (8 seedlings homogenized per family, 1 family per tube, 3 families/tubes per rust resistance level, 2 rust resistance levels per rust resistance group). PIFL NSC samples were pooled to the rust resistance group level (5-8 resistant seedlings homogenized per resistance group containing 1-2 seedlings per family resulting in 5-8 families per tube and 1 tube per rust resistance group). Therefore, raw data means (not estimated means) are shown for PIFL with no standard error. For traits with significant p-values, lowercase post-hoc letters distinguish significant differences among the five resistance groups (PIAL resistant, PIAL intermediate, PIAL susceptible, PIFL resistant, PIFL susceptible). Uppercase letters distinguish significant differences among combined resistance groups within PIAL for NSC traits only for ease of comparison with PIFL. An asterisk next to a trait name indicates a complete species difference where no post-hoc letters were shared between species (e.g., PIAL estimates were significantly lower or higher than PIFL estimates). Model estimates that required log transformations show the non-transformed estimate. The number in each trait name indicates the day post sowing (DPS) on which the trait was measured. The two numbers in the prop trait names represent the days that PIAL and PIFL were measured, respectively. Units are listed below each trait name. Emg = emerged, bf = bud formation, nb = needle burst, surv = survived.

		PIAL			PIFL		p-value	N
		Resistant	Intermediate	Susceptible	Resistant	Susceptible		
Phenology	Prop.emg.30.21	0.18 c ± 0.06	0.12 bc ± 0.05	0.12 bc ± 0.07	0.02 ab ± 0.02	0.01 a ± 0.01	**0.001**	7-16 families 5-6 families
	Prop.emg.55.56	0.40 c ± 0.07	0.28 bc ± 0.09	0.22 bc ± 0.09	0.07 ab ± 0.02	0.04 a ± 0.03	**<0.001**	7-16 families 5-6 families
	Prop.bf.30.35	0.14 b ± 0.03	0.07 a ± 0.01	0.08 ab ± 0.02	0.02 a ± 0.01	0.04 ab ± 0.02	**<0.001**	7-14 families 5-6 families
	Prop.bf.95.119	0.37 b ± 0.08	0.25 ab ± 0.09	0.20 ab ± 0.09	0.06 a ± 0.04	0.05 a ± 0.04	**0.003**	7-16 families 5-6 families
	Prop.nb.119.119	0.15 c ± 0.02	0.06 b ± 0.01	0.02 a ± 0.01	0.009 a ± 0.01	0.008 a ± 0.01	**<0.001**	6-16 families 4-6 families

Table 5 Continued

	Prop.nb.161.203	0.17 b ± 0.03	0.08 a ± 0.01	0.08 a ± 0.02	0.03 a ± 0.01	0.04 a ± 0.02	**<0.001**	6-14 families 4-6 families
	Prop.surv.95.91	0.40 b ± 0.08	0.27 ab ± 0.09	0.21 ab ± 0.10	0.06 a ± 0.04	0.05 a ± 0.04	**<0.001**	7-16 families 4-6 families
	TTE.emg days	34.28 ± 1.71	35.16 ± 2.39	34.14 ± 3.04	30.75 ± 3.54	34.05 ± 3.82	0.77	222-692 45-62
	TTE.bf days	41.60 ± 1.07	40.69 ± 0.69	40.00 ± 0.98	39.85 ± 2.54	39.24 ± 2.77	0.98	212-659 33-57
	TTE.nb days	116.60 a ± 2.57	120.43 a ± 3.14	133.64 b ± 4.45	138.71 b ± 5.83	140.34 b ± 6.27	**<0.001**	70-294 23-25
Growth - aboveground	Leaf.area.245 cm^2	25.25 ab ± 1.49	21.91 a ± 1.99	25.26 ab ± 2.48	23.30 ab ± 3.10	33.44 b ± 3.44	**0.01**	46-107 20-22
	Leaf.area.375 cm^2	23.40 ± 1.706	17.42 ± 2.94	20.66 ± 3.28	25.05 ± 4.37	28.65 ± 3.86	<u>0.08</u>	23-79 5-7
	Specific.leaf.area.245 cm^2/g	326.20 a ± 18.83	352.13 ab ± 24.83	406.08 b ± 30.69	278.12 a ± 38.86	318.11 ab ± 41.45	**0.01**	45-108 20-26
	Specific.leaf.area.375 cm^2/g	242.72 ab ± 20.84	304.76 b ± 33.23	174.40 a ± 37.15	286.11 ab ± 52.10	288.10 ab ± 46.41	**0.007**	24-79 5-8
	Leaf.mass.ratio.245 g	0.29 ab ± 0.01	0.28 a ± 0.01	0.28 a ± 0.01	0.35 c ± 0.01	0.33 bc ± 0.02	**<0.001**	45-106 20-26
	Leaf.mass.ratio.375* g	0.26 b ± 0.004	0.26 b ± 0.01	0.22 a ± 0.01	0.32 c ± 0.01	0.32 c ± 0.01	**<0.001**	21-77 5-8
	Leaf.dry.matter.content.245 g	0.43 ± 0.01	0.45 ± 0.01	0.44 ± 0.01	0.44 ± 0.02	0.43 ± 0.02	0.40	41-107 20-27
	Leaf.dry.matter.content.375 g	0.44 a ± 0.02	0.44 a ± 0.03	0.56 b ± 0.03	0.46 ab ± 0.04	0.45 ab ± 0.04	**0.006**	13-72 5-7
	Leaf.thickness.245 (m^2/g)$^{-1}$	89.37 b ± 4.32	75.72 ab ± 5.27	66.50 a ± 6.59	90.30 b ± 8.88	88.09 ab ± 9.63	**<0.001**	46-103 20-22
	Leaf.thickness.375 (m^2/g)$^{-1}$	113.03 ± 12.88	86.34 ± 16.78	138.15 ± 19.23	85.75 ± 28.47	85.51 ± 32.97	0.12	23-78 5-7
	Leaf.mass.area.245 g/m^2	36.91 ab ± 1.74	33.90 ab ± 2.29	28.92 a ± 2.84	39.15 b ± 3.58	38.03 ab ± 3.81	**0.01**	45-108 20-22

Table 5 Continued

	Leaf.mass.area.375 g/m²	50.71 ab ± 5.60	35.86 a ± 7.94	74.65 b ± 8.99	39.26 ab ± 12.96	37.16 ab ± 12.26	**0.007**	24-79 5-8
	Fresh.leaf.biomass.245 g	0.20 ab ± 0.01	0.16 a ± 0.02	0.15 a ± 0.02	0.19 ab ± 0.03	0.28 b ± 0.03	**0.003**	46-109 20-28
	Fresh.leaf.biomass.375 g	0.24 b ± 0.02	0.16 a ± 0.02	0.28 b ± 0.02	0.19 ab ± 0.04	0.24 ab ± 0.05	**<0.001**	23-77 5-6
	Dry.leaf.biomass.245 g	0.09 ab ± 0.01	0.07 a ± 0.01	0.06 a ± 0.01	0.08 ab ± 0.01	0.12 b ± 0.01	**0.002**	46-108 20-28
	Dry.leaf.biomass.375 g	0.11 b ± 0.01	0.06 a ± 0.01	0.15 c ± 0.01	0.09 abc ± 0.02	0.12 abc ± 0.02	**<0.001**	24-79 5-8
	Stem.diameter.97 mm	1.10 ± 0.05	1.00 ± 0.05	1.03 ± 0.07	0.90 ± 0.09	0.98 ± 0.10	0.18	57-139 26-39
	Stem.diameter.160 mm	1.36 b ± 0.04	1.33 b ± 0.05	1.28 ab ± 0.07	1.12 a ± 0.08	1.34 ab ± 0.08	**0.01**	56-134 22-36
	Stem.diameter.221 mm	1.59 ab ± 0.03	1.57 ab ± 0.05	1.48 a ± 0.06	1.47 ab ± 0.07	1.71 b ± 0.08	**0.006**	56-132 25-34
	Seedling.height.97 cm	2.35 ± 0.09	2.34 ± 0.12	2.42 ± 0.15	2.35 ± 0.18	2.28 ± 0.20	0.96	57-140 26-41
	Seedling.height.160 cm	2.75 ± 0.08	2.65 ± 0.12	2.72 ± 0.15	2.68 ± 0.17	2.59 ± 0.19	0.88	53-124 23-33
	Seedling.height.221 cm	3.23 ± 0.09	3.04 ± 0.12	3.10 ± 0.15	2.95 ± 0.18	2.99 ± 0.20	0.35	53-123 24-31
	Stem.diameter. growth.rate.221 mm/day	0.003 ± 0.0003	0.004 ± 0.0004	0.003 ± 0.0005	0.004 ± 0.0007	0.005 ± 0.0008	0.05	55-129 23-33
	Seedling.height. growth.rate.221 cm/day	0.002 ± 0.0002	0.002 ± 0.0002	0.002 ± 0.0002	0.002 ± 0.0003	0.002 ± 0.0004	0.28	53-119 21-30
	Fresh.stem.biomass.245 g	0.07 ± 0.004	0.06 ± 0.006	0.06 ± 0.008	0.05 ± 0.009	0.07 ± 0.01	0.08	45-108 20-28
	Fresh.stem.biomass.375 g	0.08 b ± 0.01	0.06 a ± 0.01	0.10 c ± 0.01	0.06 abc ± 0.01	0.07 abc ± 0.02	**<0.001**	22-78 5-7

Table 5 Continued

	Dry.stem.biomass.245 g	0.03 ± 0.002	0.03 ± 0.003	0.03 ± 0.003	0.02 ± 0.004	0.03 ± 0.004	0.22	46-108 19-27
	Dry.stem.biomass.375 g	0.04 b ± 0.004	0.02 a ± 0.004	0.06 c ± 0.005	0.03 ab ± 0.009	0.03 ab ± 0.008	**<0.001**	24-80 5-8
Growth - belowground	Total.root.length.245 cm	275.96 ± 24.30	262.98 ± 29.24	272.07 ± 37.51	266.65 ± 49.26	334.68 ± 56.77	0.74	45-105 20-28
	Total.root.length.375 cm	260.28 ± 17.29	224.60 ± 22.49	250.94 ± 25.80	252.91 ± 41.96	278.33 ± 38.92	0.53	23-77 5-8
	Root.diameter.245 mm	1.16 ± 0.07	1.16 ± 0.09	1.26 ± 0.11	1.31 ± 0.12	1.23 ± 0.14	0.91	45-105 20-28
	Root.diameter.375 mm	1.01 a ± 0.05	1.26 b ± 0.08	1.14 ab ± 0.09	1.32 ab ± 0.16	1.27 ab ± 0.11	<u>0.05</u>	24-80 5-8
	Root.surface.area.245 cm^2	112.28 ± 10.14	113.08 ± 13.41	122.54 ± 16.79	126.33 ± 20.03	136.70 ± 23.26	0.82	45-105 20-27
	Root.surface.area.375 cm^2	83.10 ± 5.99	95.72 ± 8.74	100.90 ± 9.82	102.01 ± 17.62	109.34 ± 14.30	0.20	24-80 5-8
	Root.volume.245 cm^3	11.01 ± 1.11	10.50 ± 1.59	11.66 ± 1.92	12.18 ± 2.17	12.84 ± 2.52	0.87	45-104 20-27
	Root.volume.375 cm^3	6.42 ± 0.56	8.12 ± 0.89	7.97 ± 1.01	8.34 ± 1.70	9.17 ± 1.33	0.13	24-79 5-8
	Specific.root.length.245 cm/g	1568.27 ± 118.41	1772.66 ± 134.80	1818.99 ± 173.38	2094.22 ± 235.96	1642.02 ± 265.61	0.13	45-103 20-27
	Specific.root.length.375 cm/g	1035.90 b ± 71.50	1559.23 c ± 101.43	618.14 a ± 115.50	1633.02 bc ± 202.08	1409.30 bc ± 169.09	**<0.001**	21-79 5-8
	Root.tissue.density.245 g/cm^3	0.45 ± 0.15	0.46 ± 0.20	0.49 ± 0.25	0.28 ± 0.30	0.19 ± 0.35	0.86	45-105 20-26
	Root.tissue.density.375 g/cm^3	0.05 b ± 0.004	0.02 a ± 0.01	0.06 b ± 0.01	0.02 ab ± 0.01	0.03 ab ± 0.01	**<0.001**	18-68 5-8
	Root.dry.matter.content.245 g	0.38 ± 0.04	0.45 ± 0.06	0.43 ± 0.07	0.42 ± 0.08	0.46 ± 0.10	0.81	44-106 20-26
	Root.dry.matter.content.375 g	0.31 ab ± 0.03	0.22 a ± 0.05	0.44 b ± 0.05	0.30 ab ± 0.06	0.30 ab ± 0.07	**0.01**	15-75 5-7

Table 5 Continued

	Root.mass.ratio.245 g	0.61 b ± 0.01	0.61 ab ± 0.01	0.61 ab ± 0.01	0.56 a ± 0.02	0.58 b ± 0.02	**0.04**	46-107 20-26
	Root.mass.ratio.375 g	0.65 b ± 0.01	0.63 ab ± 0.02	0.71 c ± 0.02	0.58 a ± 0.02	0.60 ab ± 0.02	**<0.001**	23-78 5-8
	Fresh.root.biomass.245 g	0.54 ± 0.06	0.39 ± 0.08	0.42 ± 0.10	0.40 ± 0.12	0.51 ± 0.14	0.22	46-109 20-25
	Fresh.root.biomass.375 g	0.86 ab ± 0.06	0.70 a ± 0.10	1.11 b ± 0.11	0.52 a ± 0.16	0.77 ab ± 0.15	**0.004**	24-80 5-7
	Dry.root.biomass.245 g	0.18 ± 0.01	0.15 ± 0.01	0.15 ± 0.02	0.13 ± 0.02	0.20 ± 0.03	0.05	46-109 20-28
	Dry.root.biomass.375 g	0.28 b ± 0.04	0.15 a ± 0.06	0.51 c ± 0.07	0.16 ab ± 0.09	0.22 ab ± 0.08	**<0.001**	24-76 5-8
Growth – whole plant	Total.fresh.biomass.245 g	0.80 ± 0.07	0.60 ± 0.09	0.63 ± 0.11	0.59 ± 0.14	0.84 ± 0.17	0.10	46-108 20-27
	Total.fresh.biomass.375 g	1.22 bc ± 0.07	0.92 a ± 0.10	1.50 c ± 0.12	0.76 ab ± 0.19	1.11 abc ± 0.18	**<0.001**	24-77 5-7
	Total.dry.biomass.245 g	0.29 ± 0.02	0.24 ± 0.02	0.24 ± 0.03	0.22 ± 0.04	0.34 ± 0.04	0.05	46-109 20-27
	Total.dry.biomass.375 g	0.42 b ± 0.04	0.24 a ± 0.05	0.65 c ± 0.06	0.27 ab ± 0.09	0.36 ab ± 0.09	**<0.001**	22-80 5-8
	Root:shoot.ratio.245 g	1.61 b ± 0.06	1.59 ab ± 0.08	1.59 ab ± 0.10	1.29 a ± 0.12	1.43 ab ± 0.14	**0.05**	46-107 20-26
	Root:shoot.ratio.375 g	1.89 b ± 0.07	1.70 ab ± 0.13	2.43 c ± 0.14	1.40 a ± 0.20	1.52 ab ± 0.16	**<0.001**	22-77 5-8
	Root:stem+leaves.ratio.245 g	2.54 b ± 0.08	2.63 b ± 0.10	2.68 b ± 0.13	1.87 a ± 0.17	2.20 ab ± 0.20	**<0.001**	45-106 19-26
	Root:stem+leaves.ratio.375* g	2.86 b ± 0.06	2.93 b ± 0.10	3.43 c ± 0.12	2.10 a ± 0.21	2.17 a ± 0.15	**<0.001**	21-78 5-8
		PIAL			PIFL		p-value	N
		Resistant	Intermediate	Susceptible	Resistant	Susceptible		

Table 5 Continued

NSC	Leaf.glu.375 mg/g	0.40 ± 0.03	0.44 ± 0.01	0.45 ± 0.05	0.24	0.40	NA	24-64 seedlings 5-8 seedlings
	Leaf.fru.375 mg/g	0.32 A ± 0.04	0.45 B ± 0.05	0.41 A ± 0.17	0.22	0.32	NA	16-72 seedlings 5-8 seedlings
	Leaf.glu.fru.375 mg/g	0.71 A ± 0.04	0.88 B ± 0.06	0.86 A ± 0.15	0.46	0.71	NA	24-80 seedlings 5-8 seedlings
	Leaf.suc.375 mg/g	1.34 ± 0.12	1.62 ± 0.26	1.46 ± 0.22	2.19	4.08	NA	16-72 seedlings 5-8 seedlings
	Leaf.starch.375 mg/g	0.48 A ± 0.19	0.59 A ± 0.25	0.60 B ± 0.06	0.19	0.52	NA	16-72 seedlings 5-8 seedlings
	Leaf.total.sugar.375 mg/g	2.11 ± 0.10	2.50 ± 0.28	2.32 ± 0.11	2.65	4.79	NA	24-72 seedlings 5-8 seedlings
	Leaf.total.NSC.375 mg/g	2.59 ± 0.11	3.09 ± 0.36	2.91 ± 0.08	2.84	5.32	NA	24-72 seedlings 5-8 seedlings
	Leaf.sugar:NSC.375 mg/g	0.81 B ± 0.02	0.81 B ± 0.03	0.79 A ± 0.02	0.93	0.90	NA	24-64 seedlings 5-8 seedlings
	Leaf.starch:NSC.375 mg/g	0.18 A ± 0.02	0.19 A ± 0.03	0.21 B ± 0.02	0.07	0.10	NA	24-64 seedlings 5-8 seedlings
	Root.glu.375 mg/g	0.39 ± 0.02	0.35 ± 0.05	0.38 ± 0.07	0.48	0.58	NA	16-64 seedlings 5-8 seedlings
	Root.fru.375 mg/g	0.13 A ± 0.03	0.29 B ± 0.04	0.20 AB ± 0.03	0.22	0.10	NA	16-56 seedlings 5-8 seedlings
	Root.glu.fru.375 mg/g	0.53 A ± 0.02	0.63 B ± 0.08	0.55 AB ± 0.08	0.70	0.69	NA	24-72 seedlings 5-8 seedlings
	Root.suc.375 mg/g	1.54 ± 0.11	1.65 ± 0.19	1.50 ± 0.14	1.56	1.34	NA	24-56 seedlings 5-8 seedlings
	Root.starch.375 mg/g	0.72 B ± 0.11	0.65 A ± 0.09	0.94 B ± 0.05	0.80	0.88	NA	8-48 seedlings 5-8 seedlings
	Root.total.sugar.375 mg/g	2.1 A ± 0.15	2.29 B ± 0.16	2.19 AB ± 0.17	2.26	2.02	NA	16-64 seedlings 5-8 seedlings
	Root.total.nsc.375 mg/g	2.88 A ± 0.17	2.94 B ± 0.25	3.14 AB ± 0.26	3.05	2.90	NA	16-56 seedlings 5-8 seedlings

Table 5 Continued

	Root.sugar:NSC.375 mg/g	0.72 A ± 0.03	0.78 B ± 0.02	0.70 A ± 0.002	0.74	0.70	NA	16-40 seedlings 5-8 seedlings
	Root.starch:NSC.375 mg/g	0.28 B ± 0.03	0.22 A ± 0.02	0.30 B ± 0.003	0.26	0.30	NA	16-40 seedlings 5-8 seedlings

Figures

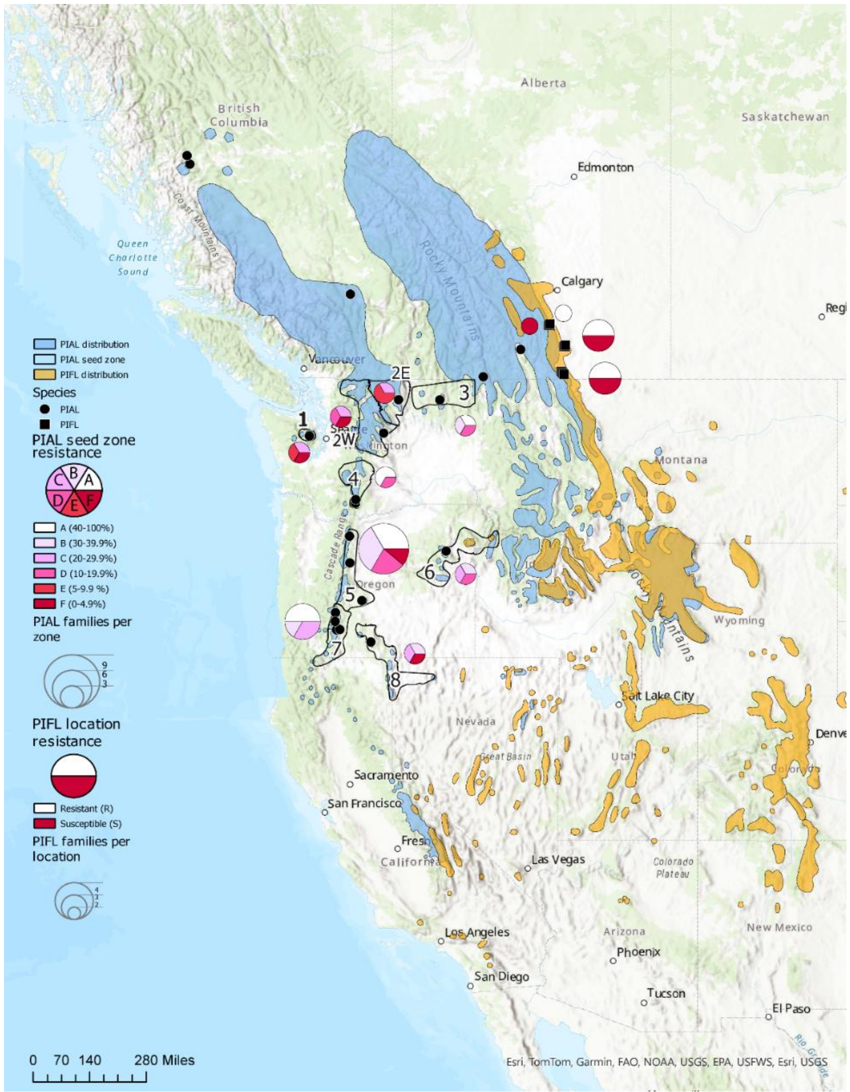

Figure 1. PIAL (whitebark pine, blue) and PIFL (limber pine, orange) species distributions with seed source family locations (black circles=PIAL, black squares=PIFL). U.S. PIAL seed zones (USFS region 6) are labeled (1-8) and outlined in black. Pie chart colors indicate the proportion of families at each resistance level for each seed zone (PIAL, A = most resistant, F = least resistant) or location (PIFL, resistant or susceptible). Pie chart size indicates the number of families per PIAL seed zone (3-9 families per seed zone) and number of families per PIFL location (2-4 families per location). B.C. PIAL did not have any rust resistance data. Seed source location details in Appx. Table 1.

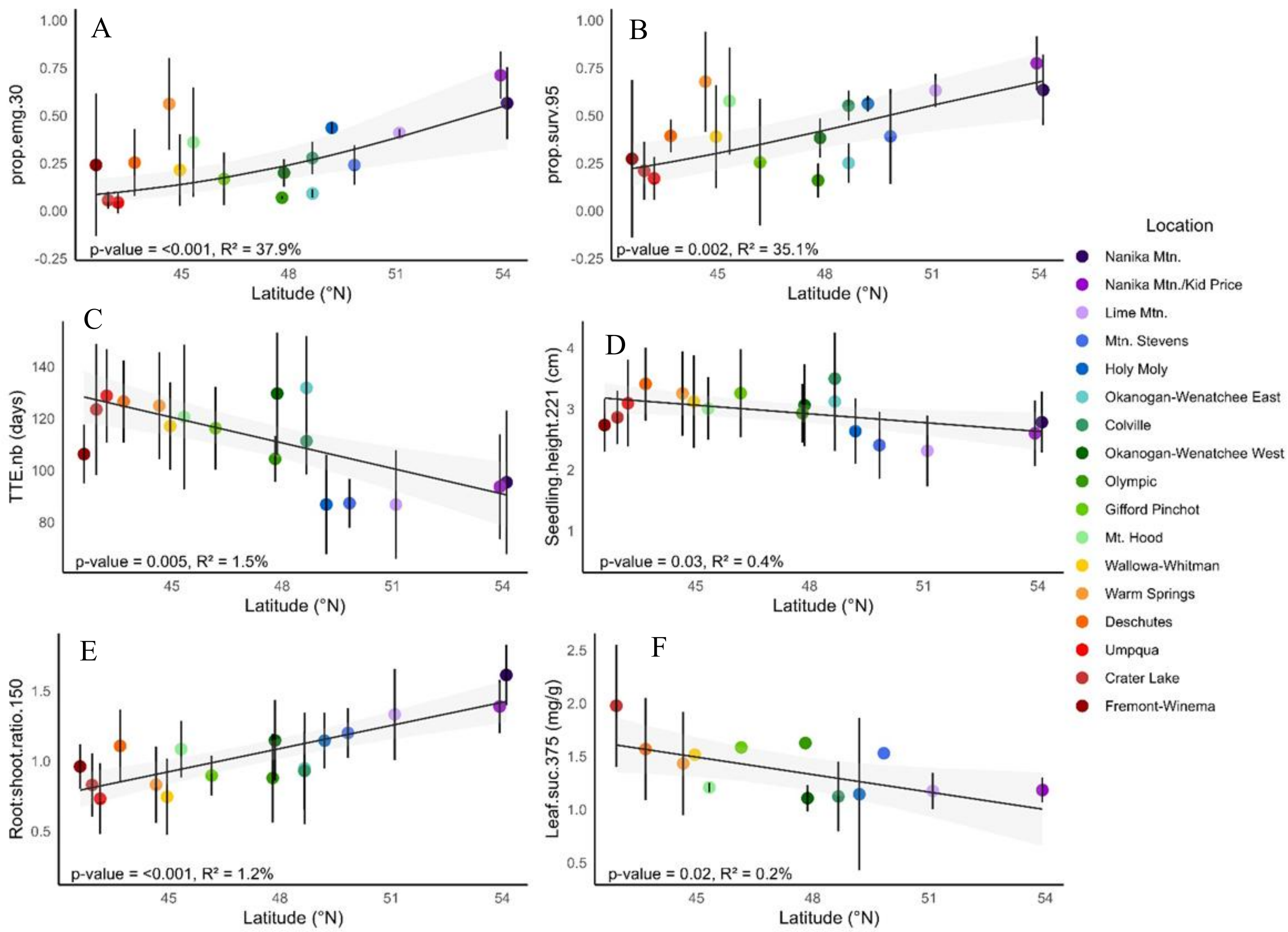

Figure 2. Selected trait relationships with latitude (˚N) for U.S. and B.C. PIAL (whitebark pine) locations (n=12 and 5 locations, respectively; 3 families per location, 51 families total) including: A) the proportion emerged at 30 days post sowing (DPS) (prop.emg.30), B) the proportion survived at 95 DPS (prop.surv.95), C) time-to-event for needle burst (TTE.nb), D) seedling height at 221 DPS (seedling.height.221; E), root-to-shoot ratio at 150 DPS (root:shoot.ratio.150), and F) leaf sucrose concentration at 375 DPS (leaf.suc.375, mg compound/g leaf dry weight). P-values and conditional R_2 (fixed + random) were obtained from binomial logistic regression models (A-B) and linear mixed effects models (C-F). The gray ribbon around the black trendline represents the 95% confidence interval. Vertical error bars represent the standard deviation of the families (n=3) within each location. Phenology proportion variables (A-B) are shown on the proportion scale (rather than log-odds) for ease of interpretation. Parent tree locations in the legend are listed from highest to lowest latitude.

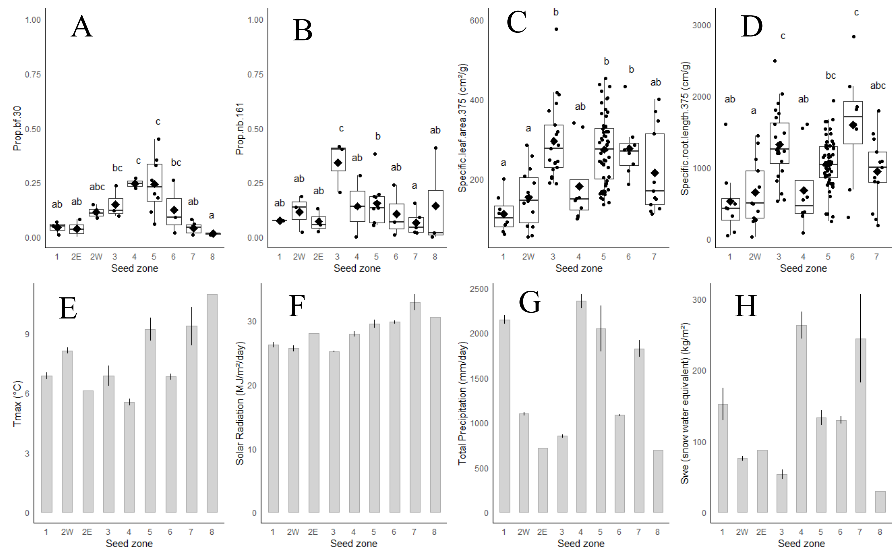

Figure 3. Selected traits that significantly (p≤0.05) differed among U.S. PIAL (whitebark pine) seed zones (USFS Region 6, OR, WA) included: A) the proportion with needle burst at 161 days post sowing (DPS) (prop.nb.161), B) the proportion survived at 95 DPS (prop.surv.95), C) specific leaf area at 375 DPS (specific.leaf.area.375), and D) specific root length at 375 DPS (specific.root.length.375). P-values were obtained from binomial logistic regression models. The height of the box represents the interquartile range (IQR), with the bottom and top of the box representing the 25th and 75th percentiles. The black horizontal line and black diamond are the median and mean, respectively. Vertical lines (whiskers) extending from the box show the smallest and largest values within 1.5x the IQR. Black circles represent raw data points with points outside of the whiskers representing values outside 1.5x the IQR. Lowercase letters distinguish significant differences in estimated means among seed zones. Selected climate variables of each seed zone were averaged over 12 months per year and then the annual average was averaged from 1992-2021 for each seed zone (n=3-9 families/zone) and included: E) Tmax (˚C), F) solar radiation (Srad, MJ/m2/day), G) total precipitation (mm/day), and H) SWE (snow water equivalent, kg/m2). Vertical error bars show the standard error of means for families within each seed zone. Climate details and calculations are included in the Methods. No error bar indicates that families within those zones (2E, 8) had the same climate value due to being in proximity. Since no data was obtained on day 375 for zones 2E and 8, no bar charts were included for those zones.

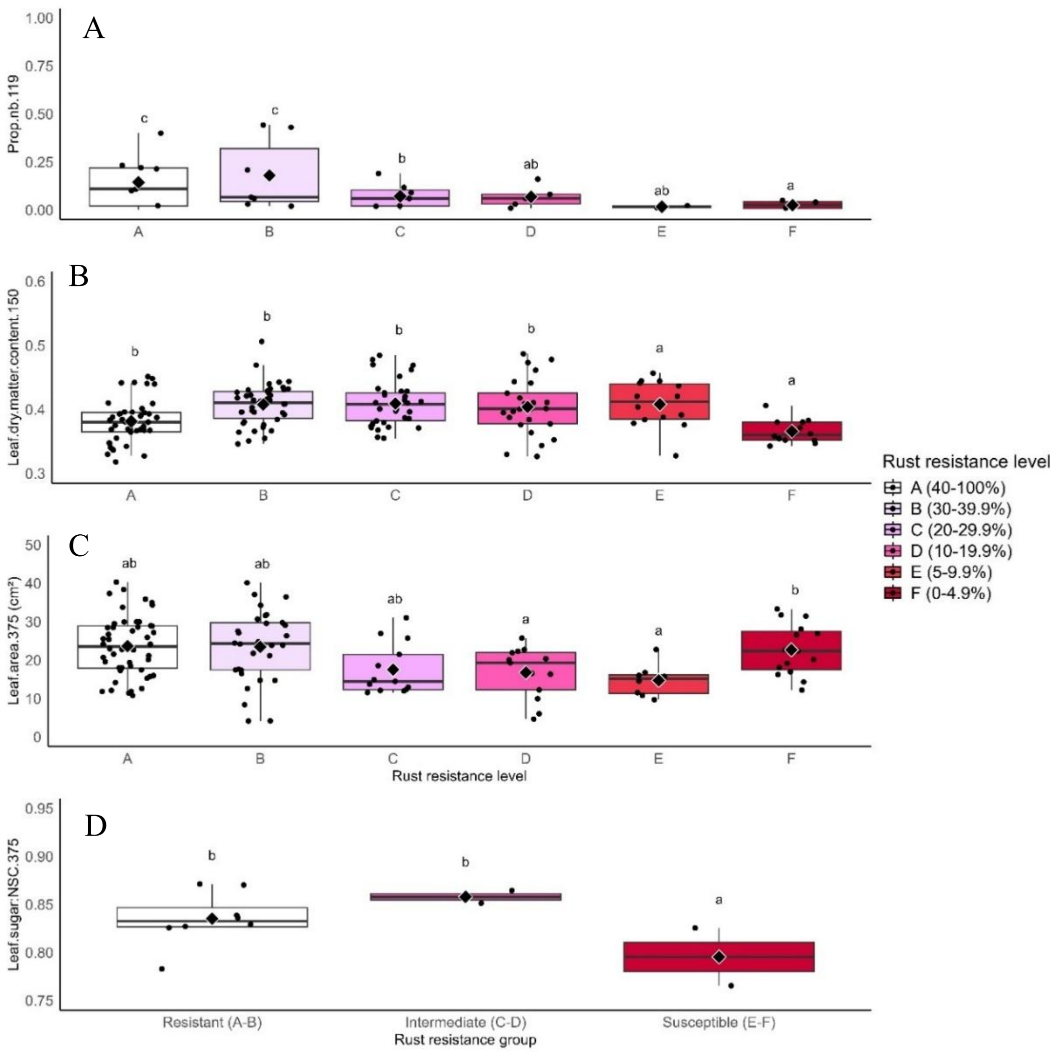

Figure 4. Selected traits that significantly ($p \leq 0.05$) differed among U.S. PIAL (whitebark pine) rust resistance levels (A-F, A = most resistant (40-100% of progeny have low to absent stem symptoms), F = least resistant (0-4.9% of progeny have low to absent stem symptoms (Sniezko et al. 2023); n= 1-6 families per level) and rust resistance groups (resistant (A-B), intermediate (C-D), susceptible (E-F); n=3-10 families per group) included: A) time-to-event for needle burst (TTE.nb), B) leaf dry matter content at 150 days post sowing (DPS) (leaf.dry.matter.content.150), C) leaf area at 150 DPS (leaf.area.150), and D) leaf sugar to total NSC at 375 DPS (leaf.sugar:NSC.375). P-values were obtained from linear mixed effects models. The height of the box represents the interquartile range (IQR), with the bottom and top of the box representing the 25th and 75th quartiles. The black horizontal line and black diamond are the median and mean, respectively. Vertical lines (whiskers) extending from the box show the smallest and largest values within 1.5x the IQR. Black circles represent raw data points with points outside of the whiskers representing values outside 1.5x the IQR. Lowercase letters distinguish significant differences in estimated means among rust resistance levels and groups.

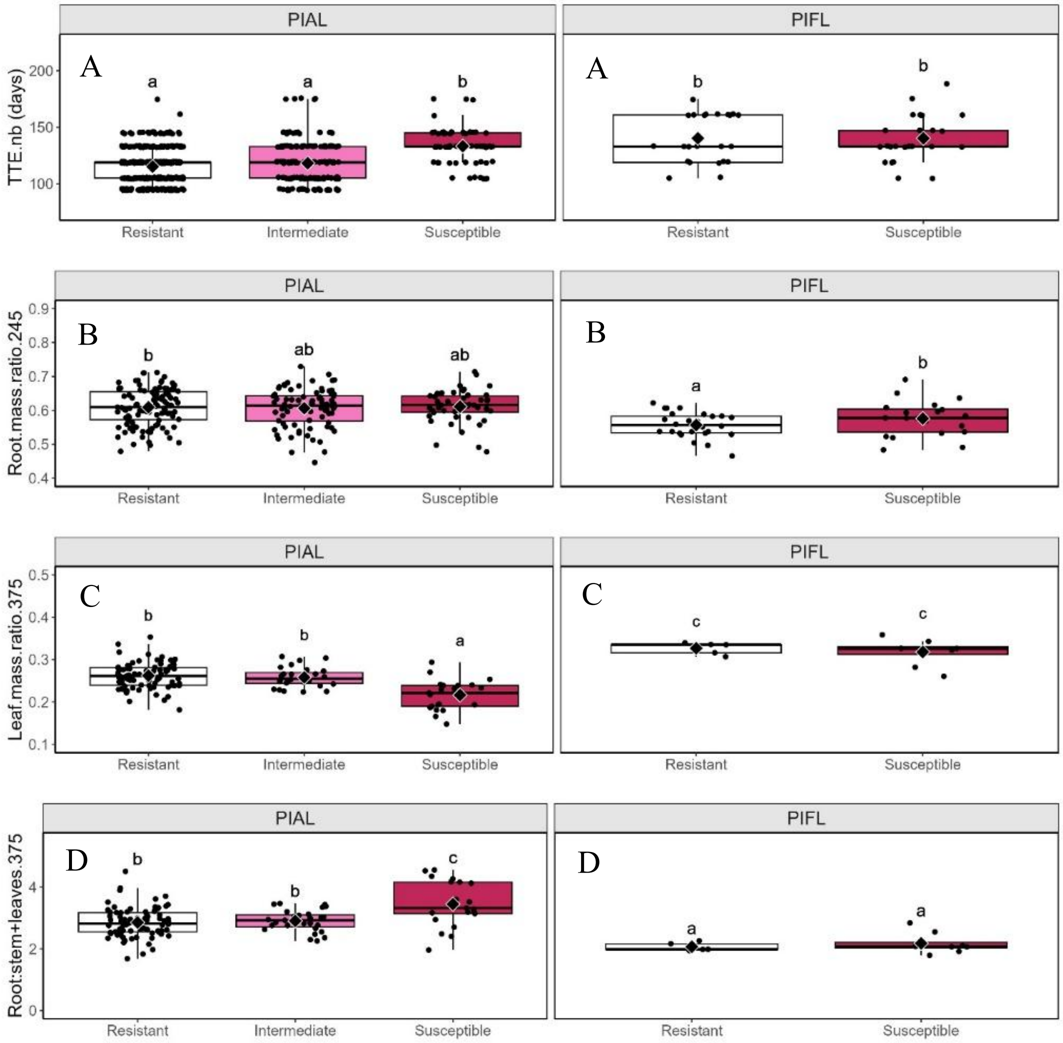

Figure 5. Selected traits that significantly ($p \leq 0.05$) differed among U.S. PIAL (whitebark pine) rust resistance groups (resistant (A-B), intermediate (C-D), susceptible (E-F); n=3-10 families per group) and PIFL (n=5-6 families per group) included: A) time-to-event for needle burst (TTE.nb; strong difference among PIAL and PIFL species), B) root mass ratio at 245 days post sowing (DPS) (root.mass.ratio.245, the only trait where PIFL R and S differed), C) leaf mass ratio at 375 DPS (leaf.mass.ratio.375, complete species difference with PIAL R and S differing but not PIFL R and S), and D) root to stem+leaves ratio at 375 DPS (root:stem+leaves.ratio.375, complete species difference with PIAL R and S differing but not PIFL R and S). P-values were obtained from linear mixed effects models. The height of the box represents the interquartile range (IQR), with the bottom and top of the box representing the 25th and 75th quartiles. The black horizontal line and black diamond are the median and mean, respectively. Vertical lines (whiskers) extending from the box show the smallest and largest values within 1.5x the IQR. Black circles represent raw data points with points outside of the whiskers representing values outside 1.5x the IQR. Lowercase letters distinguish significant differences in estimated means among rust resistance groups.

REFERENCES CITED

Aitken, S. N., Yeaman, S., Holliday, J. A., Wang, T., & Curtis-McLane, S. (2008). Adaptation, migration or extirpation: Climate change outcomes for tree populations. *Evolutionary Applications*, *1*(1), 95–111. https://doi.org/10.1111/j.1752-4571.2007.00013.x

Allen, C. D., Breshears, D. D., & McDowell, N. G. (2015). On underestimation of global vulnerability to tree mortality and forest die-off from hotter drought in the Anthropocene. *Ecosphere*, *6*(8), art129. https://doi.org/10.1890/ES15-00203.1

Allen, C. D., Macalady, A. K., Chenchouni, H., Bachelet, D., McDowell, N., Vennetier, M., Kitzberger, T., Rigling, A., Breshears, D. D., Hogg, E. H. (Ted), Gonzalez, P., Fensham, R., Zhang, Z., Castro, J., Demidova, N., Lim, J.-H., Allard, G., Running, S. W., Semerci, A., & Cobb, N. (2010). A global overview of drought and heat-induced tree mortality reveals emerging climate change risks for forests. *Forest Ecology and Management*, *259*(4), 660–684. https://doi.org/10.1016/j.foreco.2009.09.001

Alongi, F., Hansen, A. J., Laufenberg, D., Keane, R. E., Legg, K., & Lavin, M. (2020). *Using genetics to distinguish limber from whitebark pine*.

Anderegg, W. R. L., Hicke, J. A., Fisher, R. A., Allen, C. D., Aukema, J., Bentz, B., Hood, S., Lichstein, J. W., Macalady, A. K., McDowell, N., Pan, Y., Raffa, K., Sala, A., Shaw, J. D., Stephenson, N. L., Tague, C., & Zeppel, M. (2015). Tree mortality from drought, insects, and their interactions in a changing climate. *New Phytologist*, *208*(3), 674–683. https://doi.org/10.1111/nph.13477

Aubry, C. A., Goheen, D., Shoal, R., & Lorenz, T. (2008). *Aubry, C., Goheen, D. G., Shoal, R., Ohlson, T., Lorenz, T., Bower, A. D.,Mehmel, C., & Sniezko, R. A. (2008). Whitebark pine restoration strategyfor the Pacific Northwest 2009–2013. U.S. Department of Agriculture,Forest Service, Pacific Northwest Region. 212p*.

Bartoń, K. (2025). *MuMIn: Multi-Model Inference* (Version 1.48.11) [Computer software]. https://cran.r-project.org/web/packages/MuMIn/index.html

Basler, D., & Körner, C. (2012). Photoperiod sensitivity of bud burst in 14 temperate forest tree species. *Agricultural and Forest Meteorology*, *165*, 73–81. https://doi.org/10.1016/j.agrformet.2012.06.001

Bates, D., Mächler, M., Bolker, B., & Walker, S. (2015). Fitting Linear Mixed-Effects Models Using lme4. *Journal of Statistical Software*, *67*, 1–48. https://doi.org/10.18637/jss.v067.i01

Baughman, O. W., Agneray, A. C., Forister, M. L., Kilkenny, F. F., Espeland, E. K., Fiegener, R., Horning, M. E., Johnson, R. C., Kaye, T. N., Ott, J., St. Clair, J. B., & Leger, E. A. (2019). Strong patterns of intraspecific variation and local adaptation in Great Basin plants revealed through a review of 75 years of experiments. *Ecology and Evolution*, *9*(11), 6259–6275. https://doi.org/10.1002/ece3.5200

Bentz, B. J., Millar, C. I., Vandygriff, J. C., & Hansen, E. M. (2022). Great Basin bristlecone pine mortality: Causal factors and management implications. *Forest Ecology and Management*, *509*, 120099. https://doi.org/10.1016/j.foreco.2022.120099

Bisbing, S. M., Urza, A. K., Buma, B. J., Cooper, D. J., Matocq, M., & Angert, A. L. (2021). Can long-lived species keep pace with climate change? Evidence of local persistence potential in a widespread conifer. *Diversity and Distributions*, *27*(2), 296–312. https://doi.org/10.1111/ddi.13191

Blumstein, M., Gersony, J., Martínez-Vilalta, J., & Sala, A. (2023). Global variation in nonstructural carbohydrate stores in response to climate. *Global Change Biology*, *29*(7), 1854–1869. https://doi.org/10.1111/gcb.16573

Borgman, E. M., Schoettle, A. W., & Angert, A. L. (2015). Assessing the potential for maladaptation during active management of limber pine populations: A common garden study detects genetic differentiation in response to soil moisture in the Southern Rocky Mountains. *Canadian Journal of Forest Research*, *45*(4), 496–505. https://doi.org/10.1139/cjfr-2014-0399

Bower, A. D., & Aitken, S. N. (2008). Ecological genetics and seed transfer guidelines for Pinus albicaulis (Pinaceae). *American Journal of Botany*, *95*(1), 66–76. https://doi.org/10.3732/ajb.95.1.66

Bower, A. D., Clair, J. B. St., & Erickson, V. (2014). Generalized provisional seed zones for native plants. *Ecological Applications*, *24*(5), 913–919. https://doi.org/10.1890/13-0285.1

Bradley St Clair, J., & Howe, G. T. (2007). Genetic maladaptation of coastal Douglas-fir seedlings to future climates. *Global Change Biology*, *13*(7), 1441–1454. https://doi.org/10.1111/j.1365-2486.2007.01385.x

Brodersen, C. R., Germino, M. J., Johnson, D. M., Reinhardt, K., Smith, W. K., Resler, L. M., Bader, M. Y., Sala, A., Kueppers, L. M., Broll, G., Cairns, D. M., Holtmeier, F.-K., & Wieser, G. (2019). Seedling Survival at Timberline Is Critical to Conifer Mountain Forest Elevation and Extent. *Frontiers in Forests and Global Change*, *2*. https://doi.org/10.3389/ffgc.2019.00009

Brooks, M., E., Kristensen, K., Benthem, K., J. ,van, Magnusson, A., Berg, C., W., Nielsen, A., Skaug, H., J., Mächler, M., & Bolker, B., M. (2017). glmmTMB Balances Speed and Flexibility Among Packages for Zero-inflated Generalized Linear Mixed Modeling. *The R Journal*, *9*(2), 378. https://doi.org/10.32614/RJ-2017-066

Brunner, I., Herzog, C., Dawes, M. A., Arend, M., & Sperisen, C. (2015). How tree roots respond to drought. *Frontiers in Plant Science*, *6*. https://doi.org/10.3389/fpls.2015.00547

Burns, K. S., Tinkham, W. T., Leddy, K. A., Schoettle, A. W., Jacobi, W. R., & Stewart, J. E. (2023). Interactions between white pine blister rust, bark beetles, and climate over time indicate vulnerabilities to limber pine health. *Frontiers in Forests and Global Change*, *6*. https://doi.org/10.3389/ffgc.2023.1149456

Chmura, D. J., Anderson, P. D., Howe, G. T., Harrington, C. A., Halofsky, J. E., Peterson, D. L., Shaw, D. C., & Brad St.Clair, J. (2011). Forest responses to climate change in the northwestern United States: Ecophysiological foundations for adaptive management. *Forest Ecology and Management*, *261*(7), 1121–1142. https://doi.org/10.1016/j.foreco.2010.12.040

Cleaver, C. M., Jacobi, W. R., Burns, K. S., & Means, R. E. (2015). Limber pine in the central and southern Rocky Mountains: Stand conditions and interactions with blister rust, mistletoe, and bark beetles. *Forest Ecology and Management*, *358*, 139–153. https://doi.org/10.1016/j.foreco.2015.09.010

Comas, L., Becker, S., Cruz, V. M. V., Byrne, P. F., & Dierig, D. A. (2013). Root traits contributing to plant productivity under drought. *Frontiers in Plant Science*, *4*. https://doi.org/10.3389/fpls.2013.00442

Coop, J. D., & Schoettle, A. W. (2009). Regeneration of Rocky Mountain bristlecone pine (*Pinus aristata*) and limber pine (*Pinus flexilis*) three decades after stand-replacing fires. *Forest Ecology and Management*, *257*(3), 893–903. https://doi.org/10.1016/j.foreco.2008.10.034

COSEWIC. (2014). https://www.sararegistry.gc.ca/virtual_sara/files/cosewic/CESCC_1014_e.pdf

de Villemereuil, P., Gaggiotti, O. E., Mouterde, M., & Till-Bottraud, I. (2016). Common garden experiments in the genomic era: New perspectives and opportunities. *Heredity*, *116*(3), 249–254. https://doi.org/10.1038/hdy.2015.93

Dickman, L. T., Mcdowell, N. G., Sevanto, S., Pangle, R. E., & Pockman, W. T. (2015). Carbohydrate dynamics and mortality in a piñon-juniper woodland under three future precipitation scenarios. *Plant, Cell & Environment*, *38*(4), 729–739. https://doi.org/10.1111/pce.12441

Dobrowski, S. Z., Swanson, A. K., Abatzoglou, J. T., Holden, Z. A., Safford, H. D., Schwartz, M. K., & Gavin, D. G. (2015). Forest structure and species traits mediate projected recruitment declines in western US tree species. *Global Ecology and Biogeography*, *24*(8), 917–927. https://doi.org/10.1111/geb.12302

Dubos, C., & Plomion, C. (2001). Drought differentially affects expression of a PR-10 protein, in needles of maritime pine (Pinus pinaster Ait.) seedlings. *Journal of Experimental Botany*, *52*(358), 1143–1144. https://doi.org/10.1093/jexbot/52.358.1143

Dudney, J. C., Nesmith, J. C. B., Cahill, M. C., Cribbs, J. E., Duriscoe, D. M., Das, A. J., Stephenson, N. L., & Battles, J. J. (2020). Compounding effects of white pine blister rust, mountain pine beetle, and fire threaten four white pine species. *Ecosphere*, *11*(10), e03263. https://doi.org/10.1002/ecs2.3263

Dudney, J., Willing, C. E., Das, A. J., Latimer, A. M., Nesmith, J. C. B., & Battles, J. J. (2021). Nonlinear shifts in infectious rust disease due to climate change. *Nature Communications*, *12*(1), 5102. https://doi.org/10.1038/s41467-021-25182-6

Ekramoddoullah, A. K. M., & Liu, J. J. (2008). Molecular mapping of the Pinus monticola Cr2 gene using AFLP and SCAR markers. *Annals of Forest Research*, *51*, 147–148. https://doi.org/10.15287/afr.2008.153

Fajardo, A., Piper, F. I., Pfund, L., Körner, C., & Hoch, G. (2012). Variation of mobile carbon reserves in trees at the alpine treeline ecotone is under environmental control. *New Phytologist*, *195*(4), 794–802. https://doi.org/10.1111/j.1469-8137.2012.04214.x

Fox, & Weisenberg. (2019). *R Companion 3E*. https://www.john-fox.ca/Companion/

Frankham, R., Bradshaw, C. J. A., & Brook, B. W. (2014). Genetics in conservation management: Revised recommendations for the 50/500 rules, Red List criteria and population viability analyses. *Biological Conservation*, *170*, 56–63. https://doi.org/10.1016/j.biocon.2013.12.036

Geils, B. W., Hummer, K. E., & Hunt, R. S. (2010). White pines, Ribes, and blister rust: A review and synthesis. *Forest Pathology*, *40*(3–4), 147–185. https://doi.org/10.1111/j.1439-0329.2010.00654.x

Germino, M. J., & Smith, W. K. (1999). Sky exposure, crown architecture, and low-temperature photoinhibition in conifer seedlings at alpine treeline. *Plant, Cell & Environment*, *22*(4), 407–415. https://doi.org/10.1046/j.1365-3040.1999.00426.x

Gerrish, G. (1990). Relating Carbon Allocation Patterns to Tree Senescence in Metrosideros Forests. *Ecology*, *71*(3), 1176–1184. https://doi.org/10.2307/1937385

Goeking, S. A., & Izlar, D. K. (2018). *Pinus albicaulis Engelm. (Whitebark Pine) in Mixed-Species Stands throughout Its US Range: Broad-Scale Indicators of Extent and Recent Decline*. https://www.mdpi.com/1999-4907/9/3/131

Goeking, S. A., & Windmuller-Campione, M. A. (2021). Comparative species assessments of five-needle pines throughout the western United States. *Forest Ecology and*

Management, *496*, 119438. https://doi.org/10.1016/j.foreco.2021.119438

Hagedorn, F., Shiyatov, S. G., Mazepa, V. S., Devi, N. M., Grigor'ev, A. A., Bartysh, A. A., Fomin, V. V., Kapralov, D. S., Terent'ev, M., Bugman, H., Rigling, A., & Moiseev, P. A. (2014). Treeline advances along the Urals mountain range – driven by improved winter conditions? *Global Change Biology*, *20*(11), 3530–3543. https://doi.org/10.1111/gcb.12613

Hamlin, J., Kegley, A., & Sniezko, R. (2011). Genetic variation of whitebark pine (Pinus albicaulis) provenances and families from Oregon and Washington in juvenile height growth and needle color. *In: Keane, Robert E.; Tomback, Diana F.; Murray, Michael P.; Smith, Cyndi M., Eds. The Future of High-Elevation, Five-Needle White Pines in Western North America: Proceedings of the High Five Symposium. 28-30 June 2010; Missoula, MT. Proceedings RMRS-P-63. Fort Collins, CO: U.S. Department of Agriculture, Forest Service, Rocky Mountain Research Station. p. 133-139.*, *63*, 133–139.

Hankin, L. E., & Bisbing, S. M. (2021). Let it snow? Spring snowpack and microsite characterize the regeneration niche of high-elevation pines. *Journal of Biogeography*, *48*(8), 2068–2084. https://doi.org/10.1111/jbi.14136

Hankin, L. E., Leger, E. A., & Bisbing, S. M. (2023). Reforestation of high elevation pines: Direct seeding success depends on seed source and sowing environment. *Ecological Applications*, *33*(6), e2897. https://doi.org/10.1002/eap.2897

Hansen, A. J., East, A., Keane, R. E., Lavin, M., Legg, K., Holden, Z., Toney, C., & Alongi, F. (2021). Is whitebark pine less sensitive to climate warming when climate tolerances of juveniles are considered? *Forest Ecology and Management*, *493*, 119221. https://doi.org/10.1016/j.foreco.2021.119221

Harrell, F. E. (2015). Case Study in Binary Logistic Regression, Model Selection and Approximation: Predicting Cause of Death. In Jr. Harrell Frank E. (Ed.), *Regression Modeling Strategies: With Applications to Linear Models, Logistic and Ordinal Regression, and Survival Analysis* (pp. 275–289). Springer International Publishing. https://doi.org/10.1007/978-3-319-19425-7_11

Hartig, F. (2025). *Florianhartig/DHARMa* [R]. https://github.com/florianhartig/DHARMa (Original work published 2015)

Hartmann, H., & Trumbore, S. (2016). Understanding the roles of nonstructural carbohydrates in forest trees – from what we can measure to what we want to know. *New Phytologist*, *211*(2), 386–403. https://doi.org/10.1111/nph.13955

Hendry, A. P., Kinnison, M. T., Heino, M., Day, T., Smith, T. B., Fitt, G., Bergstrom, C. T., Oakeshott, J., Jørgensen, P. S., Zalucki, M. P., Gilchrist, G., Southerton, S., Sih, A., Strauss, S., Denison, R. F., & Carroll, S. P. (2011). Evolutionary principles and their practical application. *Evolutionary Applications*, *4*(2), 159–183. https://doi.org/10.1111/j.1752-4571.2010.00165.x

Hoch, G., & Körner, C. (2009). Growth and carbon relations of tree line forming conifers at constant vs. Variable low temperatures. *Journal of Ecology*, *97*(1), 57–66. https://doi.org/10.1111/j.1365-2745.2008.01447.x

Hoch, G., & Körner, C. (2012). Global patterns of mobile carbon stores in trees at the high-elevation tree line. *Global Ecology and Biogeography*, *21*(8), 861–871. https://doi.org/10.1111/j.1466-8238.2011.00731.x

Hoermiller, I. I., Naegele, T., Augustin, H., Stutz, S., Weckwerth, W., & Heyer, A. G. (2017). Subcellular reprogramming of metabolism during cold acclimation in Arabidopsis thaliana. *Plant, Cell & Environment*, *40*(5), 602–610. https://doi.org/10.1111/pce.12836

Hoff, R. J., Ferguson, D. E., McDonald, G. I., & Keane, R. E. (2001). Strategies for managing whitebark pine in the presence of white pine blister rust [Chapter 17]. *In: Tomback, Diana F.; Arno, Stephen F.; Keane, Robert E., Eds. Whitebark Pine Communities: Ecology and Restoration. Washington, D.C.: Island Press. p. 346-366.*, 346–366.

Howe, G. T., Aitken, S. N., Neale, D. B., Jermstad, K. D., Wheeler, N. C., & Chen, T. H. (2003). From genotype to phenotype: Unraveling the complexities of cold adaptation in forest trees. *Canadian Journal of Botany*, *81*(12), 1247–1266. https://doi.org/10.1139/b03-141

Jacobi, W. R., Kearns, H. S. J., Cleaver, C. M., Goodrich, B. A., & Burns, K. S. (2018). Epidemiology of white pine blister rust on limber pine in Colorado and Wyoming. *Forest Pathology*, *48*(6), e12465. https://doi.org/10.1111/efp.12465

Johnson, D. M., McCulloh, K. A., & Reinhardt, K. (2011). The Earliest Stages of Tree Growth: Development, Physiology and Impacts of Microclimate. In F. C. Meinzer, B. Lachenbruch, & T. E. Dawson (Eds.), *Size- and Age-Related Changes in Tree Structure and Function* (pp. 65–87). Springer Netherlands. https://doi.org/10.1007/978-94-007-1242-3_3

Johnson, G. R., Sorensen, F. C., Clair, J. B. S., & Cronn, R. C. (2004). Pacific Northwest Forest Tree Seed Zones: A template for native plants? *Native Plants Journal*, *5*(2), 131–140. https://doi.org/10.2979/NPJ.2004.5.2.131

Keane, R. E., Holsinger, L. M., Mahalovich, M. F., & Tomback, D. F. (2017). Restoring whitebark pine ecosystems in the face of climate change. *Gen. Tech. Rep. RMRS-GTR-361. Fort Collins, CO: U.S. Department of Agriculture, Forest Service, Rocky Mountain Research Station. 123 p.*, *361*. https://doi.org/10.2737/RMRS-GTR-361

Keane, R. E., Schoettle, A. W., & Tomback, D. F. (2022). Effective actions for managing resilient high elevation five-needle white pine forests in western North America at multiple scales under changing climates. *Forest Ecology and Management*, *505*, 119939. https://doi.org/10.1016/j.foreco.2021.119939

Kerr, K. L., Meinzer, F. C., McCulloh, K. A., Woodruff, D. R., & Marias, D. E. (2015). Expression of functional traits during seedling establishment in two populations of Pinus ponderosa from contrasting climates. *Tree Physiology*, *35*(5), 535–548. https://doi.org/10.1093/treephys/tpv034

Kinloch, B. B., Sniezko, R. A., & Dupper, G. E. (2003). Origin and Distribution of Cr2, a Gene for Resistance to White Pine Blister Rust in Natural Populations of Western White Pine. *Phytopathology®*, *93*(6), 691–694. https://doi.org/10.1094/PHYTO.2003.93.6.691

Kinloch Jr., B. B. (1992). Distribution and frequency of a gene for resistance to white pine blister rust in natural populations of sugar pine. *Canadian Journal of Botany*, *70*(7), 1319–1323. https://doi.org/10.1139/b92-165

Kolb, P. F., & Robberecht, R. (1996). High temperature and drought stress effects on survival of Pinus ponderosa seedlings. *Tree Physiology*, *16*(8), 665–672. https://doi.org/10.1093/treephys/16.8.665

Kolotelo. (2001). *Cabidigitallibrary.org/doi/full/10.5555/20023007030*. https://www.cabidigitallibrary.org/doi/full/10.5555/20023007030

Körner, C. (2003). Carbon limitation in trees. *Journal of Ecology*, *91*(1), 4–17. https://doi.org/10.1046/j.1365-2745.2003.00742.x

Kreyling, J., Buhk, C., Backhaus, S., Hallinger, M., Huber, G., Huber, L., Jentsch, A., Konnert, M., Thiel, D., Wilmking, M., & Beierkuhnlein, C. (2014). Local adaptations to frost in marginal and central populations of the dominant forest tree agus sylvatica L. as affected by temperature and extreme drought in common garden experiments. *Ecology and Evolution*, *4*(5), 594–605. https://doi.org/10.1002/ece3.971

Krist, F., Ellenwood, J. R., Woods, M. E., McMahan, A. J., Cowardin, J. P., Ryerson, D. E., Sapio, F. J., Zweifler, M. O., & Romero, S. A. (2014). *2013-2027 National Insect and Disease Forest Risk Assessment*.

Kueppers, L. M., Conlisk, E., Castanha, C., Moyes, A. B., Germino, M. J., de Valpine, P., Torn, M. S., & Mitton, J. B. (2017). Warming and provenance limit tree recruitment across and beyond the elevation range of subalpine forest. *Global Change Biology*, *23*(6), 2383–2395. https://doi.org/10.1111/gcb.13561

Lahr, E. C., & Sala, A. (2014). Species, elevation, and diameter affect whitebark pine and lodgepole pine stored resources in the sapwood and phloem: Implications for bark beetle outbreaks. *Canadian Journal of Forest Research*, *44*(11), 1312–1319. https://doi.org/10.1139/cjfr-2014-0063

Landhäusser, S. M., Chow, P. S., Dickman, L. T., Furze, M. E., Kuhlman, I., Schmid, S., Wiesenbauer, J., Wild, B., Gleixner, G., Hartmann, H., Hoch, G., McDowell, N. G., Richardson, A. D., Richter, A., & Adams, H. D. (2018). Standardized protocols and procedures can precisely and accurately quantify non-structural carbohydrates. *Tree Physiology*, *38*(12), 1764–1778. https://doi.org/10.1093/treephys/tpy118

Lazarus, B. E., Castanha, C., Germino, M. J., Kueppers, L. M., & Moyes, A. B. (2018). Growth strategies and threshold responses to water deficit modulate effects of warming on tree seedlings from forest to alpine. *Journal of Ecology*, *106*(2), 571–585. https://doi.org/10.1111/1365-2745.12837

Leck, M. A., Parker, V. T., & Simpson, R. (2008). *Seedling Ecology and Evolution*. Cambridge University Press.

Lenth, R. V., Banfai, B., Bolker, B., Buerkner, P., Giné-Vázquez, I., Herve, M., Jung, M., Love, J., Miguez, F., Piaskowski, J., Riebl, H., & Singmann, H. (2025). *emmeans: Estimated Marginal Means, aka Least-Squares Means* (Version 1.11.1) [Computer software]. https://cran.r-project.org/web/packages/emmeans/index.html

Lett, S., & Dorrepaal, E. (2018). Global drivers of tree seedling establishment at alpine treelines in a changing climate. *Functional Ecology*, *32*(7), 1666–1680. https://doi.org/10.1111/1365-2435.13137

Letts, M., Nakonechny, & Gaalen. (2009). *Physiological acclimation of Pinus flexilis to drought stress on contrasting slope aspects in Waterton Lakes National Park, Alberta, Canada*. https://doi.org/10.1139/X08-206

Lind, B. M., Friedline, C. J., Wegrzyn, J. L., Maloney, P. E., Vogler, D. R., Neale, D. B., & Eckert, A. J. (2017). Water availability drives signatures of local adaptation in whitebark pine (Pinus albicaulis Engelm.) across fine spatial scales of the Lake Tahoe Basin, USA. *Molecular Ecology*, *26*(12), 3168–3185. https://doi.org/10.1111/mec.14106

Liu, J.-J., Ekramoddoullah, A. K. M., Hawkins, B., & Shah, S. (2013). Overexpression of a western white pine PR10 protein enhances cold tolerance in transgenic Arabidopsis. *Plant Cell, Tissue and Organ Culture (PCTOC)*, *114*(2), 217–223. https://doi.org/10.1007/s11240-013-0317-z

Liu, W., Zheng, L., & Qi, D. (2020). Variation in leaf traits at different altitudes reflects the adaptive strategy of plants to environmental changes. *Ecology and Evolution*, *10*(15), 8166–8175. https://doi.org/10.1002/ece3.6519

Long, R. W., Dudley, T. L., D'Antonio, C. M., Grady, K. C., Bush, S. E., & Hultine, K. R. (2021). Spenders versus savers: Climate-induced carbon allocation trade-offs in a recently introduced woody plant. *Functional Ecology*, *35*(8), 1640–1654. https://doi.org/10.1111/1365-2435.13862

Lüdecke, D., Ben-Shachar, M. S., Patil, I., Waggoner, P., & Makowski, D. (2021). performance: An R Package for Assessment, Comparison and Testing of Statistical Models. *Journal of Open Source Software*, *6*(60), 3139. https://doi.org/10.21105/joss.03139

Lusk, C. H., Clearwater, M. J., Laughlin, D. C., Harrison, S. P., Prentice, I. C., Nordenstahl, M., & Smith, B. (2018). Frost and leaf-size gradients in forests: Global patterns and experimental evidence. *New Phytologist*, *219*(2), 565–573. https://doi.org/10.1111/nph.15202

Mahalovich, M. F. (2013). *Grizzly bears and whitebarkpine in the Greater Yellowstone Ecosystem. Futurestatus of whitebark pine: Blister rust resistance,mountain pine beetle, and climate change. Report2470 RRM-NR-WP-13-01. USDA Forest Service,Northern Region, Missoula, Montana, USA*.

Mahalovich, M. F., Burr, K. E., & Foushee, D. L. (2006). Whitebark Pine Germination, Rust Resistance, and Cold Hardiness Among Seed Sources in the Inland Northwest: Planting Strategies for Restoration. *In: Riley, L.E.; Dumroese, R.K.; Landis, T.D., Tech. Coords. 2006. National Proceedings: Forest and Conservation Nursery Associations - 2005. Proc. RMRS-P-43. Fort Collins, CO: U.S. Department of Agriculture, Forest Service, Rocky Mountain Research Station. p. 91-101*, *043*. https://research.fs.usda.gov/treesearch/26662

Mahalovich, M. F., & Hipkins, V. D. (2011). Molecular genetic variation in whitebark pine (Pinus albicaulis Engelm.) in the Inland West. *In: Keane, Robert E.; Tomback, Diana F.; Murray, Michael P.; Smith, Cyndi M., Eds. The Future of High-Elevation, Five-Needle White Pines in Western North America: Proceedings of the High Five Symposium. 28-30 June 2010; Missoula, MT. Proceedings RMRS-P-63. Fort Collins, CO: U.S. Department of Agriculture, Forest Service, Rocky Mountain Research Station. p. 118-132.*, *63*, 118–132.

Maher, E. L., & and GerminO, M. J. (2006). Microsite differentiation among conifer species during seedling establishment at alpine treeline. *Écoscience*, *13*(3), 334–341. https://doi.org/10.2980/i1195-6860-13-3-334.1

Máliš, F., Kopecký, M., Petřík, P., Vladovič, J., Merganič, J., & Vida, T. (2016). Life stage, not climate change, explains observed tree range shifts. *Global Change Biology*, *22*(5), 1904–1914. https://doi.org/10.1111/gcb.13210

Markesteijn, L., & Poorter, L. (2009). Seedling root morphology and biomass allocation of 62 tropical tree species in relation to drought- and shade-tolerance. *Journal of Ecology*, *97*(2), 311–325. https://doi.org/10.1111/j.1365-2745.2008.01466.x

Martínez-Berdeja, A., Hamilton, J. A., Bontemps, A., Schmitt, J., & Wright, J. W. (2019). Evidence for population differentiation among Jeffrey and Ponderosa pines in survival, growth and phenology. *Forest Ecology and Management*, *434*, 40–48. https://doi.org/10.1016/j.foreco.2018.12.009

Martínez-Vilalta, J., Sala, A., Asensio, D., Galiano, L., Hoch, G., Palacio, S., Piper, F. I., & Lloret, F. (2016). Dynamics of non-structural carbohydrates in terrestrial plants: A global synthesis. *Ecological Monographs*, *86*(4), 495–516. https://doi.org/10.1002/ecm.1231

McDowell, N. G., Allen, C. D., Anderson-Teixeira, K., Aukema, B. H., Bond-Lamberty, B., Chini, L., Clark, J. S., Dietze, M., Grossiord, C., Hanbury-Brown, A., Hurtt, G. C., Jackson, R. B., Johnson, D. J., Kueppers, L., Lichstein, J. W., Ogle, K., Poulter, B., Pugh, T. A. M., Seidl, R., … Xu, C. (2020). Pervasive shifts in forest dynamics in a changing world. *Science*, *368*(6494), eaaz9463. https://doi.org/10.1126/science.aaz9463

McKinney, S. T., Fiedler, C. E., & Tomback, D. F. (2009). Invasive pathogen threatens bird–pine mutualism: Implications for sustaining a high-elevation ecosystem. *Ecological Applications*, *19*(3), 597–607. https://doi.org/10.1890/08-0151.1

McLane, S. C., & Aitken, S. N. (2012). Whitebark pine () assisted migration potential: Testing establishment north of the species range. *Ecological Applications*, *22*(1), 142–153. https://doi.org/10.1890/11-0329.1

Monahan, W. B., Cook, T., Melton, F., Connor, J., & Bobowski, B. (2013). Forecasting Distributional Responses of Limber Pine to Climate Change at Management-Relevant Scales in Rocky Mountain National Park. *PLOS ONE*, *8*(12), e83163. https://doi.org/10.1371/journal.pone.0083163

Monson, R. K., Trowbridge, A. M., Lindroth, R. L., & Lerdau, M. T. (2022). Coordinated resource allocation to plant growth–defense tradeoffs. *New Phytologist*, *233*(3), 1051–1066. https://doi.org/10.1111/nph.17773

Mote, P. W., & Salathé, E. P. (2010). Future climate in the Pacific Northwest. *Climatic Change*, *102*(1), 29–50. https://doi.org/10.1007/s10584-010-9848-z

Moyes, A. B., Castanha, C., Germino, M. J., & Kueppers, L. M. (2013). Warming and the dependence of limber pine (Pinus flexilis) establishment on summer soil moisture within and above its current elevation range. *Oecologia*, *171*(1), 271–282. https://doi.org/10.1007/s00442-012-2410-0

Moyes, A. B., Germino, M. J., & Kueppers, L. M. (2015). Moisture rivals temperature in limiting photosynthesis by trees establishing beyond their cold-edge range limit under ambient and warmed conditions. *New Phytologist*, *207*(4), 1005–1014. https://doi.org/10.1111/nph.13422

Nägele, T., Gibon, Y., & Le Hir, R. (2022). Plant sugar metabolism, transport and signalling in challenging environments. *Physiologia Plantarum*, *174*(5), e13768. https://doi.org/10.1111/ppl.13768

Niinemets. (2016). *Does the touch of cold make evergreen leaves tougher? | Tree Physiology | Oxford Academic*. https://academic.oup.com/treephys/article-abstract/36/3/267/2364723?redirectedFrom=fulltext

O'Brien, M. J., Leuzinger, S., Philipson, C. D., Tay, J., & Hector, A. (2014). Drought survival of tropical tree seedlings enhanced by non-structural carbohydrate levels. *Nature Climate Change*, *4*(8), 710–714. https://doi.org/10.1038/nclimate2281

Ogle, D. (2025). *FSA package—RDocumentation*. https://www.rdocumentation.org/packages/FSA/versions/0.9.6

Overton, E. (2016). *Current Practices for Growing Whitebark Pine Seedlings at the U.S. Department of Agriculture, Forest Service, Coeur d'Alene Nursery—Reforestation, Nurseries and Genetics Resources*. https://rngr.net/publications/tpn/59-1/current-practices-for-growing-whitebark-pine-seedlings-at-the-u.s.-department-of-agriculture-forest-service-coeur-d2019alene-nursery

Pansing, E. R., & Tomback, D. F. (2019). Survival of Whitebark Pine Seedlings Grown from Direct Seeding: Implications for Regeneration and Restoration under Climate Change. *Forests*, *10*(8), Article 8. https://doi.org/10.3390/f10080677

Perkins, D. L., & Swetnam, T. W. (1996). A dendroecological assessment of whitebark pine in the Sawtooth–Salmon River region, Idaho. *Canadian Journal of Forest Research*, *26*(12), 2123–2133. https://doi.org/10.1139/x26-241

Piper, F. I., Fajardo, A., & Hoch, G. (2017). Single-provenance mature conifers show higher non-structural carbohydrate storage and reduced growth in a drier location. *Tree Physiology*, *37*(8), 1001–1010. https://doi.org/10.1093/treephys/tpx061

Poorter, H., Niinemets, Ü., Poorter, L., Wright, I. J., & Villar, R. (2009). Causes and consequences of variation in leaf mass per area (LMA): A meta-analysis. *New Phytologist*, *182*(3), 565–588. https://doi.org/10.1111/j.1469-8137.2009.02830.x

Pregitzer, K. S. (2002). Fine roots of trees – a new perspective. *New Phytologist*, *154*(2), 267–270. https://doi.org/10.1046/j.1469-8137.2002.00413_1.x

Ramsey, & Schafer. (2013). *The Statistical Sleuth: A Course in Methods of Data Analysis, 3rd Edition—9781133490678—Cengage*. https://www.cengage.com/c/the-statistical-sleuth-a-course-in-methods-of-data-analysis-3e-ramsey-schafer/9781133490678/

Rangwala, I., & Miller, J. R. (2012). Climate change in mountains: A review of elevation-dependent warming and its possible causes. *Climatic Change*, *114*(3), 527–547. https://doi.org/10.1007/s10584-012-0419-3

Rank, R., Maneta, M., Higuera, P., Holden, Z., & Dobrowski, S. (2022). Conifer Seedling Survival in Response to High Surface Temperature Events of Varying Intensity and Duration. *Frontiers in Forests and Global Change*, *4*. https://doi.org/10.3389/ffgc.2021.731267

Read, J., & Stokes, A. (2006). Plant biomechanics in an ecological context. *American Journal of Botany*, *93*(10), 1546–1565. https://doi.org/10.3732/ajb.93.10.1546

Reich, P. B. (2014). The world-wide 'fast–slow' plant economics spectrum: A traits manifesto. *Journal of Ecology*, *102*(2), 275–301. https://doi.org/10.1111/1365-2745.12211

Reinhardt, K., Germino, M. J., Kueppers, L. M., Domec, J.-C., & Mitton, J. (2015). Linking carbon and water relations to drought-induced mortality in *Pinus flexilis* seedlings. *Tree Physiology*, *35*(7), 771–782. https://doi.org/10.1093/treephys/tpv045

Robb, L. (2020). *Seed matters 3: Sowing five needle pines from Alberta seed—Open Government*. https://open.alberta.ca/publications/9781460147016

Ruddiman, W. (2013). *Earth's Climate: Past and Future* (Third edition). W. H. Freeman.

Runyon, J. B., Bentz, B. J., & Qubain, C. A. (2022). Constitutive and Induced Defenses in Long-lived Pines Do Not Trade Off but Are Influenced by Climate. *Journal of Chemical Ecology*, *48*(9), 746–760. https://doi.org/10.1007/s10886-022-01377-z

Sala, A., Woodruff, D. R., & Meinzer, F. C. (2012). Carbon dynamics in trees: Feast or famine? *Tree Physiology*, *32*(6), 764–775. https://doi.org/10.1093/treephys/tpr143

Sanaphre-Villanueva, L., Dupuy, J. M., Andrade, J. L., Reyes-García, C., Jackson, P. C., & Paz, H. (2017). Patterns of plant functional variation and specialization along secondary succession and topography in a tropical dry forest. *Environmental Research Letters*, *12*(5), 055004. https://doi.org/10.1088/1748-9326/aa6baa

Schindelin, J., Arganda-Carreras, I., Frise, E., Kaynig, V., Longair, M., Pietzsch, T., Preibisch, S., Rueden, C., Saalfeld, S., Schmid, B., Tinevez, J.-Y., White, D. J., Hartenstein, V., Eliceiri, K., Tomancak, P., & Cardona, A. (2012). Fiji: An open-source platform for biological-image analysis. *Nature Methods*, *9*(7), 676–682. https://doi.org/10.1038/nmeth.2019

Schoettle, A. W., Burns, K. S., McKinney, S. T., Krakowski, J., Waring, K. M., Tomback, D. F., & Davenport, M. (2022). Integrating forest health conditions and species adaptive capacities to infer future trajectories of the high elevation five-needle white pines. *Forest Ecology and Management*, *521*, 120389. https://doi.org/10.1016/j.foreco.2022.120389

Schoettle, A. W., & Sniezko, R. A. (2007). Proactive intervention to sustain high-elevation pine ecosystems threatened by white pine blister rust. *Journal of Forest Research*, *12*(5), 327–336. https://doi.org/10.1007/s10310-007-0024-x

Schoettle, A. W., Sniezko, R. A., Kegley, A., & Burns, K. S. (2014). White pine blister rust resistance in limber pine: Evidence for a major gene. *Phytopathology*, *104*(2), 163–173. https://doi.org/10.1094/PHYTO-04-13-0092-R

Seethepalli, A., Guo, H., Liu, X., Griffiths, M., Almtarfi, H., Li, Z., Liu, S., Zare, A., Fritschi, F. B., Blancaflor, E. B., Ma, X.-F., & York, L. M. (2020). RhizoVision Crown: An Integrated Hardware and Software Platform for Root Crown Phenotyping. *Plant Phenomics (Washington, D.C.)*, *2020*, 3074916. https://doi.org/10.34133/2020/3074916

Sevanto, S., Mcdowell, N. G., Dickman, L. T., Pangle, R., & Pockman, W. T. (2014). How do trees die? A test of the hydraulic failure and carbon starvation hypotheses. *Plant, Cell & Environment*, *37*(1), 153–161. https://doi.org/10.1111/pce.12141

Shanahan, E., Irvine, K. M., Thoma, D., Wilmoth, S., Ray, A., Legg, K., & Shovic, H. (2016). Whitebark pine mortality related to white pine blister rust, mountain pine beetle outbreak, and water availability. *Ecosphere*, *7*(12), e01610. https://doi.org/10.1002/ecs2.1610

Shepherd, B. (2018). *Ten Years of Monitoring Illustrates a Cascade of Effects of White Pine Blister Rust and Focuses Whitebark Pine Restoration in the Canadian Rocky and Columbia Mountains*. https://www.mdpi.com/1999-4907/9/3/138

Shepherd, B., Krakowski, J., Moody, R., Reid, I., Murray, M. P., Stafl, N., Sissons, R., Alger, G., Park, J., McLellan, C., Schwarz, C. J., & Smith, C. M. (2025). Climate dominates geographic influences on whitebark pine and limber pine trends and landscape patterns in Canada. *Canadian Journal of Forest Research*, *55*, 1–19. https://doi.org/10.1139/cjfr-2024-0114

Smithers, B. V. (2017). Soil Preferences in Germination and Survival of Limber Pine in the Great Basin White Mountains. *Forests*, *8*(11), Article 11. https://doi.org/10.3390/f8110423

Smithers, B. V., Alongi, F., & North, M. P. (2021). Live fast, die young: Climate shifts may favor Great Basin bristlecone pine or limber pine in sub-alpine forest establishment. *Forest Ecology and Management*, *494*, 119339. https://doi.org/10.1016/j.foreco.2021.119339

Smithers, B. V., North, M. P., Millar, C. I., & Latimer, A. M. (2018). Leap frog in slow motion: Divergent responses of tree species and life stages to climatic warming in Great Basin subalpine forests. *Global Change Biology*, *24*(2), e442–e457. https://doi.org/10.1111/gcb.13881

Sniezko, R. A., Johnson, J. S., & Savin, D. P. (2020). Assessing the durability, stability, and usability of genetic resistance to a non-native fungal pathogen in two pine species. *PLANTS, PEOPLE, PLANET*, *2*(1), 57–68. https://doi.org/10.1002/ppp3.49

Sniezko, R. A., Kegley, A., Danchok, R., & Long, S. (2018). Blister rust resistance in whitebark pine (Pinus albicaulis)—Early results following artificial inoculation of seedlings from Oregon, Washington, Idaho, Montana, California, and British Columbia seed sources. *In: Schoettle, Anna W.; Sniezko, Richard A.; Kliejunas, John T., Eds. Proceedings of the IUFRO Joint Conference: Genetics of Five-Needle Pines, Rusts of Forest Trees, and Strobusphere; 2014 June 15-20; Fort Collins, CO. Proc. RMRS-P-76. Fort Collins, CO: U.S. Department of Agriculture, Forest Service, Rocky Mountain Research Station. p. 129-135.*, *76*, 129–135.

Sniezko, R. A., & Liu, J.-J. (2022). Genetic resistance to white pine blister rust, restoration options, and potential use of biotechnology. *Forest Ecology and Management*, *520*, 120168. https://doi.org/10.1016/j.foreco.2022.120168

Sniezko, R. A., & Liu, J.-J. (2023). Prospects for developing durable resistance in populations of forest trees. *New Forests*, *54*(4), 751–767. https://doi.org/10.1007/s11056-021-09898-3

Sniezko, R. A., Mahalovich, M. F., Schoettle, A. W., & Vogler, D. R. (2011). Past and current investigations of the genetic resistance to cronartium ribicola in high-elevation five-needle pines. *In: Keane, Robert E.; Tomback, Diana F.; Murray, Michael P.; Smith, Cyndi M., Eds. The Future of High-Elevation, Five-Needle White Pines in Western North America: Proceedings of the High Five Symposium. 28-30 June 2010; Missoula, MT. Proceedings RMRS-P-63. Fort Collins, CO: U.S. Department of Agriculture, Forest Service, Rocky Mountain Research Station. p. 246-264.*, *63*, 246–264.

Stevens-Rumann, C. S., Kemp, K. B., Higuera, P. E., Harvey, B. J., Rother, M. T., Donato, D. C., Morgan, P., & Veblen, T. T. (2018). Evidence for declining forest resilience to wildfires under climate change. *Ecology Letters*, *21*(2), 243–252. https://doi.org/10.1111/ele.12889

Sturrock, R. N., Frankel, S. J., Brown, A. V., Hennon, P. E., Kliejunas, J. T., Lewis, K. J., Worrall, J. J., & Woods, A. J. (2011). Climate change and forest diseases. *Plant*

Pathology, *60*(1), 133–149. https://doi.org/10.1111/j.1365-3059.2010.02406.x

Taiz, L., Zeiger, E., Møller, I. M., & Murphy, A. (2014). *Plant Physiology & Development* (6th edition). Sinauer Associates is an imprint of Oxford University Press.

Thalmann, M., & Santelia, D. (2017). Starch as a determinant of plant fitness under abiotic stress. *New Phytologist*, *214*(3), 943–951. https://doi.org/10.1111/nph.14491

Thoma, D. P., Shanahan, E. K., & Irvine, K. M. (2019). Climatic Correlates of White Pine Blister Rust Infection in Whitebark Pine in the Greater Yellowstone Ecosystem. *Forests*, *10*(8), Article 8. https://doi.org/10.3390/f10080666

Thornton, Shrestha, & Wei. (2022). *Daymet: Annual Climate Summaries on a 1-km Grid for North America, Version 4 R1, https://doi.org/10.3334/ORNLDAAC/2130*. https://daac.ornl.gov/cgi-bin/dsviewer.pl?ds_id=2130

Tomback, D. F., & Achuff, P. (2010). Blister rust and western forest biodiversity: Ecology, values and outlook for white pines. *Forest Pathology*, *40*(3–4), 186–225. https://doi.org/10.1111/j.1439-0329.2010.00655.x

Tomback, D. F., Achuff, P., Schoettle, A. W., Schwandt, J. W., & Mastrogiuseppe, R. J. (2011). The magnificent high-elevation five-needle white pines: Ecological roles and future outlook. *In: Keane, Robert E.; Tomback, Diana F.; Murray, Michael P.; Smith, Cyndi M., Eds. The Future of High-Elevation, Five-Needle White Pines in Western North America: Proceedings of the High Five Symposium. 28-30 June 2010; Missoula, MT. Proceedings RMRS-P-63. Fort Collins, CO: U.S. Department of Agriculture, Forest Service, Rocky Mountain Research Station. p. 2-28.*, *63*, 2–28.

Tomback, D. F., Keane, R. E., Schoettle, A. W., Sniezko, R. A., Jenkins, M. B., Nelson, C. R., Bower, A. D., DeMastus, C. R., Guiberson, E., Krakowski, J., Murray, M. P., Pansing, E. R., & Shamhart, J. (2022). Tamm review: Current and recommended management practices for the restoration of whitebark pine (*Pinus albicaulis* Engelm.), an imperiled high-elevation Western North American forest tree. *Forest Ecology and Management*, *522*, 119929. https://doi.org/10.1016/j.foreco.2021.119929

Ulrich, D. E. M., Wasteneys, C., Hoy-Skubik, S., & Alongi, F. (2023). Functional traits underlie specialist-generalist strategies in whitebark pine and limber pine. *Forest Ecology and Management*, *542*, 121113. https://doi.org/10.1016/j.foreco.2023.121113

U.S. Fish and Wildlife Service. (2022, December 14). *Whitebark pine receives ESA protection as a Threatened species | U.S. Fish & Wildlife Service*. https://www.fws.gov/press-release/2022-12/whitebark-pine-receives-esa-protection-threatened-species

Vogan, P. J., & Schoettle, A. W. (2015). Selection for resistance to white pine blister rust affects the abiotic stress tolerances of limber pine. *Forest Ecology and Management*, *344*, 110–

119. https://doi.org/10.1016/j.foreco.2015.01.029

Vogan, P. J., & Schoettle, A. W. (2016). Carbon Costs of Constitutive and Expressed Resistance to a Non-Native Pathogen in Limber Pine. *PLOS ONE*, *11*(10), e0162913. https://doi.org/10.1371/journal.pone.0162913

Vogler, D. R., Maloney, P. E., Burt, T., & Snelling, J. W. (2017). First report of the white pine blister rust fungus, Cronartium ribicola, infecting Pinus flexilis on Pine Mountain, Humboldt National Forest, Elko County, northeastern Nevada, U.S.A. *Plant Disease. 101(5): 839*, *101*, 839–839. https://doi.org/10.1094/PDIS-10-16-1502-PDN

Warwell, M. V., Rehfeldt, G. E., & Crookston, N. L. (2006). Modeling contemporary climate profiles of whitebark pine (Pinus albicaulis) and predicting responses to global warming. *In: Goheen, E., Ed. Proceedings of the Conference Whitebark Pine: A Pacific Coast Perspective. R6-NR-FHP-2007-01. Ashland, OR: U.S. Department of Agriculture, Forest Service. p. 139-142.*, 139–142.

Woo, K.-S., Fins, L., McDonald, G. I., & Wiese, M. V. (2001). Differences in needle morphology between blister rust resistant and susceptible western white pine stocks. *Canadian Journal of Forest Research*, *31*(11), 1880–1886. https://doi.org/10.1139/x01-121

Woodruff, D. R., Meinzer, F. C., Marias, D. E., Sevanto, S., Jenkins, M. W., & McDowell, N. G. (2015). Linking nonstructural carbohydrate dynamics to gas exchange and leaf hydraulic behavior in *Pinus edulis* and *Juniperus monosperma*. *New Phytologist*, *206*(1), 411–421. https://doi.org/10.1111/nph.13170

Wright, I. J., Reich, P. B., Westoby, M., Ackerly, D. D., Baruch, Z., Bongers, F., Cavender-Bares, J., Chapin, T., Cornelissen, J. H. C., Diemer, M., Flexas, J., Garnier, E., Groom, P. K., Gulias, J., Hikosaka, K., Lamont, B. B., Lee, T., Lee, W., Lusk, C., … Villar, R. (2004). The worldwide leaf economics spectrum. *Nature*, *428*(6985), 821–827. https://doi.org/10.1038/nature02403

Zamani, A., Sturrock, R., Ekramoddoullah, A. K. M., Wiseman, S. B., & Griffith, M. (2003). Endochitinase activity in the apoplastic fluid of Phellinus weirii-infected Douglas-fir and its association with over wintering and antifreeze activity. *Forest Pathology*, *33*(5), 299–316. https://doi.org/10.1046/j.1439-0329.2003.00331.x

Zhang, P., Ding, J., Wang, Q., McDowell, N. G., Kong, D., Tong, Y., & Yin, H. (2024). Contrasting coordination of non-structural carbohydrates with leaf and root economic strategies of alpine coniferous forests. *New Phytologist*, *243*(2), 580–590. https://doi.org/10.1111/nph.19678

APPENDICES

APPENDIX A

TABLES

Appx. Table 1. Species (PIAL = whitebark pine, PIFL = limber pine), seed source region, seed zone (U.S. PIAL only), location (listed in chronological order within a region), family identifier (ID), rust resistance level (RR.status), total number of seed sown per family, number of early germinants (seeds that did not undergo the full stratification process due to germinating early and were removed from analysis), number of seedlings harvested at each of the four destructive harvests (DH), and seed source climate variables (latitude (degrees), longitude (degrees), Elv (elevation, m), Precip (precipitation, mm/day), Srad (solar radiation, MJ/m2/day), SWE (snow water equivalent, kg/m^2), Tmax (maximum temperature, ℃), Tmin (minimum temperature, ℃), and VP (water vapor pressure, hPa). For climate variables that significantly differed among the 17 PIAL locations (Kruskal-wallis test, p≥0.05) (NA indicates non-significance, p>0.05), lowercase letters distinguish significant differences in mean ranks between locations within species. For climate variables that significantly differed between the four PIFL locations, uppercase letters distinguish significant differences in mean ranks between locations. RR.status for U.S. PIAL is represented as levels A-F (A = most resistant, F = least resistant) and for PIFL as resistant or susceptible. For BC PIAL, no rust resistance data was available. See map in Figure 1.

Species	Region	Seed zone	Location	Family ID	RR.status	Number of seeds sown	Number of early germinants	Number harvested at:				Latitude		Longitude		Elv		Precip		Srad		SWE		Tmax		Tmin		VPD	
								DH1	DH2	DH3	DH4																		
PIAL	Washington, U.S.	1	Olympic	39	E	100	2	8	8	8	8	47.81		-123.14		1782		2143		25.5		115.1		7.18		0.14		6.47	
				41	C	120	0	10	0	8	0	47.80	abc	-123.1	abc	1911	ab	2232	abc	27.0	ab	193.6		6.60	abc	-0.30	ab	6.30	abc
				51	F	100	1	0	0	2	0	47.82		-123.13		1867		2073		26.0		148.0		6.80		-0.13		6.34	
		2E	Okanogan-Wenatchee East	33	E	100	12	0	0	8	0	48.66		-119.95		2058		719		28.0		87.2		6.11		-1.56		5.26	
				36	C	100	1	0	8	8	0	48.66	abc	-119.95	abc	2058	ab	719	abc	28.0	ab	87.2	NA	6.11	abc	-1.56	ab	5.26	abc
				38	E	100	13	8	0	8	0	48.66		-119.95		2058		719		28.0		87.2		6.11		-1.56		5.26	
		2W	Okanogan-Wenatchee West	34	C	100	8	8	8	8	0	47.86		-120.47		1775		1082		25.1		72.5		8.26		0.80		6.01	
				35	F	200	4	8	8	8	8	47.86	abc	-120.48	abc	1853	ab	1130	abc	26.6	ab	82.2		7.80	abc	0.64	b	5.96	abc
				37	D	200	4	8	8	8	8	47.86		-120.47		1775		1082		25.1		72.5		8.26		0.80		6.01	

Appx Table 1 Continued

				29	B	100	28	8	8	8	8	48.66		-118.47		1985		870		25.3		59.5		6.34		-0.78		6.30	
		3	Colville	30	D	200	1	8	8	8	8	48.66	abc	-118.45	abc	1742	ab	813	abc	24.9	ab	40.1		7.87	abc	-0.31	ab	6.42	abc
				52	A	100	0	8	8	8	8	48.66		-118.47		1985		870		25.3		59.5		6.34		-0.78		6.30	
				40	D	100	1	0	0	0	0	46.2		-121.47		2129		2198		27.1		301.2		5.17		-1.24		5.72	
		4	Gifford Pinchot	53	A	100	0	8	8	8	8	46.15	abc	-121.49	abc	1999	ab	2433	c	28.3	ab	243.8		5.69	abc	-0.52	ab	6.03	abc
				54	A	100	0	0	0	2	0	46.15		-121.49		1999		2433		28.3		243.8		5.69		-0.52		6.03	
				55	F	100	0	8	8	8	8	43.68		-121.26		2281		1211		32.4		136.7		9.68		-1.73		5.18	
			Dessc hutes	56	B	120	0	8	8	8	8	43.69	abc	-121.26	abc	2306	ab	1207	abc	31.4	ab	134.4		9.64	abc	-1.71	ab	5.19	abc
				57	B	100	0	8	8	8	8	43.68		-121.23		2189		1090		31.9		94.5		10.50		-1.48		5.16	
				47	D	100	1	8	0	8	0	45.33		-121.71		1798		2933		27.6		170.7		6.94		0.74		6.87	
		5	Mt. Hood	48	B	100	1	8	8	8	8	45.33	abc	-121.70	abc	1798	ab	2933	c	27.6	ab	170.7		6.94	abc	0.74	b	6.87	c
				50	A	100	1	8	8	8	8	45.33		-121.71		1798		2933		27.6		170.7		6.94		0.74		6.87	
	Oregon, U.S.			45	D	100	4	8	8	8	0	44.65		-121.69		1883		2071		29.4		108.7		10.69		0.44		6.64	
			Warm Springs	58	A	100	0	8	8	8	8	44.66	abc	-121.69	abc	1877	ab	2002	abc	28.5	ab	100.0		10.59	ac	0.33	ab	6.57	bc
				59	A	100	0	8	8	8	8	44.65		-121.69		1883		2071		29.4		108.7		10.69		0.44		6.64	
				46	B	100	2	10	8	8	0	44.95		-118.24		2405		1094		30.0		134.5		6.66		-0.95		5.82	
		6	Wallowa-Whitman	60	C	100	0	8	8	8	8	44.95	abc	-118.24	abc	2340	b	1059	abc	29.3	ab	118.7		7.09	abc	-0.80	ab	5.87	abc
				61	D	100	0	0	0	8	0	44.95		-118.24		2405		1094		30.0		134.5		6.66		-0.95		5.82	
		7	Crater Lake	43	A	100	14	0	0	0	0	42.97	ab	-122.14	abc	2013	ab	1681	abc	33.4	b	166.0		9.56	abc	-1.21	ab	5.28	abc

				44	A	100	2	8	0	8	8	42.93		-122.17		2082		1798		33.0		205.5		8.94		-1.02		5.40	
				62	C	100	0	8	0	8	4	42.93		-122.05		2314		1808		34.8		446.7		7.03		-2.49		4.80	
			Umpqua	42	A	100	10	0	0	7	0	43.15	abc	-122.22	abc	2335	ab	2083	abc	34.6	ab	319.6		8.31	abc	-1.76	ab	5.31	abc
				49	B	100	2	0	0	8	0	43.37		-122.20		1360		1496		26.6		6.6		13.91		1.18		6.36	
				63	C	100	0	10	0	8	0	43.15		-122.22		2335		2083		34.6		319.6		8.31		-1.76		5.31	
		8	Fremont-Winema	31	B	100	48	8	0	8	0	42.61	a	-120.94	abc	2088	ab	692	ab	30.6	ab	29.9		10.95	a	-0.81	ab	4.84	ab
				32	F	100	0	0	0	4	0	42.60		-120.94		2088		692		30.6		29.9		10.95		-0.81		4.84	
				64	C	100	0	0	0	0	0	42.61		-120.94		2088		692		30.6		29.9		10.95		-0.81		4.84	
	British Columbia, Canada		Nanika Mtn.	80		164	41	8	8	8	0	54.10	c	-127.52	c	1387	a	2058	abc	20.3	a	244.6	NA	4.10	bc	-2.34	ab	5.93	abc
				81		115	4	8	8	8	0	54.10		-127.52		1387		2058		20.3		244.6		4.10		-2.34		5.93	
				79		158	10	8	8	8	0	54.10		-127.52		1387		2058		20.3		244.6		4.10		-2.34		5.93	
			Nanika Mtn./ Kid Price Mtn.	82		102	10	8	8	8	8	53.92	bc	-127.41	bc	986	a	1928	abc	19.8	a	121.5		6.60	abc	-0.91	ab	6.45	abc
				83		126	8	8	8	8	0	53.92		-127.43		945		1924		19.6		112.0		6.85		-0.75		6.52	
				84		115	13	8	8	8	8	53.92		-127.43		945		1924		19.6		112.0		6.85		-0.75		6.52	
			Lime Mtn.	86		130	1	8	8	8	0	51.09	abc	-121.67	abc	1801	ab	571	a	25.6	ab	63.9		5.84	abc	-5.65	a	4.14	a
				85		128	3	8	8	8	8	51.09		-121.67		1888		585		26.8		80.2		5.30		-6.16		3.97	
				87		138	40	8	8	8	8	51.09		-121.67		1888		585		26.8		80.2		5.30		-6.16		3.97	
			Mtn. Stevens	92		153	7	8	8	8	8	49.83	abc	-115.58	a	2312	ab	969	abc	28.0	ab	165.0		3.53	b	-5.50	ab	4.89	abc
				93		140	4	8	8	8	8	49.83		-115.57		2312		969		28.0		165.0		3.53		-5.50		4.89	

				91		141	2	8	8	6	0	49.83		-115.58		2312		969		28.0		165.0		3.53		-5.50		4.89	
			Holy Moly Mtn.	90		96	6	8	8	8	8	49.20	abc	-116.92	ab	2034	ab	2077	abc	26.5	ab	187.3		6.20	abc	-2.09	ab	5.94	abc
				89		105	12	8	8	8	0	49.20		-116.91		2034		2077		26.5		187.3		6.20		-2.09		5.94	
				88		116	6	8	8	8	8	49.20	abc	-116.91	ab	2079	ab	2106	abc	27.1	ab	208.1		5.95	abc	-2.27	ab	5.87	abc
PIFL	Alberta, Canada		Highwood	26	Resistant	193	0	0	0	0	1	50.41	NA	-114.53	AB	4813	NA	593	NA	24.7	NA	20.3	AB	9.07	NA	-3.47	NA	5.26	AB
				27	Resistant	100	4	0	0	0	0	50.39		-114.58		4879		598		24.0		21.7		8.93		-3.57		5.25	
			Sentinel Point	65	Susceptible	200	44	0	0	5	0	50.39		-114.59	B	4879		598		24.0		21.7	AB	8.93		-3.57		5.25	B
				28	Susceptible	100	3	8	0	8	2	50.39		-114.58	B	4879		598		24.0		21.7	AB	8.93		-3.57		5.25	B
			Porcupine Hills	22	Resistant	200	14	0	0	2	0	49.94		-113.98	A	4623		543		24.1		13.4	A	9.69		-2.35		5.67	AB
				24	Resistant	100	48	0	0	0	1	49.91		-113.99		4820		562		24.2		15.3		9.33		-2.50		5.65	
				25	Susceptible	151	2	8	0	8	3	49.90		-114.02		5397		614		24.4		21.3		8.25		-2.97		5.57	
				23	Susceptible	142	4	0	0	8	4	49.90		-114.02		5397		614		24.4		21.3		8.25		-2.97		5.57	
			Prairie Bluff	20	Susceptible	125	16	0	0	4	0	49.31		-114.10	AB	5840		993		25.7		75.5	B	7.28		-2.75		5.81	A
				21	Susceptible	125	3	0	0	0	0	49.31		-114.10		5840		993		25.7		75.5		7.28		-2.75		5.81	
				19	Resistant	100	28	0	0	5	0	49.29		-114.07		5214		888		23.9		48.3		8.64		-2.13		6.03	
				18	Resistant	150	4	0	0	8	2	49.27		-114.01		5010		832		24.7		41.9		9.11		-1.94		6.09	

Appx. Table 2. Seedling group (U.S. PIAL, AB PIFL, B.C. PIAL), number of days post sowing (DPS), and date are shown for each of the chronological greenhouse processing steps and trait measurement periods (phenology proportion measurement days, start day of the destructive harvests (DH) and non-destructive harvests (ND) for growth traits and NSC). U.S. PIAL and AB PIFL were processed first (Batch 1) while B.C. PIAL was processed second (Batch 2) and were approximately 3 months apart.

	Event	U.S. PIAL (Batch 1)		AB PIFL (Batch 1)		B.C. PIAL (Batch 2)	
		Days Post Sowing (DPS)	Date	Days Post Sowing (DPS)	Date	Days Post Sowing (DPS)	Date
Greenhouse Processing	Seed Processing	-	Oct. 22nd, 2021	-	Nov. 22nd, 2021	-	Jan. 7th, 2022
	Warm stratification	-	Oct. 25th, 2021	-	-	-	Jan. 9th, 2022
	Cold stratification	-	Nov. 22nd, 2021	-	Nov. 25th, 2021	-	Feb. 6th, 2022
	Germination	-	Feb. 17th, 2022	-	Feb. 21st, 2022	-	May 15th, 2022
	Sowing	0	Feb. 21st, 2022	0	Feb. 25th, 2022	0	May 19th, 2022
	Transplanting	56	April 18th, 2022	77	May 13th, 2022	-	-
Phenology	Prop.emg.30.21	30	March 23rd, 2022	21	March 18th, 2022	30	June 18th, 2022
	Prop.emg.55.56	55	April 17th, 2022	56	April 22nd, 2022	55	July 13th, 2022
	Prop.bf.30.35	30	March 23rd, 2022	35	April 1st, 2022	30	June 18th, 2022
	Prop.bf.95.119	95	May 27th, 2022	119	June 24th, 2022	95	Aug. 22nd, 2022
	Prop.nb.119.119	119	June 20th, 2022	119	June 24th, 2022	119	Sep. 15th, 2022
	Prop.nb.161.203	161	Aug. 1st, 2022	203	Sep. 16th, 2022	161	Sep 15th, 2022
	Prop.surv.95.91	95	May 27th, 2022	91	May 27th, 2022	95	Aug. 22nd, 2022
Growth	Destructive harvest (DH1)	120	June 21st, 2022	120	June 25th, 2022	120	Sep. 16th, 2022
	Destructive harvest (DH2)	175	Aug. 15th, 2022	175	Aug. 19th, 2022	175	Nov. 10th, 2022
	Destructive harvest (DH3)	230	Oct. 9th, 2022	230	Oct. 13th, 2022	230	Jan. 4th, 2023
	Destructive harvest (DH4)	365	Feb. 21st, 2023	365	Feb. 25th, 2023	365	May 19th, 2023
	Non-destructive harvest (ND1)	97	May 29th, 2021	97	June 2nd, 2022	97	Aug. 24th, 2022

Appx Table 2 Continued

	Non-destructive harvest (ND2)	121	June 22nd, 2022	121	June 26th, 2022	121	Sep. 17th, 2022
	Non-destructive harvest (ND3)	160	July 31st, 2022	160	Aug. 4th, 2022	160	Oct. 26th, 2022
	Non-destructive harvest (ND4)	190	Aug. 30th 2022	190	Sep. 3rd 2022	190	Nov. 25th, 2022
	Non-destructive harvest (ND5)	221	Sep. 30th, 2022	221	Oct. 4th, 2022	221	December 26th, 2022
NSC	Destructive harvest (DH4)	365	Feb 21st, 2023	365	Feb 25th, 2023	365	May 19th, 2023

APPENDIX B

FIGURES

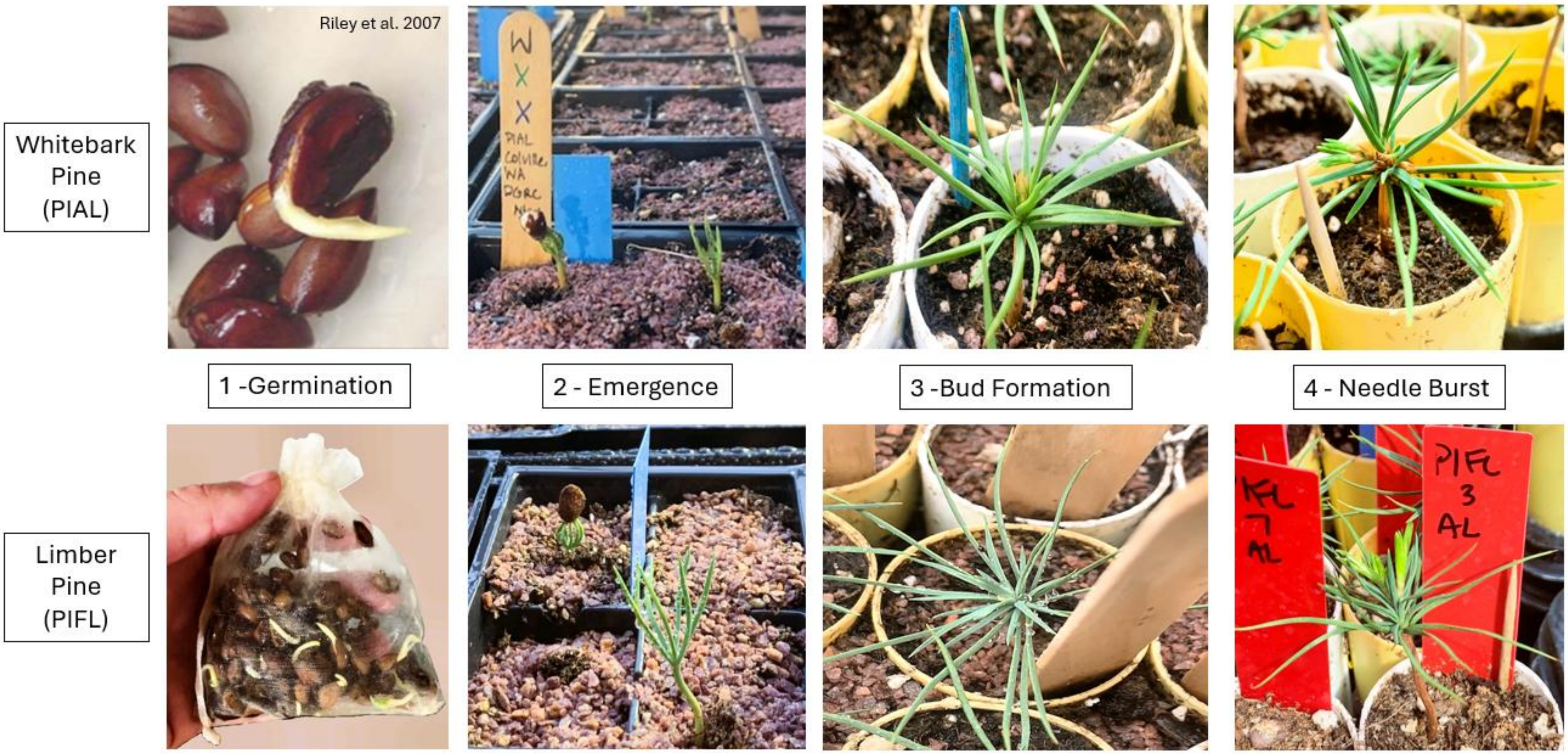

Appx. Figure 1. The four phenology stages (germination, emergence, bud formation, needle burst) that were monitored for whitebark pine (PIAL) (top row) and limber pine (PIFL) (bottom row). The analyzed traits included: proportion emerged (prop.emg), proportion with bud formation (prop.bf), proportion with needle burst (prop.nb), and proportion survived (prop.surv). All photos were obtained by Jessica Harris except for the PIAL germination photo (Riley et al., 2007).

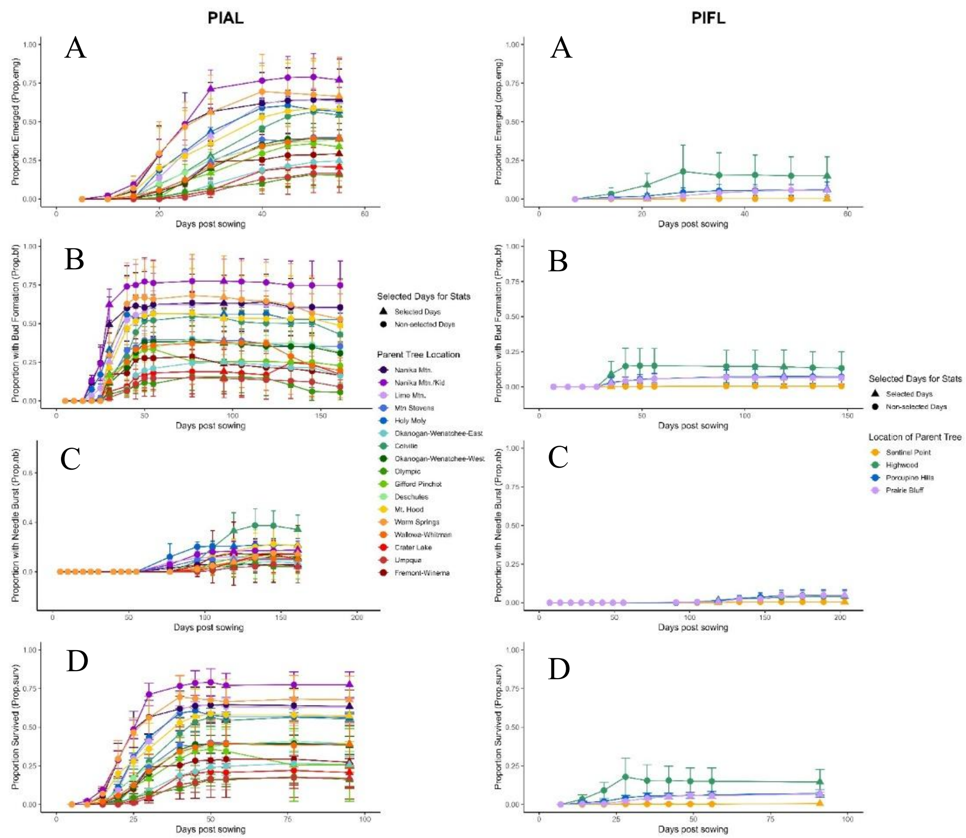

Appx. Figure 2. Proportion emerged (prop.emg) (A), proportion with bud formation (prop.bf) (B), proportion with needle burst (prop.nb) (C), and proportion survived (prop.surv) (D) for U.S. and B.C. PIAL (left) and PIFL (right) over time (days post sowing, DPS). Parent tree locations are ordered in the legend top to bottom from highest to lowest latitude. Error bars represent standard deviation for each parent tree location (N=2-3 families per location). Triangles represent the DPS on which statistical analysis was performed. For PIAL prop.emg , prop.bf , prop.nb, and prop.surv, these DPS were: 30 and 55, 30 and 95, 119 and 161, and then day 95, respectively. For PIFL prop.emg , prop.bf , prop.nb, and prop.surv, these days were 21 and 56, 35 and 119, 119 and 203, and then day 91, respectively. For each trait, the first selected day represents when proportions had the fastest rate of change (steepest slope in the curve). The second day represents the lowest rate of change (flattest slope in the curve).

APPENDIX C

STATISTICAL BACKGROUND

Grouped Binomial Logistic Regression - Example Models A-B To explain the general logic behind logistic regression models, Example Models A and B respectively show logistic regression models that used either a continuous FE (Q1) or a categorical FE (Q2-Q4) to analyze the phenology proportion traits in this project. The response variable for the logistic regression models was the number of seedlings that successfully survived to each phenology stage (emergence, bud formation, needle burst, or total survival) by the specified day divided by the total seeds sown per family (TSS_{jk}) (Ramsey and Schafer, 2013; Harrell, F., 2015). Each seedling was considered as an independent Bernoulli trial, where it either survived to the life stage on the specified day (a "success", denoted by a 1) or it did not (a "failure" denoted by a 0). The total number of seeds sown were the total number of trials (the number of opportunities for a seedling within a family to reach the life stage on the specified day). These trials aggregate into a proportion, bound between 0 and 1. Because the seedling stage is a bottleneck for PIAL and PIFL populations (Smithers et al. 2020), these proportions can be used as an approximation of how many seedlings in a family will survive through the seedling stage to the juvenile and adult life stages. Surviving to the life stage on the specified day will be called surviving to the event from hereafter.

For line 1 in Example Model A below, y_{jk} represents the binomially distributed response variable, which is the proportion of seedlings that reached the event for the *kth* family within the *jth* location. The proportion of seedlings that reached the event can be modeled as a probability ($Prob_{jk}$) constrained between 0 and 1 that represents the probability of a given seedling reaching the event within the *kth* family within the *jth* location. Probabilities follow an s-shaped sigmoid curve when plotted against a continuous predictor. Small changes in X have little effect on a probability when its near 0 or 1 (near the top or bottom of the "S") but changes rapidly near the middle of the range (~0.5 probability in the middle of the "S")(Apdx, Figure 3). Because probabilities naturally have a curve-linear relationship with a continuous predictor, probabilities depend on specific values of the predictor to estimate an outcome (Ramsey and Schafer, 2013; Harrell, F., 2015). This makes it challenging to use typical linear regression techniques like a GLMM or to obtain a slope.

To overcome the curve-linear nature of probabilities, probabilities can be transformed to the log-odds scale using the link function (left-hand side of line 2 equation in Example Model A). In line 2, ($Prob_{jk}$) represents the probability of the event occurring in the *kth* family within the *jth* location (seedling gets a "1") while ($1\text{-}Prob_{jk}$) represents the probability that the event does not occur (Seedling gets a "0"). Therefore, ($Prob_{jk}/(1\text{-}Prob_{jk})$) is the odds of the event happening for a given seedling. The logit function transforms the probability into log-odds, mapping the probability from (0,1) to an unbounded scale ($-\infty$, $+\infty$). The logit transformation ensures that the effects of predictor variables are additive and linear on the log-odds scale. The right-hand side of the equation is the systematic component which contains the linear predictors (β = fixed effects, b = random effects). β_0 represents the intercept (baseline log-odds for the event occurring when the continuous FE variable (FE_cont) is at its mean value due to centering) while β_1 represents the change in log-odds of the event occurring per unit increase in the FE variable (the slope). Line 3 shows how the odds ratio (OR) can be obtained from the exponentiated log-odds estimate (est_{LO}) (which is calculated from the completed linear predictor equation in the systematic component). The inverse logit function can also be used to transform the log-odds estimate (est_{LO}) back to a probability on the response scale by exponentiating the (est_{LO}) divided by (1 +

exponentiated (est_{LO})) (Ramsey and Schafer, 2013; Harrell, F., 2015).

Line 4 shows that the variables, b_j and b_{jk} represent the RE intercept for location and family respectively where b_j accounts for the variation between locations while b_{jk} accounts for the variation between families within a location. These RE follow a normal distribution on the log-odds scale where the mean is 0 and the variance is described by $\sigma^2_{location}$ or σ^2_{family}, for location and family respectively. Line 5 shows the variance (Var) on the log-odds scale which is the sum of the variability accounted for by the RE and the assumed residual variance. The assumed residual variance is the remaining variation that was not explained by the FE + RE, which is assumed to be $\frac{\pi^2}{3}$ for the binomial distribution with the logit link. Line 6 shows the variance on the response scale which describes the variation in the expected probability. This variance depends on the total number of trials (TSS_{jk}), the odds of the event occurring (($Prob_{jk}$)/(1−$Prob_{jk}$). In logistic regression, families with fewer seeds sown (TSS_{jk}) have lower variance because there are fewer trials. These proportions are more stable near 0 or 1 (top or bottom of the "S" curve). In contrast, families with more seeds sown have greater variance because there are more trials. This allows for more uncertainty in the proportion, making it more likely to be near 0.5 (middle of the "S" curve). Therefore, families with a larger TSS_{jk} contribute more information as they provide better estimates of the underlying probability (Ramsey and Schafer, 2013; Harrell, F., 2015).

Example Model A. Grouped Binomial Logistic Regression (Continuous FE)

$$1)\ y_{jk} \sim Binomial\ (TSS_{jk}, Prob_{jk})$$

$$2)\ logit(p_{jk}) = \log\left(\frac{Prob_{jk}}{1 - Prob_{jk}}\right) = \beta_0 + \beta_1 FE\_cont_{jk} + b_j + b_{jk}$$

$$3)\ OR = \exp\ (est_{LO})\ ;\ Prob_{jk} = \frac{\exp(est_{LO})}{1+\exp\ (est_{LO})}$$

$$4)\ b_j \sim N(0, \sigma^2_{location});\ b_{jk} \sim N(0, \sigma^2_{family})$$

$$5)\ Var(logit(Prob_{jk})) = \sigma^2_{location} + \sigma^2_{family} + \frac{\pi^2}{3}$$

$$6)\ Var(Prop_{jk} | FE\_cont,\ location, family) = TSS_{jk} * Prob_{jk} * (1 - Prob_{jk})$$

For Example Model B below, the equation and variables are the same as Example Model A except that the FE is now categorical instead of continuous. The interpretation of β_x now changes. For the categorical model, β_0 represents the intercept (baseline log-odds for the event occurring for the reference level of the categorical FE (FE_cat)) while β_1 represents the difference in the log-odds of the event occurring between the reference level and the next categorical level. Each β_x represent the difference between the reference level and level of interest. Below FE_cat2, FE_cat3, and FE_cat8 stand for categorical FE level 2, categorical FE level 3, and categorical FE level 8, respectively. (Ramsey and Schafer, 2013; Harrell, F., 2015).

Example Model B. Grouped Binomial Logistic Regression (Categorical FE)

$$1)\ y_{jk} \sim Binomial\ (TSS_{jk}, Prob_{jk})$$

$$2)\ logit(p_{jk}) = \log\left(\frac{Prob_{jk}}{1 - Prob_{jk}}\right)$$
$$= \beta_0 + \beta_1 FE\_cat2_{jk} + \beta_2 FE\_cat3_{jk} + \cdots + \beta_8 FE\_cat8_{jk}\ b_j + b_{jk}$$

$$3)\ OR = \exp\ (est_{LO})\ ;\ Prob_{jk} = \frac{\exp(est_{LO})}{1+\exp\ (est_{LO})}$$

$$4)\ b_j \sim N(0, \sigma^2_{location});\ b_{jk} \sim N(0, \sigma^2_{family})$$

$$5)\ Var(logit(Prob_{jk})) = \sigma^2_{location} + \sigma^2_{family} + \frac{\pi^2}{3}$$

$$6)\ Var(Prop_{jk} | FE\_cat, location, family) = TSS_{jk} * Prob_{jk} * (1 - Prob_{jk})$$

Linear Mixed Effects – Example Models C-D To explain the general logic behind LME models, Example Models C and D respectively show LME models that used either a continuous FE to analyze the phenology TTE, growth, and NSC traits for Q1 (Example Model C) or a categorical FE that were used to analyze the phenology TTE, growth, and NSC traits for Q2-Q4 (Example Model D). The same model was used for NSCs except there was only *jk* in the model instead of *ijk* as depicted below (reasons listed above). Line 1 shows that the response trait (RT) was normally distributed with a mean of the *ith* observation within the *kth* family, within the *jth* location (M_{ijk}) with standard deviation (σ^2). Line 2 shows that the expected mean (M_{ijk}) is determined by the linear predictors (β = fixed effects, b = random effects). β_0 is the fixed intercept (trait value centered at the mean of the first continuous FE variable (FE_cont1) and the second continuous FE variables (FE_cont2), while β_1 and β_2 represent the change in RT for each unit increase of the FE_cont1 and the FE_cont2 (the slope) respectively while holding the other FE variable constant for the *ith* observation within the *kth* family in the *jth* location. Line 3 shows that the variables, b_j and b_{jk} represent the RE intercept for location and family respectively where b_j accounts for the variation between locations while b_{jk} accounts for the variation between families within a location. These RE follow a normal distribution where the mean is 0 and the variance is described by $\sigma^2_{location}$ or σ^2_{family}, respectively for each RE. Line 4 shows the residual error, ε_{ijk}, which represents the remaining variation that was not explained by the FE and RE in the model. The residual error, ε_{ijk}, is normally distributed with a mean of 0 and standard deviation (σ^2) divided by the total sown seeds (TSS_{ijk}) for the *ith* observation within the *kth* location in the *jth* location. To control for unbalanced seedling sample size within a family, the families with a greater number of total sown seeds are given a greater weight. Because those families have more reliable estimates, they contribute more to the model. Line 5 shows the variance (Var) for the RT for the *ith* observation within the *kth* location in the *jth* location with the FE variables and location and family as RE. The variance is the sum of the variation explained by the RE and the residual variation that is weighted by TSS$_{ijk}$ (Ramsey and Schafer, 2013; Bates et al. 2015)

Example Model C. Linear Mixed Effects (LME) Model (FE continuous)

$$1)\ RT_{ijk} \sim N(\mu_{ijk}, \sigma^2)$$

$$2)\ \mu_{ijk} = \beta_0 + \beta_1 FE\_cont1_{ijk} + \beta_2 FE\_cont2_{ijk} + \ b_j + b_{jk} + \ \epsilon_{ijk}$$

$$3)\ b_j \sim N(0, \sigma^2_{location});\ b_{jk} \sim N(0, \sigma^2_{family})$$

$$4)\ \epsilon_{ijk} = N(0, \frac{\sigma^2}{TSS_{ijk}})$$

$$5)\ Var(RT_{ijk} | FE\_cont1, FE\_cont2,\ Location, Family) = \ \sigma^2_{location} + \ \sigma^2_{family} + \frac{\sigma^2}{TSS_{ijk}}$$

For Example Model D below, the equation and variables are the same as Example Model C except that the FE is now categorical instead of continuous. The same model as example D (below) was used for NSCs except there was only *jk* in the model instead of *ijk* as depicted below. The intercept, β_0, now represents the trait mean for the category reference level while β_1 represents the difference in the trait mean between the reference level and the next level. Each β_x represents the difference between the reference level and the level of interest (Ramsey and Schafer, 2013; Bates et al. 2015). Below FE_cat stands for categorical FE, where FE_cat2, FE_cat3, and FE_cat8 stand for categorical fixed effect level 2, categorical fixed effect level 3, and categorical fixed effect level 8, respectively.

Example Model D. Linear Mixed Effects (LME) Model (FE categorical)

$$1)\ RT_{ijk} \sim N(\mu_{ijk}, \sigma^2)$$

$$2)\ \mu_{ijk} = \beta_0 + \beta_1 FE\_cat2_{ijk} + \beta_2 FE\_cat3_{ijk} + \cdots + \beta_2 FE\_cat8_{ijk}\ b_j + b_{jk} + \ \epsilon_{ijk}$$

$$3)\ b_j \sim N(0, \sigma^2_{location});\ b_{jk} \sim N(0, \sigma^2_{family})$$

$$4)\ \epsilon_{ijk} = N(0, \frac{\sigma^2}{TSS_{ijk}})$$

$$5)\ Var(RT_{ijk} | FE\_cat1, FE\_cat2,\ Location, Family) = \ \sigma^2_{location} + \ \sigma^2_{family} + \frac{\sigma^2}{TSS_{ijk}}$$